Functional characterization of the human renal organic anion transporter 3 (hOAT3) and comparison to hOAT1

Dissertation
zur Erlangung des Doktorgrades
der Mathematisch-Naturwissenschaftlichen Fakultäten
der Georg-August-Universität zu Göttingen

vorgelegt von

Nadiya Bakhiya
aus Sochi, Russland

Göttingen 2004

D7

Referent: Prof. Dr. R. Hardeland

Korreferent: Prof. Dr. K. v. Figura

Tag der mündlichen Prüfung: Mittwoch, 28 April 2004

CONTENTS

List of Abbreviations

Å	Angstrom
ATP	adenosine triphosphate
bp	base pairs
C	Celsius
cAMP	cyclic adenosine monophosphate
C-terminus	carboxy-terminus
cDNA	complementary DNA
CKII	casein kinase II
cRNA	complementary RNA
Da	Dalton
dNTP	deoxyribonucleotide phosphate
DHEA-S	dehydroepiandrosterone sulfate
ES	estrone sulfate
GA	glutaric acid
NaDC3	sodium/dicarboxylate cotransporter 3
fOAT	flounder organic anion transporter
hr	hour
HCTZ	hydrochlorothiazide
HEK293	human embryonic kidney cell line
hNLT	human novel liver transporter
hOAT1	human organic anion transporter 1
hOAT2	human organic anion transporter 2
hOAT3	human organic anion transporter 3
hOAT4	human organic anion transporter 4
α-KG	α-ketoglutarate
k	kilo
K_m	Michaelis Menten constant
LB	Luria Bertani broth
M	molar (moles per litre)
μM	micromolar
ml	milliliter
mRNA	messenger RNA
NCC	Na^+-Cl^- cotransporter
NKCC	Na^+-K^+-$2Cl^-$ cotransporter
N-terminus	amino-terminus
NKT	novel kidney transporter
NLT	novel liver transporter
NSAIDs	non-steroidal anti-inflammatory drugs
OAT	organic anion transporter
OAT1	organic anion transporter 1

OAT3	organic anion transporter 3
OAT4	organic anion transporter 4
OAT5	organic anion transporter 5
OATv1	voltage-driven organic anion transporter
OCT	organic cation transporter
ORI	oocyte Ringer's solution
PAH	para-aminohippurate
PCR	polymerase chain reaction
PGE_2	prostaglandin E_2
$PGF_{2\alpha}$	prostaglandin $F_{2\alpha}$
PKA	cAMP-associated protein kinase
PKC	protein kinase C
pmol	picomole
RACE	rapid amplification of cDNA ends
rOAT1	rat organic anion transporter 1
rOAT2	rat organic anion transporter 2
rOAT3	rat organic anion transporter 3
rpm	revolutions per minute
RST	renal solute transporter
RT-PCR	reverse transcriptase PCR
SLC	solute carriers
TAL	thick ascending limb
TCA	tricarboxylic acid cycle
TMD	trams-membrane domain
U	unit
URAT1	urate transporter 1
UTR	untranslated region
UST	unidentified solute transporter
V_{max}	maximum velocity

ABSTRACT

Renal secretion of organic anions is critically dependent on their basolateral uptake against the electrochemical gradient. Due to their localization, two transporters are likely involved, namely OAT1 and OAT3. While OAT1 as an exchanger clearly operates in the secretory direction, OAT3 in its previously supposed mode as a uniporter should move substrates from cell to blood. Therefore, in the present study the driving forces of human OAT3 were re-investigated. Additionally, hOAT3 was compared to hOAT1 under identical conditions, for a better understanding of their contribution to renal handling of some common physiologically and clinically important substrates (urate, diuretics). As the hOAT3 obtained from a resourcecenter (RZPD) was not functional, it was corrected by site-directed mutagenesis. Using the *Xenopus laevis* oocyte expression system, hOAT3-mediated transport of estrone sulfate (ES) and glutarate was assayed for cis-inhibition and/or trans-stimulation. The substrate uptake by hOAT3 showed characteristics similar to hOAT1 – it was chloride dependent and was most potently inhibited by the C-5 dicarboxylates α-ketoglutarate (α-KG) and glutarate by 90 and 95%, respectively. Both were also substrates for hOAT3, although the apparent affinity of hOAT3 for glutarate (K_m=23.5 μM) was about one order of magnitude lower than that of hOAT1 (K_m=2.5 μM). It was demonstrated that hOAT3-mediated efflux of glutarate, in contrast to ES, can be significantly trans-stimulated by a variety of ions, including GA (280%), α-KG (480%), *p*-aminohippurate (180%), and, most notably, urate (170%). These results prove the ability of hOAT3 to operate as an organic ion/dicarboxylate exchanger. Thus, similar to hOAT1, hOAT3 likely functions in the secretory direction in vivo, and possibly also driven by outwardly directed α-KG gradient. hOAT3 showed a higher sensitivity for urate than hOAT1, which was also true when both were expressed in cultured mammalian cells. Thus, hOAT3 is likely to be involved in renal urate secretion and may even predominate over hOAT1 in this process. As for the potential contribution of hOAT3 and hOAT1 to the renal secretion of diuretics, the efflux by both carriers was trans-stimulated by furosemide, as well as hydrochlorothiazide, showing that both can translocate diuretics and thus participate in basolateral uptake of these compounds in exchange for α-KG. While hOAT3 exhibited a far higher sensitivity to inhibition by loop diuretic furosemide than hOAT1 (IC_{50} of 3μM for hOAT3 versus 490μM for hOAT1), it may play the major role in secretion of this drug. Taken together, the present study establishes hOAT3 as an anion exchanger involved in the secretion of endogenous and exogenous compounds.

1 INTRODUCTION

1.1 Secretion of organic anions in proximal tubules

Organic anions are substances containing a carbon backbone and one or more negative charges at physiological pH. A great number of potentially toxic substances can be classified as organic anions. These include endogenous compounds such as waste products, as well as exogenous compounds such as environmental and industrial xenobiotics, plant and animal toxins, and numerous anionic pharmaceutical drugs. The elimination of organic anions is an important protective task and it is performed by liver and kidneys. In the kidneys, the proximal tubules are the site of organic anion secretion.

Over the past century many studies have been performed on the characterization of the renal organic anion secretory mechanism, using model systems such as isolated non-perfused and perfused proximal tubules, kidney slices and membrane vesicles (Pritchard and Miller 1993). A “classical organic anion transport system” was described, by which the secretion process occurs in two main steps, namely the uptake of organic anions from the blood into the proximal tubule cell across the basolateral membrane, and the efflux into the tubular lumen across the apical (or brush-border) membrane (Roch-Ramel 1998). As cells maintain an inside negative membrane potential, movement of negatively charged compounds across the basolateral membrane requires energy. Moreover, the uptake of the organic anions is concentrative. Therefore these substances are moved against their electrical and chemical gradients.

The current model for the driving force of organic anion uptake was proposed by Burckhardt and co-workers (Shimada *et al* 1987) and Pritchard (Pritchard 1988) based on experiments with rat renal basolateral vesicles. In this model, the Na^+,K^+-ATPase generates the inwardly directed sodium gradient, which drives sodium-dicarboxylate cotransport via NaDC-3 (sodium-dicarboxylate cotransporter). The secondary active Na^+-cotransport from the blood side together with metabolism maintain an outwardly directed dicarboxylate gradient (Shuprisha *et al* 1999), which drives cellular organic anion uptake via anion / dicarboxylate exchange. This process is called tertiary active, because the uptake of the organic anion is driven by ATP hydrolysis through two intermediate steps. After basolateral uptake, which is considered to be the rate-limiting step in the process of secretion, the organic anions are sequestered within vesicles of

unknown origin and translocated to the luminal side (Miller *et al* 1993). Luminal exit of organic anions is a less well defined process. In contrast to the highly conserved basolateral uptake (Pritchard and Miller 1991), the apical efflux mechanisms differs among species (Roch-Ramel and Diezi 1997). Efflux occurs via anion / anion exchange, anion / dicarboxylate exchange and/or membrane potential-dependent transport (Burckhardt and Pritchard 2000).

1.2 Organic Anion Transporter (OAT) family

1.2.1 OAT family members

The first carrier molecules involved in organic anion secretion have been identified in 1997, when, the protein now termed organic anion transporter 1 (OAT1) was cloned from rat (originally named as ROAT), winter flounder (originally named as fROAT) and mouse (originally named as NKT) (Lopez-Nieto *et al* 1997, Sekine *et al* 1997, Sweet *et al* 1997, Wolff *et al* 1997). Later, the human OAT1 homologue was cloned in our laboratory (Reid *et al* 1998). When expressed in *Xenopus laevis* oocytes or cultured cells, OAT1 exhibited the functional properties of the basolateral organic anion transporter determined earlier. The carrier mediated high-affinity uptake of *p*-aminohippurate (PAH) – the classical model substrate used for characterization of the renal organic anion secretory system (Kuze *et al* 1999, Lu *et al* 1999, Sekine *et al* 1997, Sweet *et al* 1997, Wolff *et al* 1997). OAT1 also showed interaction with a wide range of organic substances of endogenous and exogenous origin, such as cyclic nucleotides, prostaglandin E_2, dicarboxylates, β-lactam antibiotics, and non-steroidal anti-inflammatory drugs (Apiwattanakul *et al* 1999, Jariyawat *et al* 1999, Sekine *et al* 1997). The OAT1-mediated PAH uptake was dose-dependently *cis*-inhibited and *trans*-stimulated by α-ketoglutarate or glutarate, demonstrating that OAT1 functioned as an anion / dicarboxylate exchanger (Kuze *et al* 1999, Sweet *et al* 1997).

Since then several OAT isoforms have been identified, and their transport properties characterized. These isoforms are also multispecific transporters that show between 39% (OAT2 vs. OAT3) and 49% (OAT1 vs. OAT3) amino acid sequence identity (Sekine *et al* 2000), and they form the organic anion transporter (OAT) family. The OAT family members are structurally related to the OCT family of organic cation transporters (Burckhardt and Wolff 2000). A phylogenetic tree of the OAT family is presented in Figure 1.1. So far, at least 9 OAT isoforms have been functionally characterized (they

are marked by shading in the diagram). These are OAT1, OAT2, OAT3, OAT4, the recently isolated OAT5, OAT from winter flounder (fOAT), OAT from Caenorhabditis elegans (CeOAT), the human urate transporter URAT1 (originally cloned as RST), and the voltage-driven OATv1 recently cloned from pig kidney (Jutabha *et al* 2003).

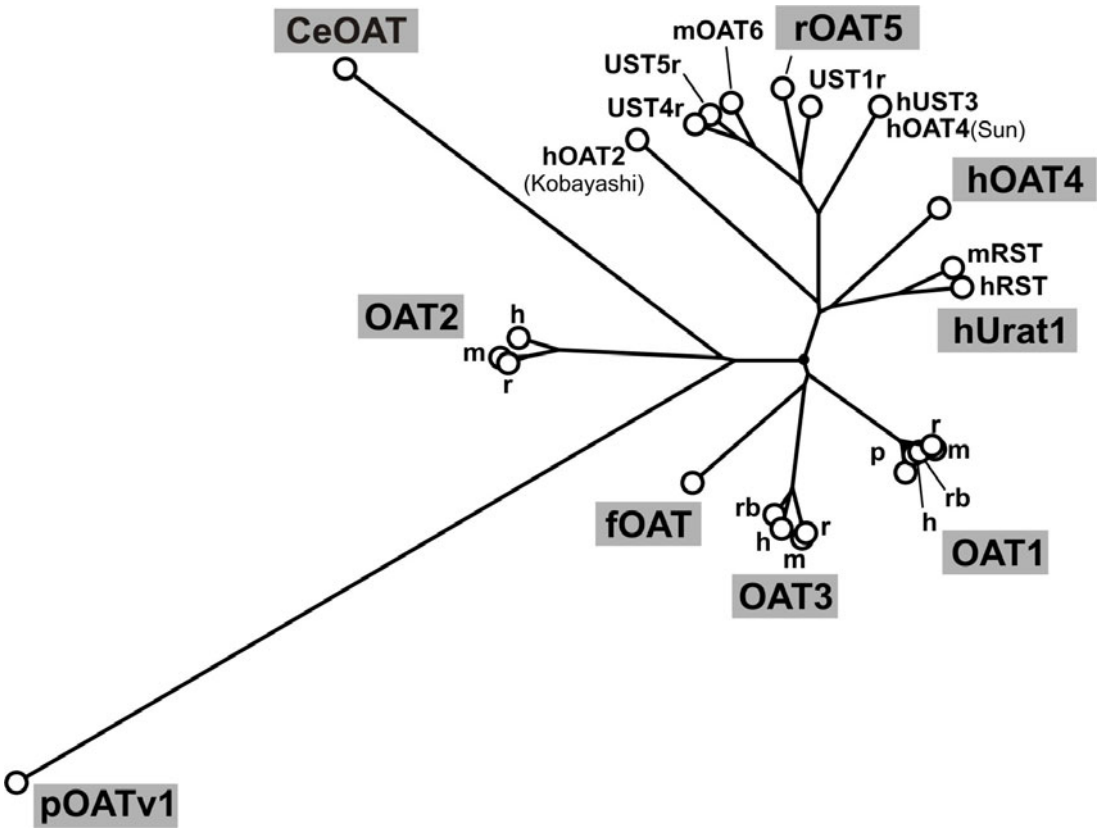

Figure 1.1: Phylogenetic tree of OAT family proteins. The dendrogram was generated with the GenTree Program of the Computational Biochemistry Research Group (CBRG) in the Eidgenössische Technische Hochschule, Zürich. The functionally characterized OAT isoforms are shaded. Meaning of the abbreviations: RST, renal specific transporter; UST, unidentified solute transporter; URAT1, Urat-Transporter 1; h, human; r, rat; m, mouse; rb, rabbit; p, pig; f, flounder; Ce, Caenorhabditis elegans.

The closest relatives of the OAT1 proteins are the OAT3 proteins (the subject of interest in the present study). Notably, the genes of hOAT1 and hOAT3 are closely linked and located on chromosome 11q12.3. (Table 1.1.) (Eraly *et al* 2003). As detailed below, both carriers are co-expressed in the basolateral membrane of the proximal tubules. The common relative of OAT1s and OAT3s appears to be the flounder OAT, which branches off very near the branch point between the OATs1 and OATs3. Of the apical transport proteins, hOAT4 cloned by Cha et al. (Cha *et al* 2000) and URAT1 – form the next cluster. In the human genome (see Table 1.1.), OAT4 and URAT1 genes

are localized close to each other on the chromosomal band 11q13.1 (Eraly *et al* 2003). OAT2 is the most distant among the OAT1-OAT4 isoforms. The gene of this family member is physically isolated from the others and located on chromosome 6p21.1 (Eraly *et al* 2003, Kok *et al* 2000). The OAT5 protein, recently isolated from a rat kidney cDNA library, is located in a large cluster of further cloned, but not yet functionally characterized related proteins. These are OAT6, and a group of putative transporters named UST1, UST3 and UST4. Several inconsistencies are present in the nomenclature of these transporter proteins. The human OAT4 cloned by Sun et al. (Sun *et al* 2001) is not identical to the hOAT4 cloned by Cha et al. (Cha *et al* 2000) and the function of the former has not been described. The same problem exists for the hOAT2 cloned by Kobayashi.

Name	Species	Alternative Name	Accession No(s)	AA	Chromosome localization	Human gene name
rOAT1	rat		AB004559 AF008221	551		
hOAT1	human	hPAHT	AF057039 AB009697	550	11q12.3	SLC22A6
mOAT1	mouse	NKT	U52842	546		
fOAT1	winter flounder		Z97028			
rOAT2	rat	NLT	L27651 L30107	535		
hOAT2	human		AF097518 AF210455	548	6p21.1-2	SLC22A7
rOAT3	rat		AB017446			
mOAT3	mouse	Roct	AF078869	537		
hOAT3	human		AF097491 AB042505	568	11q12.3	SLC22A8
hOAT4	human		AB026116	550	11q13.1	SLC22A11
rOAT5	rat		BAB78471	551		
URAT1	human	RST	AB071863	553	11q13.1	SLC22A12

Table 1.1: Properties of organic anion transporters. Meaning of the abbreviations: AA, amino acids; hPAHT, human PAH transporter; NKT, novel kidney transporter; NLT, novel liver transporter; Roct, reduced in osteosclerosis transporter; URAT1, Urat-Transporter 1; RST, renal specific transporter; h, human; r, rat; m, mouse; rb, rabbit; p, pig; f, flounder; SLC – solute carriers.

1.2.2 Structure of OATs

All transporters of OAT the family possess common structural characteristics (Burckhardt and Wolff 2000). The OAT proteins are between 535 and 568 amino acids long (as summarized in Table 1.1), and have a predicted transmembrane topology as shown in Figure 1.2. The OAT proteins are assumed to have twelve α-helical

transmembrane domains (TMDs) and intracellular N- and C-termini. A long extracellular hydrophilic loop, containing a cluster of potential glycosylation sites, is found in all OATs between the first and second predicted TMDs. In a study with mOAT1, expressed in COS7 cells, inhibition of glycosylation by tunicamycin resulted in a decrease of surface expression of the transporter protein and accumulation of newly synthesized transporters in an intracellular compartment (Kuze *et al* 1999). This suggests that glycosylation is required for proper sorting of OAT1 into the plasma membrane. Finally, an intracellular loop between TMD6 and TMD7 is predicted for all members of the OAT family, which carries multiple potential phosphorylation sites – mostly for protein kinase C (PKC) (Figure 1.2). Several consensus sequences for phosphorylation are also clustered in the C-terminus. However, while there is evidence confirming that transport function of OATs (namely OAT1 and OAT3) is downregulated by PKC (Lu *et al* 1999, Takeda *et al* 2000b, Uwai *et al* 1998), at least in hOAT1 the conserved canonical PKC sites do not appear to be involved (Wolff *et al* 2003)

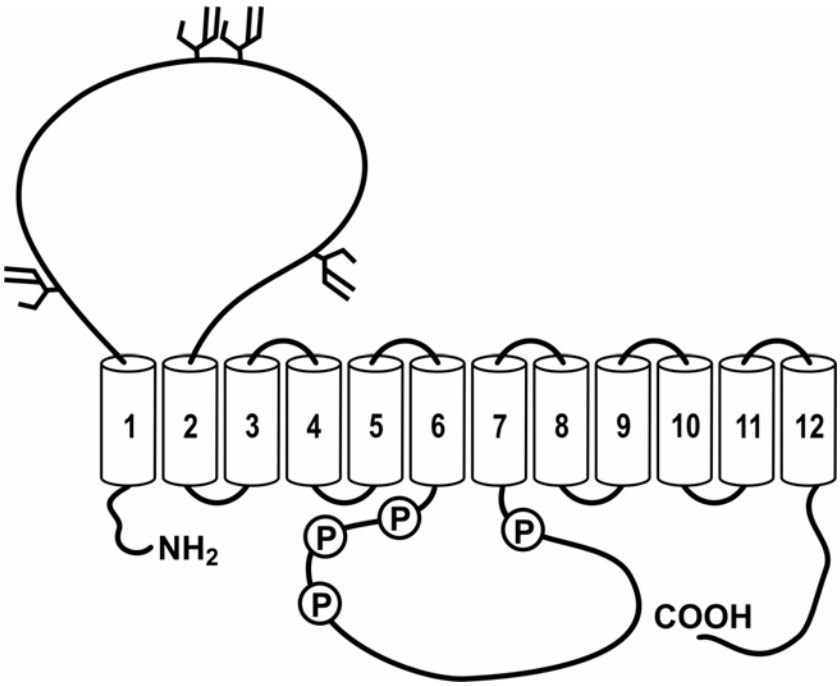

Figure 1.2: Predicted transmembrane topology model of organic anion transporters. OATs are assumed to have twelve transmembrane domains with intracelullar N- and C-termini. Several consensus sequences for N-glycosylation (the branched structures) are present in the large extracellular loop between the first and second transmembrane domains (TMDs) and several protein kinase C phosphorylation sites (P) are predicted in the large intracellular loop between the sixth and seventh TMDs. *Re-drawn from (Sekine et al 2000)*

1.2.3 Tissue distribution and localization of OATs

The distribution of the OATs was assessed by the Northern blot technique and by immunocytochemistry. As summarized in Table 1.2, mRNA for almost all of the functionally characterized OAT-type transporters is found in the kidneys, and for OAT1, OAT3, OAT4, OAT5 and URAT1, the proximal tubules seem to be the predominant site of expression, although some species differences in expression patterns were found.

OAT subtype	Species	Organs	Nephron segment(s)	Cell side
OAT1	mouse	kidney >> brain		
	rat	kidney >> brain (choroid plexus)	proximal tubule	basolateral
	human	kidney >> brain, liver	proximal tubule	
OAT2	mouse	kidney >> liver		
	rat	liver > kidney (M); kidney >> liver (F)	TAL, collecting duct	apical
	human	liver >> kidney	proximal tubule	basolateral
OAT3	mouse	kidney > choroid plexus		
	rat	kidney >> liver (M only), brain	proximal tubule, TAL, collecting duct	basolateral
	human	kidney >> brain	proximal tubule	basolateral
OAT4	human	kidney >> placenta	proximal tubule	apical
OAT4	rat	kidney only	proximal tubule	apical
URAT1	human	kidney only	proximal tubule	apical

Table 1.2: Tissue distribution and intra-renal localization of organic anion transporters. Meaning of the abbreviations: URAT1, Urate-Transporter 1; F, female; M, male; TAL, thick ascending limb.

The OAT1 from human (Hosoyamada *et al* 1999, Lu *et al* 1999, Race *et al* 1999), rat (Sekine *et al* 1997, Sweet *et al* 1997) and mouse (Kuze *et al* 1999, Lopez-Nieto *et al* 1997) were most strongly expressed in kidneys and to a lesser extent in brain. The hOAT1 was also found in skeletal muscle (Hosoyamada *et al* 1999, Takeda *et al* 2004) and liver (Cihlar *et al* 1999). Immunohistochemical analyses of the human kidney revealed that the hOAT1 protein was expressed in the basolateral membrane of all three segments (S1, S2 and S3) of proximal tubules (Motohashi *et al* 2002). In contrast, rat rOAT1 was shown to localized in the basolateral membrane of only the S2 segment of proximal tubules (Sekine *et al* 1997, Tojo *et al* 1999). The expression pattern of hOAT3 has some similarities with that of hOAT1. It was found to be strongly expressed in the kidneys and weakly in brain (Kusuhara *et al* 1999, Race *et al* 1999).

Within the human kidney, positive staining for hOAT3 was detected in the basolateral membrane of the S1, S2 and S3 segments of the proximal tubules, where it co-localized with hOAT1 (Motohashi *et al* 2002). Interestingly, the expression level of hOAT3 mRNA in the human kidney was highest among the organic ion transporter family (Motohashi *et al* 2002). Recent immunohistochemical studies revealed the presence of hOAT3 together with hOAT1 also in the cytoplasmic membrane and cytoplasm of the human choroid plexus (Alebouyeh *et al* 2003). In rats, highest signals of OAT3 mRNA were found in kidney, and less intensive signals in brain and liver (Buist *et al* 2002). In contrast to humans, rat OAT3 protein was detected not only in the proximal tubules, but also in the thick ascending limb (TAL) and collecting duct (CD), where it was localized in the basolateral membrane (Kojima *et al* 2002). The expression of hepatic rOAT3 mRNA was much higher in male rats than in females (Buist *et al* 2002). In the rat brain, rOAT3 (but not rOAT1) was localized in the apical membrane of the choroid plexus, where its possible function is the removal of organic anions from the cerebrospinal fluid (Nagata *et al* 2002).

Among the OAT isoforms, only OAT2 is highly expressed in the liver. Furthermore, the distribution of OAT2 shows gender- and species-related differences. In humans, OAT2 was found to be highly expressed in liver and at a lower level in kidneys (Sun *et al* 2001). Within the human kidney the hOAT2 protein was localized at the basolateral side of proximal tubules (Enomoto *et al* 2002b). Rat OAT2, first cloned from rat liver and named “novel liver transporter” (NLT), was found in liver and at lower levels in kidneys (Simonson *et al* 1994). While rOAT2 expression in males were highest in liver, it was in females considerably higher in kidneys than in liver (Buist *et al* 2002). Moreover, the total amount of OAT2 mRNA in females was much higher than that in males (Kudo *et al* 2002). In contrast to human OAT2, rOAT2 was localized to the apical surface of the TAL and collecting duct (Kojima *et al* 2002). In mouse, OAT2 was abundantly expressed in the male kidney but faintly expressed in the male liver, whereas it’s expression level was almost equal in female liver and kidney (Kobayashi *et al* 2002). There are no data available on the existence of such differences in humans. The human OAT4 was found to be predominantly expressed in the kidney and at a lower levels in placenta (Cha *et al* 2000). In the kidney, hOAT4 mRNA was the least abundant among the OAT isoforms (Motohashi *et al* 2002), and the hOAT4 protein was localized to the apical membrane of proximal tubule cells (Babu *et al* 2002). The expression of the human urate transporter URAT1 appears to be restricted to the kidney, where it was localized to the apical membrane of proximal tubule cells

(Enomoto *et al* 2002a). Expression of the newly identified rat OAT5 was also detected exclusively in the kidney. There it was immunolocalized to the apical membrane of the proximal tubules. The mRNA for voltage-driven organic anion transporter OATv1 was found in kidneys and liver. By the western blot technique, the OATv1 protein was detected only in brush-border membranes of the pig kidney cortex (Jutabha *et al* 2003). Thus, OATs are consistently found in barrier epithelia, where they function in the elimination of endogenous and exogenous organic anions (Sweet *et al* 2001). In the kidneys, OAT1 together with OAT3 are believed to be responsible for the basolateral step of organic anion secretion, and OAT4, OAT5 and OATv1 involved in the apical release.

1.2.4 Substrates of OATs

The functional characteristics of OAT family members were studied using heterologous expression systems, such as *Xenopus laevis* oocytes or cultured mammalian cells. Different compounds have been tested either for transport by OATs, mostly by applying them in radiolabeled form to the extracellular uptake medium, or for inhibition of OAT-mediated uptake of labeled model substrates, when added in non-labeled form to the uptake medium. The common feature of all OATs (at least of OAT1-OAT4) is polyspecificity: they interact with compounds of different chemical structure and even of different charge. Their substrates include many endogenous compounds (α-ketoglutarate, prostaglandins, cyclic nucleotides and urate) as well as exogenous substances, such as widely prescribed drugs (diuretics, antiviral drugs, antibiotics and non-steroidal anti-inflammatory drugs). Although there are notable differences in the selectivity, the substrate specificities of OATs overlap. In the following, some examples of common endogenous and exogenous substrates of different human OATs are discussed.

The dicarboxylates α-ketoglutarate and/or its non-metabolizable analogue glutarate have been shown to be substrates for hOAT1 (Cihlar and Ho 2000, Lu *et al* 1999), hOAT2 (Sun *et al* 2001) and hOAT3 (Cha *et al* 2001), but apparently not for hOAT4, since this transporter was not even inhibited by glutarate (Cha *et al* 2000). Another example of common endogenous substrates are prostaglandins E_2 and $F_{2\alpha}$, for which hOAT1, hOAT2, hOAT3 and hOAT4 have been shown to have a high affinity (Enomoto *et al* 2002b, Kimura *et al* 2002). The second messenger cAMP was accepted by hOAT2 (Sun *et al* 2001) and hOAT3 (Cha *et al* 2001). For hOAT4 interaction with cAMP has not been tested, while its transport has been shown for rat OAT1 (Sekine *et*

al 1997). The conjugated bile acid taurocholate was taken up into hOAT3-expressing oocytes and showed inhibition on hOAT1-mediated PAH uptake (Islinger *et al* 2001) and hOAT4-mediated estrone sulfate (ES) uptake (Cha *et al* 2000), but was not tested for interaction with hOAT2. Indoxyl sulfate, the uremic toxin derived from dietary protein, has been shown to be transported by hOAT1, hOAT3 and hOAT4, but not by hOAT2 (Enomoto *et al* 2003, Motojima *et al* 2002). The nephrotoxic agent ochratoxin A was found to be a high-affinity substrate for both basolateral carriers hOAT1 and hOAT3 (Jung *et al* 2001) as well as for the apical hOAT4 (Babu *et al* 2002).

With respect to drugs, widely used non-steroidal anti-inflammatory drugs or NSAIDs (such as diclofenac, ibuprofen and salicylate) were described to interact with hOAT1, hOAT3 and hOAT4 (Khamdang *et al* 2002,Mulato *et al* 2000). However, due to this characteristic, NSAIDs are able to prevent nephrotoxicity caused by antiviral drugs (Mulato *et al* 2000). The OATs have also been shown to react with β-lactam antibiotics and tetracyclines. For example hOAT1 (Hosoyamada *et al* 1999), hOAT3 (Cha *et al* 2001) and hOAT4 (Cha *et al* 2000) where inhibited by penicillin G; the organic anion transport by hOAT1, hOAT3 and hOAT4 was significantly inhibited by cephaloridine (Takeda *et al* 2002a); human OAT1, hOAT2, hOAT3 and hOAT4 have been found to transport tetracycline (Enomoto *et al* 2002a). Several antiviral drugs have also been shown to be OATs substrates. For example, acyclovir, gancyclovir, cidofovir and adefovir were transported by hOAT1, valacyclovir was transported by hOAT3 and zidovudine was transported by hOAT1-hOAT4 (Cihlar *et al* 1999, Ho *et al* 2000, Takeda *et al* 2002c). Therefore, OATs are believed to play a role in antiviral drug-induced nephrotoxicity. The cytostatic drug methotrexate, which is eliminated with the urine, and was found to cause toxic effects when co-administrated with NSAIDs, probenecid or penicillin G, is transported with high affinity by hOAT3 and hOAT4 (Takeda *et al* 2002b), and by hOAT2 (Sun *et al* 2001). Another common feature of all characterized OAT family members is their interaction with diuretics. Since many diuretics such as loop diuretics and thiazides act from the tubule lumen (Okusa and Ellison 2000) and because of the protein binding poorly filtrated in glomerulus, the secretion in the proximal tubules plays a critical role in targeting these drugs. The loop diuretics furosemide and bumetanide have been shown to potently inhibit organic anion uptake by hOAT1 (Hosoyamada *et al* 1999, Lu *et al* 1999, Race *et al* 1999), as well as by hOAT3 (Cha *et al* 2001), hOAT4 (Cha *et al* 2000) and URAT1 (Enomoto *et al* 2002a). One more common feature of the OATs is their sensitivity to probenecid. This well-known inhibitor of renal organic anion secretion powerfully blocked the substrate

transport by hOAT1, hOAT2, hOAT3 as well as hOAT4 (Burckhardt and Burckhardt 2003, Cha *et al* 2000). As for their mode of operation, at the time of the outset of this study only OAT1 had been shown to function as an anion / dicarboxylate exchanger, while OAT2, OAT3 and OAT4 where believed to be uniporters (Sekine *et al* 2000, Sweet *et al* 2001). However, as OAT1 appeared to be the best characterized of all OAT members, it remained possible that other OATs could also exchange their substrates against yet undefined counterions.

1.3 Comparison of hOAT3 with hOAT1

The subject of interest in this study were the two human organic anion transporters hOAT1 and hOAT3, which are localized at the basolateral membrane of the proximal tubule cells (Cha *et al* 2001, Hosoyamada *et al* 1999). Both are candidates for basolateral uptake systems of anionic compounds from the blood into renal proximal tubule cells. The transport properties of hOAT1 have been more intensively examined than those of hOAT3. Similar to hOAT1, hOAT3 appears to handle a wide range of organic anions, including estrone sulfate (ES), *p*-aminohippurate (PAH), benzylpenicillin, taurocholate, and several potentially toxic neurotransmitter metabolites (Cha *et al* 2001, Kusuhara *et al* 1999, Sweet *et al* 2002).

1.3.1 Mode of operation of hOAT3

The main difference between OAT1 and OAT3 appeared to be its mode of transport. While hOAT1 had been shown to function as an organic anion / dicarboxylate exchanger (Lu *et al* 1999), the driving forces of the hOAT3-mediated organic anion transport remained unclear. Since efflux of the model substrate estrone sulfate (ES) from hOAT3-expressing *Xenopus laevis* oocytes was not trans-stimulated by ES or other organic anions in the extracellular medium (Cha *et al* 2001, Kusuhara *et al* 1999), hOAT3 has been regarded as a uniporter, mediating facilitated diffusion. Nevertheless, due to its basolateral localization, hOAT3 was always considered as a carrier involved in organic anion secretion. However, as was already mentioned, the uptake of organic anions against their concentration gradient and an inside negative membrane potential could not occur without energy input. Therefore, in its suggested mode as a uniporter OAT3 would facilitate the outward flux of its substrates, providing reabsorption rather than secretion. Since the substrate specificities of hOAT1 and hOAT3 overlap and both transporters co-localize at least in the S2 segment (Tojo *et al* 1999), if not all along the proximal tubule (Kojima *et al* 2002, Motohashi *et al* 2002), hOAT3 would allow the

back-leak of the substances enriched in the cells via hOAT1, if operating in the reabsorptive direction (Figure 1.3). Thus, hOAT3 would impair secretion of substrates shared with hOAT1 and thus dissipate energy, which is unlikely to occur in vivo. Therefore, it was important to identify the driving force for organic anion uptake via hOAT3.

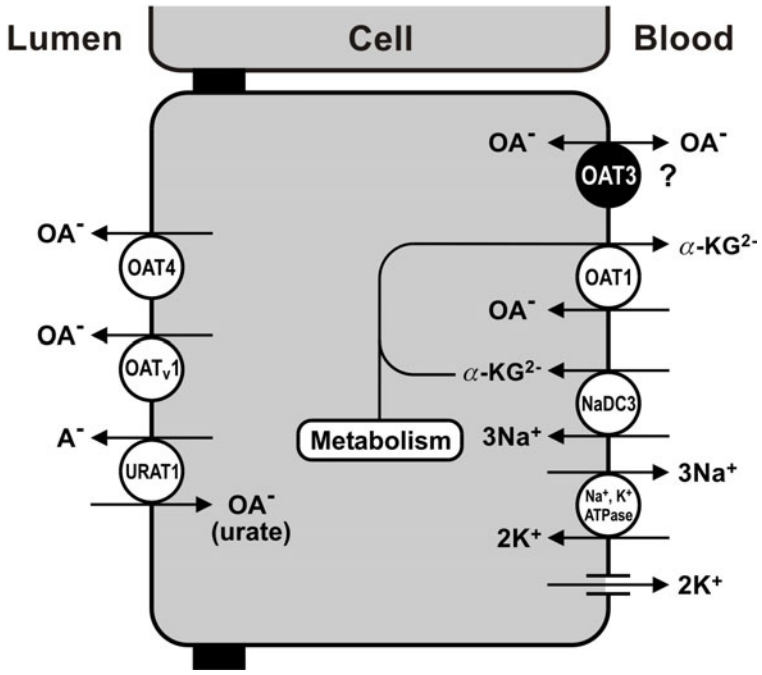

Figure 1.3: Scheme of proximal tubular organic anion secretion. OA^-, organic anion; A^-, anion; $\alpha\text{-}KG^-$; α-ketoglutarate; NaDC3; sodium-dicarboxyate cotransporter;

1.3.2 Substrate specificity of hOAT3 and hOAT1

Although, as was mentioned above, the substrate specificities of hOAT1 and hOAT3 show a considerable overlap, they by far not identical and often the affinities of both carriers even for common substrates differ. These differences should result in an unequal contribution of hOAT1 and hOAT3 to the secretion of such compounds. Thus, increased knowledge of the hOAT1 and hOAT3 substrate specificities is of physiological and clinical importance.

The comparison of hOAT1 and hOAT3 with respect to their interaction with some substrates is shown in the Table 1.3. The main model substrate of hOAT3 and also one of the best is estrone sulfate (ES). The affinity of hOAT3 for ES is very high, with reported K_m-values between 2.2 µM (Takeda *et al* 2001) and 7.5 µM (Takeda *et al* 2000a). Other high-affinity substrates for hOAT3 are the hormone metabolites

dehydroepiandrosterone sulfate (DHEA-S) and estradiol glucuronide (Cha *et al* 2001). In contrast, hOAT1 does not transport any of these substances, such that hOAT3, but not hOAT1, appears to be involved in transport of sulfated and glucuronidated steroid hormones. The affinity of hOAT3 for PAH, the classic substrate of OAT1, is much lower than that of hOAT1. The apparent K_m of hOAT3 for PAH has been determined to be 87.2 µM (Cha *et al* 2001), while for hOAT1 this value ranges from 3.9 µM (Islinger *et al* 2001) to 22 µM (Motojima *et al* 2002) when measured in different expression systems (Table 1.3.). This suggests that transport of PAH across the basolateral membrane of renal proximal tubule cells is predominantly mediated by hOAT1. Another difference from hOAT1 is the ability of hOAT3 to transport the cytostatic methotrexate with a K_m value of 10.9 µM (Cha *et al* 2001) or 21 µM (Takeda *et al* 2002b), while hOAT1 has been shown to transport this drug with very low affinity with a K_m value of 554 µM (Takeda *et al* 2002b), or did not transport it at all in an other study (Lu *et al* 1999)

	hOAT1			**hOAT3**		
Compound	Transport or K_m (µM)	Inhibition or IC_{50} (µM)	Expression system	Transport or K_m (µM)	Inhibition or IC_{50} (µM)	Expression system
PAH	3.9 - 9.3 22	+	*Oocytes* *OK cells*	87.2	+	*Oocytes*
ES	– (mOAT1)		*Oocytes*	3.1 2.2 / 7.5	+ 	*Oosytes* *Mouse PTC*
DHEA-S				+	+	*Oocytes*
Estradiol glucuronide		– (rOAT1)	*LLC-PK1*	+		*Oocytes*
PGE_2	– 0.97	 +	*HeLa cells* *Mouse PTC*	+ 0.35	 +	*Oocytes* *Mouse PTC*
PGF_2	 0.58	– +	*HeLa cells* *Mouse PTC*	 1.09	 +	 *Mouse PTC*
Taurocholate		+	*Oocytes*	+	+	*Oocytes*
Ochratoxin A	 0.42		 *Mouse PTC*	+ 0.75		*Oocytes* *Mouse PTC*
Glutarate	10.7	4.9	*CHO cells*	+	+	*Oocytes*
α-KG	+		*HeLa cells*			
Urate	– 943	– / +	*Oocytes* *Mouse PTC*	+		*Oocytes*
Methotrexate	– 553.8	–	*HeLa cells* *Mouse PTC*	10.9 21.1		*Oocytes* *Mouse PTC*
Cimetidine		+	*Mouse PTC*	57.4	+	*Oocytes*
Bumetanide		+	*Oocytes*		+	*Oocytes*
Furosemide		+	*Oocytes*		+	*Oosytes*
HCTZ		–	*Oocytes*			

Table 1.3: The interaction of hOAT1 and hOAT3 with (and affinities to) some of their typical substrates. Meaning of the abbreviations: PAH, *p*-aminohippurate; ES, estrone sulfate; α-KG, α-ketoglutarate; PGE_2, prostaglandin E_2; $PGF_{2\alpha}$, prostaglandin $F_{2\alpha}$; HCTZ, hydrochlorothiazide; PTC, proximal tubule cells. If the compound was not tested with human OAT1 or OAT3, then data on its interaction with a homologue from another species is given.

Some examples of common substrates (together with affinities, if they are known) for hOAT1 and hOAT3 are given in the Table 1.3. Among these are the mycotoxin ochratoxin A and prostaglandins PGE_2 and $PGF_{2\alpha}$, which have been found to have the high affinities for hOAT3 and hOAT1 (Jung *et al* 2001, Kimura *et al* 2002). However, in another study hOAT1 did not transport PGE_2 and was not inhibited by $PGF_{2\alpha}$ (Lu *et al* 1999). The reason for this discrepancy is not known. The dicarboxylate glutarate is another example of common substrates for both basolateral carriers, although the affinity of hOAT3 for glutarate was not determined, while for hOAT1 the K_m for glutarate was around 10 µM (Cihlar and Ho 2000). Conflicting results were reported concerning the ability of OAT1 to transport the organic anion urate. The human OAT1 as well as its rat homologue was found to transport urate in some studies (Ichida *et al* 2003, Sekine *et al* 1997), but not in others (Cihlar *et al* 1999, Sweet *et al* 1997). hOAT3 has been shown to mediate uptake of urate in hOAT3-expressing oocytes in one study (Cha *et al* 2001). Thus, the question of involvement of both OATs to proximal tubule urate secretion remained to be elucidated. No data existed concerning the ability of hOAT1 and hOAT3 to translocate diuretics. Although inhibition of carrier-mediated transport by the loop diuretics furosemide and bumetanide had been shown for hOAT1 (Hosoyamada *et al* 1999, Lu *et al* 1999, Race *et al* 1999) and hOAT3 (Cha *et al* 2001), these drugs were not directly tested as substrates. Only the rat OAT1 homologue has been shown not only to be inhibited by acetazolamide, thiazides and loop diuretics, but to actually translocate furosemide, though not the others (Uwai *et al* 2000). Thus, the role and contribution of hOAT1 and hOAT3 to the process of diuretics secretion is not clear.

1.4 Aims of the present study

The present study focused on hOAT3, with the primary aim to establish the mode of operation of hOAT3. Therefore, using *Xenopus laevis* oocytes as an expression system, hOAT3-mediated organic anion transport was studied in the uptake and efflux directions. A next focus was the sensitivity of hOAT3 for urate. Finally, hOAT3 was compared to hOAT1 with respect to interaction with diuretics and it was investigated whether both transporters could also translocate these drugs.

2 MATERIALS

2.1 Oligonucleotide Primers

Sequence specific primers for RT-PCR, sequence analysis and for site-directed mutagenesis were obtained from IBA or MWG Biotech and are listed in Table 2.1

Primer name	Primer sequence	Primer use
hOAT3(283)F	CAATGCCTCCACAGGGCCTTG G	hOAT3-specific RT-PCR primer
hOAT3(365)F	AATGCCAGCCTGCCCAATGAC	hOAT3-specific RT-PCR primer
hOAT3(1540)R	GAAGGGCTGTACCTCACCCGT G	hOAT3-specific RT-PCR primer
hOAT3(778)F	CACCTTTGGCCAGTTCATTCTG	hOAT3-specific RT-PCR primer
hOAT3(1199)R	GGAGGATGTAGAGGTTGACTC C	hOAT3-specific RT-PCR primer
5'RACE-hOAT3(304)R	CCAAGGCCCTGTGGAGGCATT G	hOAT3-specific 5'RACE primer
5'RACE-hOAT3(383)R	CATTGGGCAGGCTGGCATTGG	hOAT3-specific 5'RACE primer
5'RACE-hOAT3(511)R	GAAGATAGACTGGGCCATCTC C	hOAT3-specific 5'RACE primer
3'RACE-hOAT3(1240)F	CACCATCCTCTCCTTAAGCTAC	hOAT3-specific 3'RACE primer
3'RACE-hOAT3(1519)F	CACGGGTGAGGTACAGCCCTT C	hOAT3-specific 3'RACE primer
QoQi-dT	CGCAGATGTACGTCCTACCAT CGC-CTCTAGACCAGCCTACGAGC(T)17	Universal RACE "anchor" primer
Qo	CGCAGATGTACGTCCTACCAT CGCC	Universal RACE "nested" primer
Qi	ATCGCCTCTAGACCAGCCTAC GAGC	Universal RACE "nested" primer
hOAT3(cl)-F	GCTTGCTCGAGCTGAGCTGCC CTAC	hOAT3-specific primer for the amplification of full-length clone
hOAT3(cl)-R	ACGGGTACCGATGTCGAC(T)1 5	hOAT3-specific primer for the amplification of full-length clone
hOAT3-P22A(F)	CCAGTTCCTGCATGTAGCCAT ACT-GGGCCTC	Forward primer for the generation of the hOAT3 P22A point mutation
hOAT3-P22A(R)	GAGGCCCAGTATGGCTACATG CAG-GAACTGG	Reverse primer for the generation of the hOAT3 P22A point mutation
hOAT3-K271E(F)	CTGGAAAGTCCTCGGAGGCCC	Forward primer for the

	TGA-AGATAC	generation of the hOAT3 K271E point mutation
hOAT3-K271E(R)	GTATCTTCAGGGCCTCCGAGG ACT-TTCCAG	Forward primer for the generation of the hOAT3 K271E point mutation
M13forward	GTAAAACGACGGCCAGT	Vector specific
M13reverse	GGAAACAGCTATGACCATG	Vector specific
T7	TAATACGACTCACTATAGGG	Specific for T7 RNA polymerase promoter
SP6	ATTTAGGTGACACTATAG	Specific for SP6 RNA polymerase promoter

Table 2.1: Oligonucleotide primers used in this study. F stands for forward; R stands for reverse; cl – stands for cloning.

2.2 Chemicals

All chemicals used in this study were obtained from Merck, Sigma, Boehringer, Serva, Roth or Applichem, unless otherwise stated in the text. Radioactively labeled chemicals were obtained from PerkinElmer or ICN Biomedicals.

2.3 Enzymes

Taq DNA polymerase was purchased from Promega GmbH. The restriction endonucleases were purchased from New England Biolabs® Inc (Beverly, MA, USA) or MBI Fermentas (Vilnius, Lithuania). T4 DNA ligase was purchased from Boehringer Mannheim (Mannheim, Germany). Calf intestinal alkaline phosphatase (CIP) was purchased from New England Biolabs® Inc (Beverly, MA, USA). Collagenase CLS II was purchased from Biochrom KG (Berlin, Germany).

2.4 Plasmid vectors

pCMV-SPORT6 vector

The hOAT3 cDNA sequence was obtained from the Resource Center/ Primary Database (RZPD, Deutsches Ressourcenzentrum für Genomforschung GmbH, Berlin), clone IMAGE: 5184914 (5'), GenBank accession number BI760120, in the cloning vector pCMV-SPORT6. The expression vector pCMV-SPORT6 is 4396 bp in length. It contains multiple cloning sites. The hOAT3 cDNA was cloned by EcoRV site at the 5' end (EcoRV site was destroyed), and Not1 restriction site at the 3' end. The map of the pCMV-SPORT6 vector is shown in the Figure 2.1.

pCR®2.1 vector

For the cloning and sequencing of PCR products, vector pCR®2.1 (Invitrogen™ life technologies) was used. The vector consists of 3929 bp. It contains T7 RNA polymerase promoter, necessary for in vitro transcription, a multiple cloning site (polylinker), containing sites for different restriction endonucleases, and primer sequences (universal and reverse primers), necessary for DNA sequencing. The PCR products can be inserted in the linearized vector, which has single, overlapping deoxythymidine (T) residues. The pCR®2.1vector map is shown in the Figure 2.2.

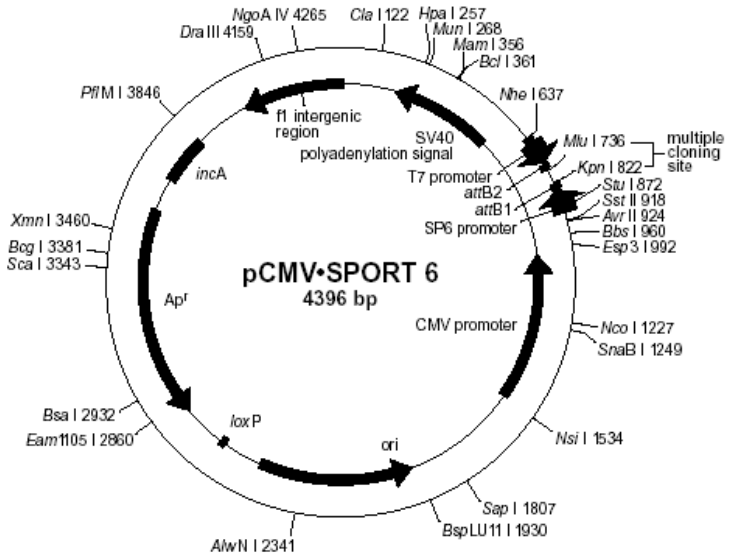

Figure 2.1: Structure of the pCMV-SPORT6 vector. The vector contains a CMV promoter upstream of the *att*B1 site followed by restriction endonuclease sites and *att*B2. Downstream of the *att*B2 sequence is the SV40 small t-intron and polyadenylation signal. This vector contains the SP6 and T7 RNA polymerase promoters flanking the *att*B1 and *att*B2 sites, respectively; pUC origin of replication, and F1 intergenic region, and an ampicillin resistance marker. From the MGC (Mammalian Gene Collection) web-page http://mgc.nci.nih.gov/Vectors/

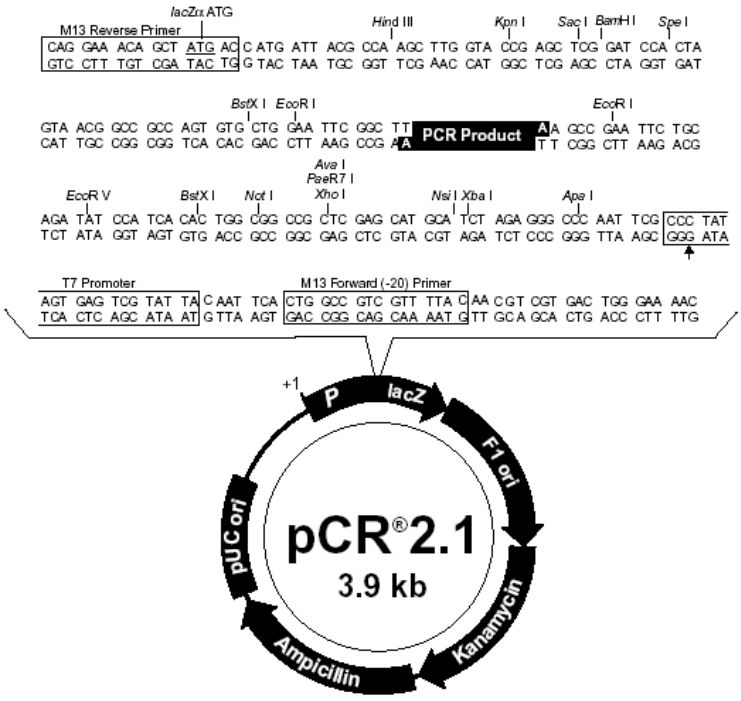

Figure 2.2: Structure of the plasmid pCR®2.1. The vector contains two origins of replication, f1 and pUC, the ampicillin and kanamycin resistance genes for antibiotic selection, and the LacZ gene encoding β-galactosidase for blue/white color selection of recombinant colonies. The multiple cloning sites are flanked by T7 promoter and by the sequences for universal and reverse sequencing primers. *From the Invitrogen™ web-page: http://www.invitrogen.com*

pcDNA3.1/myc-His(-) vector

pcDNA3.1/*myc*-His(-) A, B, and C (Invitrogen™ life technologies) are 5.5 kb vectors designed for expression of recombinant proteins in mammalian cell lines. The vectors are supplied in three reading frames to facilitate in frame cloning. Its C-terminal peptide contains a polyhistidine metal-binding tag (that permits purification of recombinant protein on metal-chelating resin) and the *myc* epitope (that allows detection of recombinant protein with Anti-*myc*-antibody). The human cytomegalovirus immediateearly (CMV) promoter provides high-level expression in a wide range of mammalian cells.

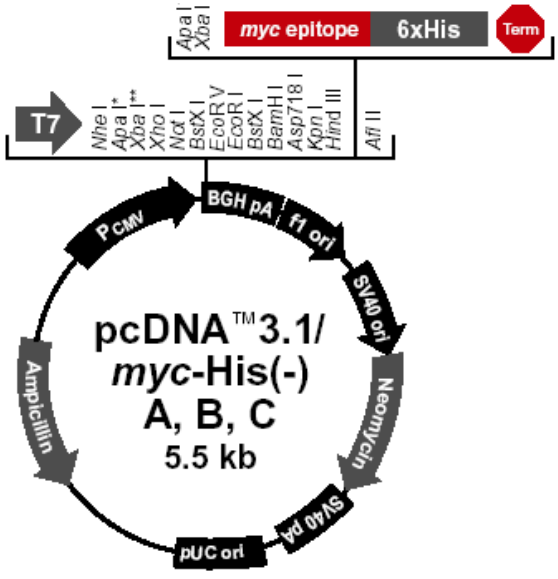

Figure 2.3. Structure of the plasmid pcDNA3.1/*myc*-His(-)A,B,C. The vector contains two origins of replication, f1 and pUC; the ampicillin resistance gene for antibiotic selection in *E.coli*; neomycin (Geneticin®) resistance gene for selection of transfectants in mammalian cells. The multiple cloning site is flanked by T7 promoter and by BGH reverse priming site. *From the Invitrogen™ web-page: http://www.invitrogen.com*

2.5 Bacteria

Bacteria strains used for maintenance of plasmid constructs are listed in the Table 2.2.

strain name	company	genotype
XL1-Blue	Stratagene	*recA1, endA1, gyr96, thi-1, hsdR17, supE44, relA1,lac* [F' *proAB lacI*^{q}*ZΔM15* Tn10(Tet^r)]^c
INVaF'	Invitrogen	F', *end*A1, *rec*A1, *hsd*R17(r_k^-,m_k^+), *sup* E44, *thi*-1, *gyr*A96, *rel*A1, ø80*lac* ZΔM15, Δ(*lac*ZYA-*arg*F)U169λ$^-$
TOP10F'	Invitrogen	F'{*lac*I^{q}Tn*10*(Tet^R)}, *mcr*A, Δ(*mrr-hsd*RMS-*mcr*BC), ø80*lac* ZΔM15, Δ*lac*X74, *rec*A1, *ara*D139, Δ(*ara-leu*)7697,*gal* U, *gal* K, *rps* L (Str^R) *end*A1, *nup*G

Table 2.2: Bacterial (E.coli) strains used in the study.

2.6 Kits

All kits used are listed in Table 2.3 below

Application	Kit	Manufacturer
Nucleic acid purification	MinElute Gel Extraction Kit	QIAgen (Hilden, Germany)
	QIAquick PCR Purification Kit	
	QIAprep Spin Miniprep Kit	
	NucleoSpin Plasmid Kit	Macherey-Nagel (Düren, Germany)
	NucleoSpin Extpact Kit	
PCR cloning	TA Cloning Kit	Invitrogen (Carlsbad, CA, USA)
Mutagenesis	QuikChange Site-directed Mutagenesis Kit	Stratagene (La Jolla, CA, USA)
CDNA cynthesis	CDNA Cycle Kit	Invitrogen (Carlsbad, CA, USA)
CRNA synthesis	T7 mMessage mMachine Kit	Ambion (Austin, TX, USA)
	SP6 mMessage mMachine Kit	

Table 2.3: Kits used in this study.

2.7 Software

Software		
Program	Use	Reference
Chromas	sequence reading program	Technelysium Pty Ltd
Generunner	primer design	Hastings Software Inc
Microsoft Excel	evaluation of uptake and efflux experiments	Microsoft Corporation
SigmaPlot	enzyme kinetic	Jandel Corporation
InStat	statistical analyses	GraphPad Software Inc
Reference Manager	managing of bibliographic references	Wintertree Software Inc
Online sequence analysis servers		
Program	Use	Reference
Entrez Browser	sequence retrieval	http://www.ncbi.nlm.nih.gov/Entrez/
MAP	multiple sequence alignments	http://genome.cs.mtu.edu/map.html
TopPred 2	secondary structure prediction	http://www.biokemi.su.se/~server/toppred2/
Webcutter	restriction maps	http://www.medkem.gu.se/cutter/
Translation tool	N sequence to aa sequence	http://www.expasy.ch/tools/dna.html
Blast	Sequences alignments	http://www.ncbi.nlm.nih.gov/BLAST/

Table 2.4: Software used in this study.

2.8 Equipment

All equipment are listed in table 2.5 below

Appliance	Model	Manufacturer
Automated DNA sequencer	ABI Prism	Applied Biosystems (Laguna Beach CA, USA)
Centrifuges	Biofuge fresco	Heraeus (Osterode, Germany)
	5417R	Eppendorf (Hamburg, Germany)
Circulating water baths	D8	Haake (Karlsruhe, Germany)
Dissection microscope	Stemi1000	Zeiss (Jena, Germany)
Gel chamber	Midi	MWG-Biotech (Ebersberg, Germany)
Gel documentation	Gel Print 2000 I	Biophotonics (Ann Arbor, MI, USA)
Electroporator	Easyject	Equibio (Monchelsea, England)
Microwave	Privileg 8017	Quelle Schikedanz (Fürth, Germany)
Nanoliter injector		World Precision Instruments (Sarasota FL, USA)
pH meter	pH-Meter 611	Orion Research Inc (Beverly MA, USA)
Power pack	P24	Biometra (Göttingen, Germany)
	LKBBromma2297	Pharmacia (Uppsala, Sweden)
Scintillation counter	1500 Tri-Carb	Packard Instrument Co (Meriden CT,USA)

	2100 TR	Packard Instrument Co (Meriden CT,USA)
Shaking incubator	3031	GFL (Burgwedel, Germany)
Spectrophotometer	GeneQuant II	Pharmacia (Uppsala, Sweden)
Speed vacuum concentrator	SVC 100E	Savant (Holbrook NY, USA)
Thermocycler	PTC-200	MJ Research (Watertown MI, USA)
UV transilluminator	TM40	UVP Inc (Upland, CA, USA)
Vortexer	MS1	IKA (Staufen, Germany)

Table 2.5: Equipment used in this study.

3 METHODS

3.1 Molecular Biological Methods

3.1.1 Site-Directed Mutagenesis

The QuikChange™ Site-Directed Mutagenesis Kit (Stratagene) was the method of choice for the introduction of single base mutations into hOAT3-RZPD clone and generation of the restriction enzyme recognition sites. The QuikChange kit allows site-specific mutation in any double-stranded plasmid, thus eliminating the need for subcloning into M13-based bacteriophage vectors and for ssDNA rescue. The basic procedure involves a double-stranded DNA (dcDNA) vector with an insert of interest and two synthetic oligonucleotide primers containing the desired mutation. The oligonucleotide primers, each complementary to opposite strands of the vector, extend during temperature cycling by means of *Pfu* DNA polymerase. This generates a mutant plasmid with staggered nicks, and the template can be removed by digestion with *Dpn*I (a methylation-dependent endonuclease, with reacts only with the methylated template plasmid isolated from bacteria, target sequence: 5'-G^{m6}ATC-3'). The nicked vector DNA incorporating the desired mutation can be then transformed into E. coli, where the nicks are repaired.

Reagents used

Pfu DNA polymerase	2.5 U/µl
10x reaction buffer	100 mM KCl, 100 mM $(NH_4)_2SO_4$, 200 mM Tris-HCl (pH8.8), 20 mM $MgSO_4$, 1% Triton X-100, 1 mg/ml BSA
Oligonucleotide primers	Forward and reverse primers, specific for each mutation, 125 ng/µl
dNTP mix	Composition not supplied by manufacturer
Dpn I restriction enzyme	10 U/µl
Competent cells	Epicurian Coli XL1-Blue supercompetent cells, 50µl
SOC medium	10 mM NaCl, 2.5 mM KCl, 10 mM $MgCl_2$, 10 mM $MgSO_4$, 20 mM Glucose, 2% Tryptone, 0.5% Yeast Extract

For introducing of each specific mutation, the mutagenic oligonucleotide primers were designed individually according to the desired nucleotide base substitution. The following consideration was taken for designing mutagenic primers: both primers contained the desired mutation and annealed to the same sequence on opposite strands of the plasmid; they were between 30 and 45 bases in length with the melting temperature (T_m) of around 78°C; the desired nucleotide base substitution was situated

in the middle of the primer with approximately 15 bases of correct sequence on both sides; primers had a minimum GC content of 40% and terminated in C or G bases. All primers, used for mutagenesis are listed in Table. The cycling reaction mix consisted of 5µl of 10x reaction buffer, 40 ng of template plasmid (4µl of 10ng/µl diluted plasmid DNA), 125 ng of each oligonucleotide primer, 1µl of dNTP mix, 1µl of *Pfu* DNA polymerase (2.5 U/µl) and ddH_2O was added to a final volume of 50µl. Cycling parameters were: 95°C for 30 seconds, followed by 16 cycles of: 95°C for 30 seconds, 55°C for 1 minute, and 68°C for 2 minutes per 1 kb of plasmid length. Following temperature cycling, the reaction was placed on ice for cooling to less than 37°C. Afterwards, the template DNA was digested by adding of 1µl of the *Dpn* I restriction enzyme (10 U/µl) to amplification reaction and incubation at 37°C for 1 hour. Once *Dpn* I digestion was complete, 1 µl of the extension mix was added to pre-thawed Epicurian Coli® XL1-Blue super-competent cells, gently mixed and incubated on ice for 30 min. The cells were then exposed to a 45 seconds heat shock at 42°C, and then transferred immediately on ice. After 2 minutes incubation on ice, 450 µl SOC medium was added and the tube with cells were shaken horizontally at 37°C at 220 rpm for 1-2 hours. Afterwards, 200 µl aliquot was spread on a pre-warmed LB agar plate, supplemented with antibiotics specific for the plasmid used (routinely ampicillin) and incubated at 37°C overnight. On the following day colonies, containing insert, were picked and cultured in LB medium (overnight). Plasmid DNA was isolated and sequenced to verify the presence of desired mutation.

3.1.2 cDNA Synthesis

Reagents used

Total RNA in sterile water	1-2µg
Oligo dT primer	1µl
RNase inhibitor	10 U/µl
5x RT buffer	375 mM KCl, 15 mM $MgCl_2$, 250 mM Tris-HCl (pH8.3)
dNTP mix	100 mM of each dATP, dCTP, dGTP, dTTP
Sodium pyrophosphate	80 mM
AMV Reverse Transcriptase	10 U/µl

First-strand cDNA was synthesized from total human kidney RNA for use as a template in subsequent Polymerase Chain Reaction (PCR). Synthesis was carried out using the cDNA Cycle® Kit (Invitrogen™ Life Technologies), according to the manufacturer's protocol. 1-2µg of the total RNA was diluted in the RNase-free tube in sterile water to

the total volume of 11.5 µl. After addition of 1 µl of Oligo dT Primer, the vial was heated in a 65°C water bath for 10 minutes for removing of secondary structure, and then placed at room temperature for 2 minutes. To collect the reaction mixture the vial was shortly centrifuged and the following reagents were added in the order listed: 1 µl of RNase inhibitor, 4 µl of 5x RT buffer, 1 µl of dNTPs, 1 µl of sodium pyrophosphate and 0.5 µl of AMV reverse transcriptase. The solution was mixed by tapping the tube, collected on the bottom by short centrifuging and the tube was placed in a water bath for 60 minutes. After completion of reverse transcription, the solution was placed to 95°C for 2 minutes for denaturation of RNA-cDNA hybrids. Before freezing and storing, the cDNA was purified by phenol extraction and ethanol precipitation. Therefore, 1µl of 0.5 M EDTA (pH 8.0) and 20 µl of phenol-chloroform was added to the tube, mixed and centrifuged for 3 minutes. The top aqueous layer, containing cDNA, was carefully removed and placed into a new, sterile tube. Next, 22 µl of ammonium acetate, 1 µl of a 2 mg/ml glycogen solution and 88 µl of ethanol was added, mixed by vortexing and frozen in dry ice for 10 minutes. After thawing, cDNA was collected by centrifuging at 4°C at maximum speed for 15 minutes. The supernatant was removed and the pellet was resuspended in 20 µl of sterile water. The purified cDNA was stored at -20°C for future use in PCR reactions.

3.1.3 Polymerase Chain Reaction

The PCR technique was used for amplification of hOAT3 cDNA. Polymerase Chain Reaction is the enzymatic method of making multiple copies of pre-selected segment of DNA. The basic components of the reaction are: the cDNA template, containing the sequence of interest; two synthetic oligonucleotide primers, designed with homology to the 5' and 3' ends of the target sequence; four deoxyribonucleoside triphoshpates (dNTPs); thermostable DNA polymerase and the buffer, usually containing Mg^{2+}. The reaction mixture are undergoes the temperature cycling. Cycling begins with heating to 95°C, with is required for the denaturation of the DNA template. Then it is rapidly cooled to the temperature necessary for the annealing of the oligonucleotide primers to their target on the single-stranded template. The primers annealing temperature (T_m) depends on their length and nucleotide base composition. After annealing, the temperature goes to 72°C, optimal for the functioning of DNA polymerase, which extends the primers at their 3'-ends. Since the 3'-ends of the primers directed towards each other, repeated cycles of heating and cooling lead to the chain reaction, an exponential synthesis of many copies of the specific segment of interest. After cycling,

the PRC results usually visualized by an agarose gel electrophoresis, purified with the help of adequate PCR-purification kits and analyzed by sequencing.

3.1.3.1 Standard RT-PCR

For amplification of hOAT3 cDNA fragments, primers were designed on the basis of the published human sequence (nucleotides 1 to 2179, GenBank accession number AB042505). For the primer design, the regions were chosen that indicated both greatest homologies between OAT3s from different species whilst at the same time maximal divergence from the OAT1s.

Reagents used

Template	1 µl of cDNA, reverse transcribed with Oligo dT Primer
Forward Primer	20 pmol
Reverse Primer	20 pmol
5x PCR Buffer	2 µl (50 mM KCl, 10 mM Tris, pH 9.0, 1.5 mM $MgCl_2$, 0.1% Tritone-X-100)
dNTPs	200 µM of each
DNA Polymerase	Takara Tag, 1U
Nuclease-free H_20	To a final volume of 20 µl

The thermo-cycling parameters were: 94°C for 1 minute followed by 15 cycles with comprised: 94°C for 30 seconds, 61°C (-0.4°C per cycle) for 45 seconds, and 72°C for 1 minute; followed by 15 cycles of: 94°C for 30 seconds, 55°C for 45 seconds, and 72°C for 1 minute; and finally 72°C for 7 minutes. The PCR fragments obtained were purified and cloned into pCR™II and sequenced.

3.1.3.2 Rapid amplification of cDNA ends (RACE)

The RACE (rapid amplification of cDNA ends) technique was used to amplify 5' and 3'-ends of hOAT3 cDNA. The basic principles of this method are following. From the already known internal stretch of sequence gene-specific primers are chosen, that are oriented in the direction of the missing sequence. Extension of the partial cDNAs from the unknown end of the message back to the known region is achieved using primers that anneal to the preexisting poly(A) tail (3'-end) or an appended homopolymer tail (5'-end).

3' RACE

To generate "3' end" partial cDNA clone, mRNA was reverse transcribed using the universal RACE "anchor" primer (QoQi-dT) that consists of 17 nucleotides of oligo(dT)

followed by a unique 35-base oligonucleotide sequence (QoQi; table 2.2). Amplification was than performed using a primer containing part of the “anchor” sequence (Qo) and a primer derived from the gene of interest gene specific primer 1 (GSP1). To quench the amplification of nonspecific products, a second set of amplification cycles was then carried out using “nested” primers Qi and GSP2.

Reagents used

	First amplification set	Nested amplification set
Template	cDNA, reverse transcribed with QoQi-dT primer	1 µl initial PCR reaction
Primer	Q_O, 200 ng	Qi, 200 ng
Gene-Specific Primer	GSP1, 200 ng	GSP2, 200 ng
5x PCR Buffer		
dNTPs	200 µM	200 µM
DNA Polymerase	Takara Tag, 1U	Takara Tag, 1U

For amplification of 3’-end of hOAT3, in the first nest reaction as primers were used universal RACE primer Qo and GSP1 (3’RACE-hOAT3(1240)F primer, specific for hOAT3). Thermo-cycling conditions for first stage PCR were: 35 cycles of 94°C for 20 seconds, 65°C for 30 seconds and 72°C for 1.5 minute. For the second nested PCR were used universal “nested” RACE primer Qi and GSP2 (3’RACE-hOAT3(1519)F primer, specific for hOAT3). 1 µl of initial PCR reaction was used as a template for the “nested” reaction. The cycling conditions were the same as used for the initial stage. The product of reaction was cloned into pCR™II vector and sequenced.

5’ RACE

Reagents used

	Synthesis of poly(A) tail	
Template	50ng cDNA, reverse-transcribed with random hexanucleotides	
dATP	200 µM	
Terminal Transferase	15 U	
RNase-free Water	To 20 µl of total volume	
	First amplification set	Nested amplification set
Template	Tailed first-strand cDNA,	1 µl initial PCR reaction
Primer	QoQi-dT, 20 ng and Q_O, 200 ng	Qi, 200 ng
Gene-Specific Primer	So, 200 ng	Si, 200 ng
5x PCR Buffer		
dNTPs	200 µM	200 µM
DNA Polymerase	Takara Tag, 1U	Takara Tag, 1U

To isolate the 5' end of a cDNA, reverse transcription was carried out using random hexanucleotides (Invitrogen™ life technologies) to generate first-strand product. Then, a poly(A) tail was appended using terminal deoxynucleotidyltranserase (TdT) and dATP. Amplification was then achieved using the hybrid "anchor" primer (QoQi-dT) to form second strand of cDNA, the Qo primer and the gene specific primer oriented in the 5'-end direction (So). Finally, a second set of PCR cycles was carried out using nested primers (Qi and Si) to increase specificity. The conditions for the tailing reaction were: 10 minutes at 37°C and then 15 minutes at 65°C, necessary for inactivation of enzyme. In the first stage reaction the primers used were: "anchor" primer QoQi-dT, universal RACE primer Qo and gene-specific primer So (5'RACE-hOAT3(383)R, specific for hOAT3). Thermo-cycling conditions for first stage PCR were: 3 cycles of 94°C for 20 seconds, 42°C for 2 minutes and 72°C for 3 minutes; followed by 35 cycles of 94°C for 20 seconds, 65°C for 20 seconds and 72°C for 1.5 minutes. The second "nested" PCR was carried out with 1 µl of initial PCR reaction, universal "nested" RACE primer Qi and sequence-specific primer Si (3'RACE-hOAT3(511)R, specific for hOAT3). The cycling conditions were: 35 cycles of 94°C for 20 seconds, 65°C for 20 seconds and 72°C for 1.5 minutes. The product of reaction was cloned into pCR™II vector and sequenced.

3.1.3.3 Amplification of full-length clone

Based on the RT-PCR data, sequence-specific primers (with restriction sites incorporated) were designed for PCR- amplification of the full-length hOAT3 clone from human kidney cDNA. The amplification reaction composition was as for usual PCR. The template was cDNA synthesized using the "anchor" (QoQi-dT) primer. The thermocycling parameters were: 94°C for 2 minutes; 10 cycles of 94°C for 20 seconds, 58°C for 30 seconds and 72°C for 2 minutes; followed by 20 cycles of 94°C for 20 seconds, 58°C for 30 seconds, and 72°C for 2 minutes + 5 seconds per each next cycle; followed by a final extension period of 10 minutes at 72°C. The required extension time was empirically calculated from the expected product length. The full-length cDNA was cloned into pCR™II vector and sequenced.

3.1.4 The TA Cloning

To clone RT-PCR products the TA Cloning® Kit (Invitrogen™,) was used. This system is designed for cloning PCR products into bacteria directly from a PCR reaction without the need for modifying enzymes, purification, or restriction digestion. The TA Cloning® vector, pCR™II, contains the lacZ-alpha complementation fragment for blue-white color

screening, ampicillin and kanamycin resistance genes for selection, and a versatile polylinker (more detailed vector data is given in the material section). The method relies on the nontemplate-dependent activity of *Taq* DNA polymerase, which adds a single deoxyadenosine (A) to the 3' ends of the PCR products. The linearized pCR™II vector contains 3' deoxythymidine (T) overhangs, which allows the PCR-product to ligate efficiently with the vector. The system is also supplied with the OneShot™ module, which contains all of the reagents necessary for transformation.

Reagents used

pCR™II, linearized	25 ng/µl
10x Ligation Buffer	60 mM Tris-HCl (pH7.5), 60 mM $MgCl_2$, 50 mM NaCl, 1mg/ml BSA, 70 mM β-mercaptoethanol, 1 mM ATP, 20 mM dithiothreitol, 10 mM spermidine
T4 DNA Ligase	4.0 U/µl
Sterile water	
OneShot competent cells	Competent *E-coli* TOP10F' or INVαF' cells, in 50 µl aliquots
β-mercaptoethanol	0.5 M
SOC Medium	2% Tryptone, 0.5% Yeast Extract, 10 mM NaCl, 2.5 mM KCl, 10 mM $MgCl_2$, 10 mM $MgSO_4$, 20 mM glucose

The fresh PCR-products were separated and visualized by gel electrophoresis; the bands of interest were excised from the gel and extracted using the NucleoSpin® Gel Extraction kit (Macherey-Nagel) or the MinElute™ Gel Extraction kit (Qiagen). After purification and quantification, the ligation reaction was set, that consisted of: the required amount of PCR product (usually no more then 1-2 µl); 1 µl of 10x ligation buffer, 2 µl (50 ng) of pCR™II vector, sterile water to the total volume of 9 µl and 1 µl of T4 DNA ligase. The reaction was incubated at 14°C for a minimum of 4 hours, or (preferably) overnight. After incubation, 1-3 µl of the ligation product and 1 µl of β-mercaptoethanol were added to the pre-thawed OneShot competent cells (50 µl aliquot) and gently stirred with a pipette tip. The cells were then incubated for 30 min on ice, exposed to a 45 seconds of heat shock at 42°C, and immediately placed on ice for 2 minutes. The 450 µl of the SOC medium (room temperature) was added to the vial, and it was incubated for 1-2 hours at 37°C at 220 rpm in a shaking incubator. The aliquots of 50 and 200 µl were plated on LB agar plates, containing 0.4% X-gal and 50 µg/ml ampicillin, and incubated overnight at 37°. The next day, the single white colonies were picked for plasmid isolation and restriction analysis (for determination the presence and orientation of insert).

3.1.5 cRNA Synthesis

cRNAs for the oocyte microinjection were synthesized by means of the T7 mMESSAGE mMACHINE kit (for hOAT1 in pSport1 plasmid) or SP6 mMESSAGE mMACHINE kit (for hOAT3 in pSport6 plasmid). These kits enable the synthesis of large amounts of capped RNA from a linearized cDNA template, by incorporation of cap analog (m_7G(5')ppp(5)'G) during polymerization reaction.

Reagents used

10x Enzyme Mix	A combination of bacteriophage T7 or SP6 RNA polymerase, ribonuclease inhibitor and other unlisted components
10x Transcription Buffer	T7 or SP6 Reaction Buffer, composition not provided by manufacturer
2x Ribonucleotide Mix	T7 kit: 15 mM ATP, CTP, UTP, 3mM GTP and 12 mM Cap Analog; SP6 kit: 10 mM ATP, CTP, UTP, 2mM GTP and 8mM Cap Analog
DNase I	Rnase-free (2 U/µl), supplied in 50% glycerol buffer
Template DNA	Linearized with *Not*I restriction enzyme
Precipitation solution	7.5 M LiCl, 75 mM EDTA

Before cRNA synthesis, the double-stranded DNA template should be digested to completion with a suitable restriction enzyme that cleaves distal to the promoter, downstream of the insert to be transcribed. In both cases (hOAT1 and hOAT3) *Not*I was the restriction enzyme of choice. The composition of digestion reaction was: 5µg of template cDNA, 3 µl of 10x NEBuffer 3 (100 mM NaCl, 50 mM Tris-HCl, 10 mM $MgCl_2$, 1 mM dithiothreitol, pH 7.9 at 25°C), 3 µl of 10x BSA (to final concentration of 100µg/ml), 2.5 µl of 10U/µl *Not*I restriction enzyme (5-fold overdigest condition) and H_2O to a final volume of 30µl. Digestion was carried out at 37°C for 3 hours, and its efficiency was checked on agarose gel. The linearized product was purified by ethanol precipitation, re-suspended in 10µl of nuclease-free H_20 and measured for the DNA concentration. For the cRNA synthesis, transcription reaction was assembled at room temperature, and consisted of: 2µl of 10x reaction buffer, 10 µl of 2x ribonucleotide mix, 1 µg of linear template DNA, 2µl of enzyme mix, and nuclease-free H_2O to a final volume of 20µl. The reaction was incubated at 37°C for 2 hours, after with template DNA was removed by the addition of 1 µl Rnase-free DnaseI and incubation at 37°C for 15 minutes. Following incubation, the synthesized cRNA was precipitated by adding of 30 µl of nuclease-free H_2O, 25 µl of LiCl precipitation solution, and chilling the sample at -20°C for at least 2 hours. Afterwards, the cRNA was collected by centrifugation for 30 min at 4°C, 2 times washed and re-centrifuged with 1 ml of 70%

ethanol. After removal of the ethanol, the cRNA was dried at room temperature for ~ 20 minutes and re-suspended in 15 µl of nuclease-free H_2O. The concentration was determined and adjusted to either 0.87 µg/µl (20 ng of cRNA in 23 nl) or 1.3µg/µl (30 ng of cRNA in 23 nl). The cRNA samples were stored at -80°C.

3.1.6 DNA-modifications

3.1.6.1 Restriction digestion

Restriction digestion was used as a part of subcloning procedure and for linearization of .cDNA template in the procedure of site-directed mutagenesis.

Reagents used

DNA template	1-5µg
10x Enzyme Buffer	10% v/v; composition depends on enzyme used
100x BSA	1% v/v; added when necessary for enzyme activity
Restriction Enzyme	2-5 U/µg DNA; less then 10% of the final reaction volume
Nuclease-free H_20	Up to required volume

After setting, the reaction was incubated at 37°C for 1-4 hours, depending on efficiency of enzyme used. The completion of digestion was controlled on the gel electrophoresis.

3.1.6.2 Dephosphorylation

To prevent recirculation of cloning vectors after cutting with restriction endonucleases, they were treated with Calf Intestinal Alkaline Phosphatase (CIP). This enzyme catalyzes the removal of 5'-phosphate groups from nucleic acids; therefore since CIP-treated fragments lack the 5'-phosphoryl termini required by ligases, they cannot self-ligate.

Reagents used

Vector DNA	1-5µg
1x NEBBufer 3	100mM NaCl, 50mM Tris-HCl, 10mM $MgCl_2$, 1mM dithiothreitol (pH 7.9 at 25°C)
CIP	1 U/µg vector DNA
Nuclease-free H_20	Up to required volume

Following restriction, vector DNA was first precipitated with ethanol, and then treated with CIP (optimal conditions) or 1µl of CIP was directly added to the restriction reaction mix and incubated for 1 hour at 37°C. Dephosphorylated vector was then purified by gel purification or spin-column purification and used in a standard ligation reaction.

3.1.6.3 Ligation

T4 DNA ligase was used for joining DNA fragments with compatible cohesive ends generated by restriction digestion or by RT-PCR. For its catalytic activity the enzyme requires the presence of ATP and Mg^{2+}.

Reagents used

Vector DNA	~100ng
DNA to be inserted	50-150ng (the amount was calculated my the formula below)
10x ligation buffer	1µl (66 mM Tris-HCl, 5 mM $MgCl_2$, 1 mM dithiothreitol 1 mM ATP (pH 7.5)
T4 DNA Ligase	1µl (4U/µl)
Sterile H_20	Up to total volume of 10 µl

The amount of DNA insert needed for to ligate with 100ng of vector reaction was estimated using the formula: X (ng) of insert = (Ybp of insert * 100ng of vector)/(size in bp of the vector), where X ng is the amount of insert of Y base pairs to be ligated for a 1:1 molar ration. Routinely, 1:3 (vector: insert) ratio was used for better yield of ligation. After mixing the ligation reaction was incubated at 14°C for a minimum 4 hours (preferably overnight). Afterwards, 1-3 µl aliquot was used for the transformation procedure (section 3.2.1).

3.1.7 DNA isolation and purification

3.1.7.1 Agarose gel electrophoresis

Agarose gel electrophoresis was used for visualization or/and isolation of DNA after PCR amplification or restriction digestion. Agarose gels were from 0.7% to 1.5%, depending on the size of the DNA molecule to be separated. Agarose was dissolved in TBE buffer (45 mM Tris, 45 mM borate, 1 mM EDTA) by heating in a microwave for ~ 1 minute. After cooling to 60-70°C, 10mg/ml ethidium bromide solution was added to a final concentration of 0.5 µg/ml, mixed thoroughly, and the solution was immediately poured into the mold. Gel was completely set after 30-45 minutes at room temperature and run at 60-100 V for 1-2 hours, depending on the size if the DNA molecules to be separated. Results of electrophoresis were visualized using Dual Intensity Ultraviolet Transilluminator (UniEquip) and photo-documented. Required DNA fragments were excised with a scalpel from gel, and isolated using the NucleoSpin® Gel Extraction kit (Macherey-Nagel) or the MinElute™ Gel Extraction kit (Qiagen), according to the protocols.

3.1.7.2 Isolation of plasmid DNA

E.coli colonies, transformed with plasmid of interest (as described in section 3.2.1), were cultured overnight in 5-7 ml of LB medium (10 g/l trypton, 5 g/l yeast extract, 10 g/l NaCl, pH adjusted to 7.3 with NaOH, medium sterilized by autoclaving), containing 100µg/ml ampicillin. Cells from 3-6 ml of culture, depending on culture density, were harvested by centrifugation. Plasmid DNA was isolated by the principle of SDS/alkaline lysis, according to the manufacturer's instructions (NucleoSpin Plasmid kit; Macherey-Nagel). Therefore, the cells were resuspended in 250 µl of buffer A1, containing Rnase, and lysed by addition of 250 µl of A2 buffer, containing SDS. Once lysis had occurred, 300 µl of neutralizing buffer A3 was added and mixed until formation of precipitate. Afterwards the SDS precipitate and cell debris were pelleted by centrifugation at maximum speed for 10 min, and the supernatant was loaded onto a NucleoSpin Plasmid column. Contaminations were washed away by centrifuging first with 500 µl of pre-warmed to 50°C AW buffer and then 600 µl of ethanol-containing buffer A4. The remaining ethanol was removed by additional centrifugation for 2 minutes and drying at 37°C for 5 minutes. Finally, plasmid DNA was eluted with 50 µl of buffer AE (5 mM Tris-HCl, pH 8.5) by centrifuging the column for 1 minute.

3.1.7.3 Ethanol precipitation

Precipitation with ethanol was used as the rapid technique for concentrating nucleic acids. Therefore 3M sodium acetate (pH 5.2) to a final concentration of 0.3 mM and 2.5 volumes of ice-cold ethanol were added to the DNA solution. After mixing the ethanolic solution was placed on -20°C for 15-30 minutes to allow precipitation of DNA. Afterwards DNA was recovered by centrifugation at 4°C at maximum speed for 20 minutes and supernatant was carefully removed without disturbing the pellet of nucleic acid. Pellet was washed 2 times by recentrifuging with 250 µl of 70% ethanol at 4°C at maximum speed for 5 minutes, and dried at room temperature or 37°C until the last traces of fluid have evaporated. DNA was dissolved in the desired volume of Nuclease-free water or TE buffer (pH 8.0).

3.1.8 DNA sequencing and Analysis

The sequencing was performed by dye terminator cycle sequencing method (Applied Biosystems), according to the manual. In this method a premix solution, containing four didesoxynucleotides (ddNTPs), each labeled with a different fluorescent dye, and unlabeled desoxynucleotides was mixed with the template DNA and one sequencing primer. Therefore in the sequencing reaction DNA fragments of different size labeled at

their 3'-ends with base specific fluorescent dyes were synthesized. After ethanol precipitation and denaturation, the probes were loaded on the gel (4.75% polyacrylamide DNA sequencing gel) and electrophoretically separated in the sequence service laboratory. The fluorescence of dye-containing polynucleotides was stimulated by 40 mW argon laser (488 nm and 514 nm) and the fluorescent signal was identified by the detector system of the DNA sequencer (automatic sequencer: ABI Prism, Applied Biosystems) and quantificated.

Composition of sequencing reaction

DNA template	300-400 ng
Primer	10 pmol
Sequencing premix	2.5 µl (Ready Reaction BigDye Terminator Kit: AmpliTag® DNA polymerase FS, thermostabile pyrophosphate, dNTPs, dITP, BigDye labeled ddNTPs and buffer with not specified composition (PE Biosystems)
HPLC H_2O	Up to 10 µl volume

The sequencing reaction comprised 25 cycles of: 96°C for 10 seconds, 50°C for 15 seconds and 60°C for 4 minutes. After completing of reaction, amplification products were precipitated by addition of 1 µl of 3M Na Acetate and 50 µl of 95% ethanol, followed by centrifugation for 20 minutes at 14000 U. Supernatant was discarded carefully, without disturbing the pellet. Afterwards the product was washed with adding of 250 µl of 70% ethanol and centrifugation for 10 minutes at 14000 U. Supernatant was removed completely and pellet was dried in the vacuum dessicator (Speedy Vac) for 3 minutes and finally resuspended in 25 µl of HPLS H_2O. The sequence was assembled and analyzed with various software packages, as listed in Table 2.5. Sequence homology searches were performed using the BLAST network service.

3.2 Cell Biological Methods

3.2.1 Transformation of competent E. coli cells

3.2.1.1 Electroporation

Electrocompetent cells were prepared according to the manufacturer's protocol and stored at -80°C. Electroporation was carried out using the electroporator (EasyjecT Prima®, Equibio). The output voltage was set at 2500 V. After defrosting the 40 µl aliquot of electrocompetent cells, 1 to 2 µl of ligation mix was added to it, mixed and kept on ice for 1 minute. Then the cell suspension was loaded into pre-chilled 2 mm cuvette and electroporation was done by triggering the pulse. The cells were

immediately cooled on ice for 1 minute and 450 µl of SOC was added. For selection of antibiotic-resistance, the cells were incubated at 37°C for 1-2 hours in shaking incubator. After incubation, 50 and 200 µl aliquots were plated on LB agar plates, containing 0.4% X-gal and 50 µg/ml ampicillin and incubated overnight at 37°C.

3.2.1.2 Heat chock

The chemycompetent cells (Invitrogen) were transformed according to the standard protocol. After thawing the 50 µl aliquot of competent cells, 1-3 µl of the plasmid DNA was added to them, mixed and the cells suspension was incubated for 30 min on ice. The cells were then exposed to a 45 seconds of heat shock at 42°C water bath, and immediately placed on ice for 2 minutes. The 450 µl of the SOC medium was added to the vial, and transformants were elaborated for 1-2 hours at 37°C at 220 rpm in a shaking incubator. The aliquots of 50 and 200 µl were plated on LB agar plates, and incubated overnight at 37°C.

3.2.2 Expression of OATs in Xenopus laevis oocytes

Xenopus laevis oocytes were used for functional characterization hOAT3 and hOAT1. Therefore, oocytes were injected with cRNA synthesized from the cDNA of interest and, after 3 days of expression period, uptake or efflux assays were carried out as described below. The schematic representation of the oocyte assay system is shown on Figure 3.1.

3.2.2.1 Preparation of oocytes

Reagents used

Barth's	88 mM NaCl, 1 mM KCl, 0.3 mM $Ca(NO_3)_2$, 0.41 mM $CaCl_2$, 0.82 mM $MgSO_4$, 15 mM HEPES, 12 µg/ml gentamycin, pH set at 7.6 with NaOH
ORI (oocyte Ringer's solution)	90 mM NaCl, 3 mM KCl, 2 mM $CaCl_2$, 1 mM $MgCl_2$, 5 mM HEPES, pH set at 7.6 with 1 mM Tris

Individual stage V-VI oocytes were defolliculated by collagenase treatment. It involved overnight incubation of several ovarian lobes in 20 ml Barth's solution containing 0.5 mg/ml collagenase (Type CLSII, Biochrom KG) at 18°C. On the following day, oocytes were washed several times with oocyte Ringer's solution (ORI), incubated for 10 min in Ca^{2+} free medium and then washed again 2-3 times with ORI solution. Oocytes were sorted and the "healthy" looking oocytes were used for the cRNA injection.

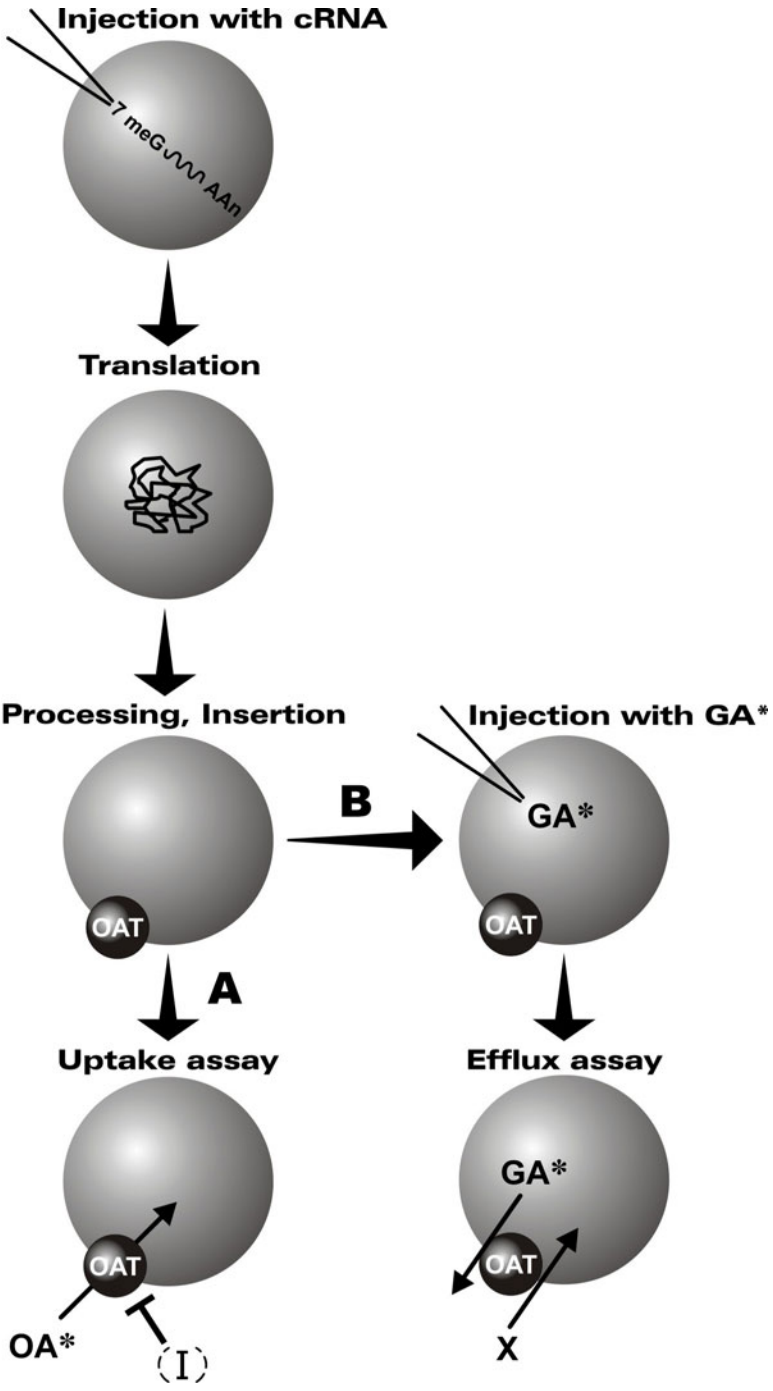

Figure 3.1. Schematic representation of the oocyte assay system. *Xenopus laevis* oocytes are injected with in vitro synthesized cRNA, with cap and poly-A tail. Then follows the expression period, necessary for translation of the polypeptide encoded by the cRNA, its processing and insertion into membrane. On the 3rd day, the functions of transporter could be studied by: (A) uptake assay, when the uptake of radioactively labeled substances (OA*) in the absence or presence of inhibitor compounds (I) is or (B) efflux assay, when oocytes injected with radioactively labeled substances, here it is glutaric acid (GA*), and then trans-stimulation of GA efflux by different compounds (X) from the extracellular is measured.

3.2.2.2 Oocyte Injection

cRNA were injected into the oocyte cytoplasm using a nanoliter microinjector with glass capillaries (Word Precision Instruments). Oocytes were injected with 20-30 ng of cRNA in a 23-46 nl volume, or the equivalent volume of water as a control. Oocytes were arranged on a specially designed plastic support chamber with grooves to facilitate the injection process. Injection was carried out in ORI solution, and upon injection, the oocytes were incubated for three days at 18°C in Barth's solution. On the third day after injection, surviving oocytes were sorted to remove unhealthy or maturated oocytes and used for transport assays.

3.2.2.3 Uptake Experiments

The selected oocytes were divided into groups of 8-11 and after equilibration in ORI medium, transferred to a 10 ml vial with 1 ml of ORI uptake medium, containing radioactively labeled substrate. Radio-labeled substances used were: [^{3}H]ES (0.44 µCi/ml) (estrone sulfate, ammonium salt, [6,7-^{3}H(N)]-, 40-60 Ci/mmol), [^{3}H]PAH (5 µCi/ml) (aminohippuric acid, *p*-[glycyl-2-^{3}H]-, 1-5 Ci/mmol, NEN), [^{14}C]glutaric acid (2.5 µCi/ml) (glutaric acid, [1,5-^{14}C]-, 30.8 mCi/mmol, ICN), or [^{14}C]α-KG (2.5 µCi/ml) (ketoglutaric acid, sodium salt, α-[^{14}C(U)]-, 273.1 mCi/mmol). For the ion dependence studies, the uptake medium was of altered composition, as detailed in results. For *cis*-inhibition studies, a stock solution of each potential inhibitor was made in ORI. Uptake was assayed at room temperature for time periods of 5 minutes to 1 hour, as required. After completion of the incubation period, the uptake was terminated by aspiration of the incubation medium and 3 x 4 ml washes with ice-cold ORI buffer. Individual oocytes were then transferred to 5 ml scintillation vials and each was dissolved in 100 µl of 1 N NaOH for 2 hours and, after neutralization with 100 µl of 1 N HCl and addition of 2.5 ml Lumasafe scintillation fluid (Lumac-LSC), the ^{3}H or ^{14}C content was assayed in a scintillation counter over 10 minutes.

3.2.2.4 Efflux Experiments

For measurements of [^{14}C]GA efflux, oocytes, expressing hOAT3 or hOAT1, were injected, using a nanoliter microinjector, with 2.6 nCi [^{14}C]glutarate corresponding to 84 pmol glutarate in a volume of 23 nl (the procedure of injection was the same as for injection with cRNA as described above). On the basis of an average oocyte diameter of 1.3 mm and a free cellular water volume of 35% (Horowitz and Miller 1984), this would approximate an intracellular concentration of 200 µM. After injection, oocytes were individually placed in 100 µl of the same basic buffer as that used for uptake

medium without or with compound to be tested for trans-stimulation. After an initial period of 2 minutes, during which oocytes showed a highly variable leak because of the injection, medium was changed on the 100 µl of same new buffer, and the efflux then assayed over the following 28 minutes. At the end of the efflux period, the aspirated buffers from 2 and 28 minutes efflux periods were assayed for ^{14}C content by liquid scintillation counting, and oocytes were dissolved as before to determine the remaining [^{14}C]glutarate content. Total glutarate injected was calculated from glutarate remaining in the oocytes plus total efflux.

3.2.3 Expression of OATs in T-REx™-HEK293 cells

3.2.3.1 Cultivation of T-REx™-HEK-293 cells

The Tetracycline-Regulated Expression (T-REx™) HEK293 cells, stably expressing OAT1 or hOAT3 were used for radioactive uptake inhibition studies as an expression system, alternative to *Xenopus laevis* oocytes. Originally, the T-Rex cells were designed for using with the T-REx™ System (Invitrogen, Life Technologies) and they stably express the tetracycline (Tet) repressor. These T-REx™-HEK293 cells were stably transfected with hpcDNA6/TR-based expression constructs, containing OAT1, hOAT3 or only vector (negative control), and the dual selection made with Geneticin® and blasticidin by Dr. Ugele, Universitäts-Frauenklinik, München.

Reagents used

T-REx culture medium	DMEM high glucose, 2mM L-glutamine, 1% Pen/Strep stock solution, 10% heat-inactivated FCS, 5 µg/ml blasticidin
"Milieu C"	1 mM EGTA, 85 mM NaCl, 17.5 mM $NaHCO_3$, 3.9 mM KCl, 0.8 mM KH_2PO_4 and 10 mM glucose
Freezing medium	45% of complete medium, 45% of conditioned medium (medium one day feed by the cells) and 10% DMSO
Polylysine solution	0.1 ml polylysine per 1 ml PBS
PBS buffer	0.9% NaCl, 10 mM sodium phosphate buffer, pH 7.2

Cells were cultivated routinely in T-REx culture medium, and passaged 1:5 every forth or fifth day. Before splitting, medium was removed and cells were rinsed once with PBS. Then, 2.5 ml of pre-warmed EGTA-containing "milieu C" was added per 25 cm^2-flask. After incubation at 37°C for 2-3 minutes (time required for detachment the cells from the plate), 2.5 ml of complete medium per 25 cm^2-flask was added and the cell suspension was transferred into a sterile 15 ml Falcon tube. The cells were collected by centrifugation at room temperature at 1000 rpm for 5 minutes. Supernatant was

aspirated and cells were resuspended 1:2 in fresh complete medium, counted using the Hemacytometer (before the counting, 20 µl of cell suspension was diluted with 180 µl of medium for better accuracy) and seeded in the required density. Because of the property of the HEK293 cells to easily come off the plate, culture dishes were coated with polylysine (Sigma). Therefore, 200 µl of polylysine solution was pipetted onto each well of 24 well plates shortly before seeding and aspirated after a few minutes. Cells were seeded directly onto the polylysine-wet surface. For using in transport experiments cells were plated into the 24 well plates at the density of approximately 2 x 10^5 cells per well 1 day before transfection.

3.2.3.2 Radioactive uptake into the cells

For the uptake experiments, confluent cell cultures were used. Therefore cells were cultured in 24-well plates for at least 48 hours before the beginning of transport studies.

Regents used

Mammalian Ringer solution	130 mM NaCl, 4 mM KCl, 1 mM $CaCl_2$, 1 mM $MgSO_4$, 20 mM HEPES, 1 mM NaH_2PO_4, 18 mM glucose, pH 7.4
Radio-labeled substrates	[^{3}H]ES (0.44 µCi/ml) (estrone sulfate, ammonium salt, [6,7-^{3}H(N)]-, 40-60 Ci/mmol) and [^{3}H]PAH (5 µCi/ml) (aminohippuric acid, *p*-[glycyl-2-^{3}H]-, 1-5 Ci/mmol, NEN),

Directly before uptake, cells were washed three times with 1 ml of mammalian Ringer solution, pre-warmed to 37°C. The transport media was pre-warmed mammalian Ringer solution, containing radioactively labeled substance (10 µM [^{3}H]PAH or 50 nM [^{3}H]ES) and, in inhibition studies, compound tested for inhibition. The volume of 500 µl of uptake solution was carefully added in each well, not directly on the cells, but on the well wall, not to cause cells detachment. Cells were incubated in the transport media at the room temperature for the required time period (usually 15 min). After finishing the incubation, the uptake was terminated by aspiration of transport solution and washing the cells 3 times with 1 ml of ice-cold Ringer solution. Then 500 µl of 1 N NaOH was added in each well and the plates were incubated in this solution for 1 hour. After complete cells lysis, of 500 µl of 1 N HCl was added for neutralization and the solution was mixed. From this 1 ml of cell lysate, 2x50 µl were transferred into Eppendorf tubes for the subsequent protein estimation using the Bradford method. The Lumasafe scintillation fluid (2.5 ml) was added to the rest 900µl of solution and the ^{3}H content was assayed in a scintillation counter over 10 minutes.

3.3 Statistical analysis

Statistical analysis was performed using the GraphPad InStat program, version 3.00 for Windows 95, GraphPad Software, www.graphpad.com. n is given as the number of experiments on oocytes from different donor animals, with the number of oocytes used per treatment in each individual experiment indicated.

4 RESULTS

4.1 Generation of a functional hOAT3 clone

4.1.1 RT-PCR amplification of human OAT3

4.1.1.1 Standard RT-PCR

As at the beginning of this study no hOAT3 clone was available, a RT-PCR approach was used to isolate hOAT3. First, for amplification of hOAT3 cDNA fragments, hOAT3-specific primers were designed on the basis of the published human sequence (nucleotides 1 to 2179, GenBank accession number AB042505). For the primers, the regions that exhibited both greatest homologies between OAT3s from different species and at the same time maximal divergence from the OAT1s were chosen. A successful amplification was obtained with hOAT3(283)F and hOAT3(1540)R primers. The Figure 4.1.A shows the bands of around 1250 base pairs that were amplified from human kidney cDNA synthesized with “anchor” primer and with oligo-dT primer. The PCR fragments obtained were purified, cloned into pCR^{TM}II and sequenced with vector-specific primers. The coding sequence was identical to the published hOAT3 sequence.

4.1.1.2 5’ and 3’ RACE

The sequence-specific primers for performing the 5’- and 3’-RACE reactions were again designed based on the hOAT3 published sequence. The same strategy as for initial RT-PCR was used for primer design. The 3’-RACE reaction yielded a product of around 660 base pairs (Figure 4.1.B), which was also cloned into pCR^{TM}II and sequenced. The sequence was again identical to the corresponding region of the published hOAT3 sequence and included a polyadenylation signal. With the 5’-RACE reaction, a product of around 300 base pairs was amplified (Figure 4.1.C). After cloning and sequencing, the amplificate was found to be identical to 5’-part of published hOAT3 sequence with additional 12 base pairs of untranslated region at the 5’-end: 5’-AGCTTGTTAGAG-3’

4.1.1.3 Amplification of full-length clone

Based on the 5’ and 3’RACE data, sequence-specific primers where designed for amplification of the entire hOAT3 cDNA sequence from human kidney cDNA. Since the amplification of the full-length clone with proof-reading polymerases was not successful

for unknown reasons, the *Taq*-Polymerase was used to confirm the ability to amplify the right-size product with the primers. chosen Figure 4.1.D shows the product of around 2200 base pairs, which after cloning into the pCR™II vector and sequencing was fund to be hOAT3.

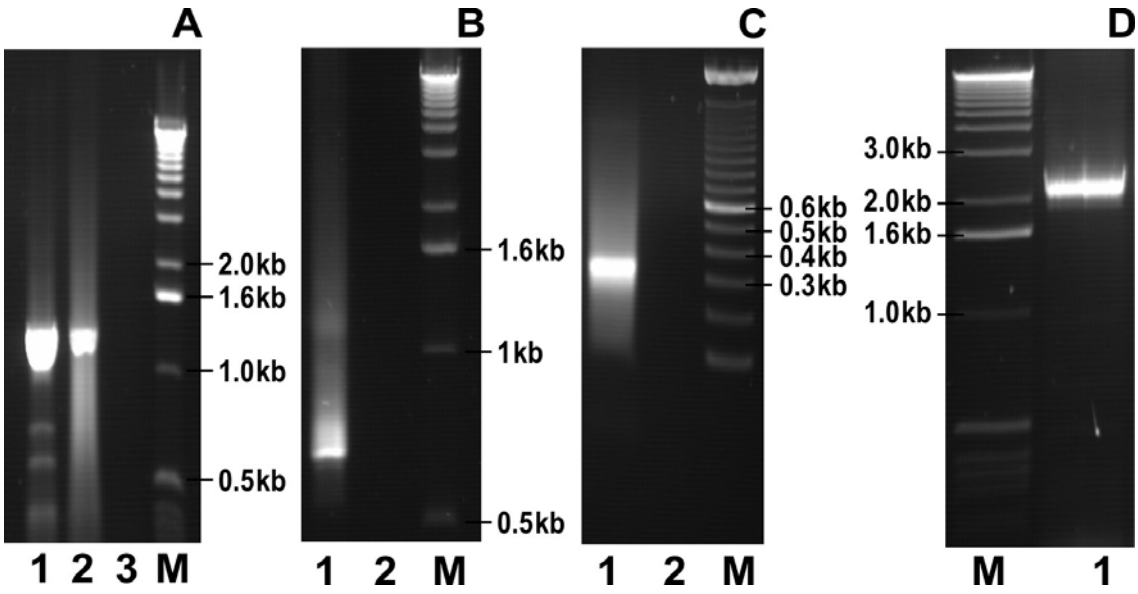

Figure 4.1: Amplification of hOAT3 from human kidney cDNA. A. Initial RT-PCR with hOAT3-specific primers. Lane 1: amplification from cDNA, synthesized with anchor primer; lane 2: amplification from cDNA, synthesized with oligo-dT primer; lane 3: negative control; M: molecular weight markers (kb stands for kilo base pairs). **B.** 3'-RACE. Lane 1: 3'RACE-product; lane 2: negative control; M: molecular weight markers. **C.** 5'-RACE. Lane 1: 5'RACE-product; lane 2: negative control; M: molecular weight markers. **D.** Amplification of the full-length clone. M: molecular weight markers; Lane 1: amplification product.

4.1.2 Analysis and correction of the hOAT3-RZPD clone

In this point in time a hOAT3 clone could be obtained from the Resource Center / Primary Database (RZPD) human cDNA library (IMAGp998L0311461Q2; Gene Bank accession number BI760120). First, the function of this original hOAT3-RZPD clone was investigated by expression in *Xenopus laevis* oocytes. hOAT3-RZPD-cRNA-injected oocytes showed no increase in 10 µM PAH or 10 nM ES uptake as compared with water-injected oocytes (see below). Subsequent comparison of the hOAT3-RZPD clone sequence with the published hOAT3 sequence (Cha *et al* 2001) and our own RT-PCR data revealed two single nucleotide exchanges that resulted in two amino acid exchanges: a proline residue instead of the alanine residue at position 22, and a lysine residue instead of the glutaric acid residue at position 271. The A22P exchange lies in the first predicted trans-membrane domain of the hOAT3 protein.

Figure 4.2 shows an alignment of hOAT3 with its rat and mouse homologues including the deviating amino-acids in the RZPD clone.

```
                *      20      *      40      *      60
    rOAT3  : MTFSEILDRVGSMGPFQYLHVTLLALPVLGIANHNLLQIFTATTPVHHCRPPPNASIGPW :
60
    mOAT3  : MTFSEILDRVGSMGPFQYLHVTLLALPILGIANHNLLQIFTATTPDHHCRPPPNASLEPW :
60
    hOAT3  : MTFSEILDRVGSMGHFQFLHVAILGLPILNMANHNLLQIFTAATPVHHCRPPHNASTGPW :
60
                ----------P---------
                *      80      *     100      *     120
    rOAT3  : VLPLDPNGKPEKCLRFVHLPNASLPNDTQRATEPCLDGWIYNSTRDTIVIEWDLVCSSNK :
120
    mOAT3  : VLPLGPNGKPEKCLRFVHLPNASLPNDTQGATEPCLDGWIYNSTRDTIVTEWDLVCGSNK
: 120
    hOAT3  :
VLPMGPNGKPERCLRFVHPPNASLPNDTQRAMEPCLDGWVYNSTKDSIVTEWDLVCNSNK : 120

                *     140      *     160      *     180
    rOAT3  : LKEMAQSIFMAGILVGGPVIGELSDRFGRKPILTWSYLMLAASGSGAAFSPSLPVYMIFR :
180
    mOAT3  : LKEMAQSVFMAGILVGGPVFGELSDRFGRKPILTWSYLLLAASGSSAAFSPSLTVYMIFR :
180
    hOAT3  : LKEMAQSIFMAGILIGGLVLGDLSDRFGRRPILTCSYLLLAASGSGAAFSPTFPIYMVFR :
180
             ---------------------          ----------------- --
                *     200      *     220      *     240
    rOAT3  : FLCGCSISGISLSTVILNVEWVPTSMRAISSTSIGYCYTIGQFILSGLAYAIPQWRWLQL : 240
    mOAT3  : FLCGCSISGISLSTIILNVEWVPTSTRAISSTTIGYCYTIGQFILPGLAYAVPQWRWLQL : 240
    hOAT3  : FLCGFGISGITLSTVILNVEWVPTRMRAIMSTALGYCYTFGQFILPGLAYAIPQWRWLQL :
240
           ------------------          ----------------------     -
                *     260      *     280      *     300
    rOAT3  : TSSAPFFIFSLLSWWVPESIRWLVLSGKYSKALKTLQRVATFNGKKEEGKKLTIEELKFN :
300
    mOAT3  : SVSAAFFIFSLLSWWVPESIRWLVLSGKFSRALKTLQRVATFNGKKEEGEKLTVEELKFN
: 300
    hOAT3  : TVSIPFFVFFLSSWWTPESIRWLVLSGKSSEALKILRRVAVFNGKKEEGERLSLEELKLN :
300
           ----------          K
                *     320      *     340      *     360
    rOAT3  : LQKDITSAKVKYGLSDLFRVSILRRVTFCLSLAWFSTGFAYYSLAMGVEEFGVNIYILQI :
360
    mOAT3  : LQKDITSAKVKYGLSDLFRVSILRRVTFCLSLAWFATGFAYYSLAMGVEEFGVNIYILQI :
360
    hOAT3  : LQKEISLAKAKYTASDLFRIPMLRRMTFCLSLAWFATGFAYYSLAMGVEEFGVNLYILQI :
360
                          ----------          -----
                *     380      *     400      *     420
    rOAT3  : IFGGVDIPAKFITILSLSYLGRRITQSFLLLLAGGAILALIFVPSEMQLLRTALAVFGKG : 420
    mOAT3  : IFGGVDIPAKFITILSISYLGRRITQGFLLILAGVAILALIFVSSEMQLLRTALAVFGKG : 420
    hOAT3  : IFGGVDVPAKFITILSLSYLGRHTTQAAALLLAGGAILALTFVPLDLQTVRTVLAVFGKG :
420
           ------------          ----------          -----
                *     440      *     460      *     480
    rOAT3  : CLSGSFSCLFLYTSELYPTVLRQTGMGISNVWARVGSMIAPLVKITGELQPFIPNVIFGT :
480
    mOAT3  : CLSGSFSCLFLYTSELYPTVLRQTGMGISNIWARVGSMIAPLVKITGELQPFIPNVIFGT :
480
    hOAT3  : CLSSSFSCLFLYTSELYPTVIRQTGMGVSNLWTRVGSMVSPLVKITGEVQPFIPNIIYGI :
480
           ----------------     ----------          -----
                *     500      *     520      *     540
```

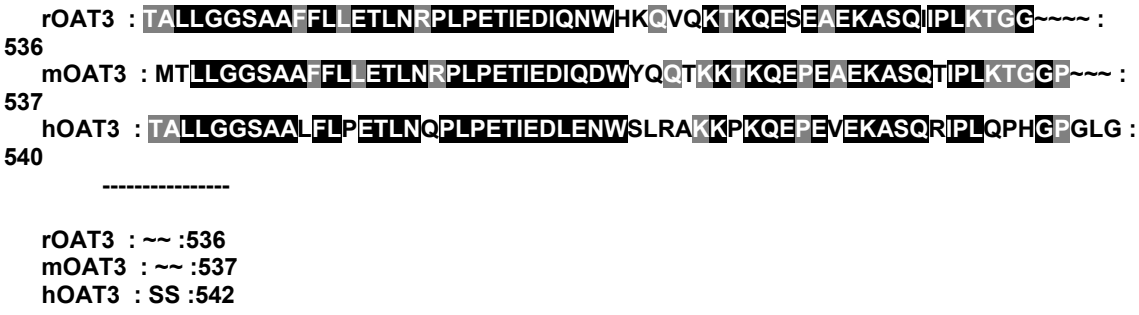

Figure 4.2: Alignment of three OAT3 homologues. Residues shaded in black are those conserved between the human, mouse and rat homologues. Residues shaded in gray are those identical in two of these homologues. Residues in boxes, placed under hOAT3 sequence are those different between published hOAT3 sequence and the hOAT3-RZPD (Resource Center/ Primary Database) clone. Positions of the trans-membrane domains in the hOAT3-protein as predicted by TMpred (Hofmann & Stoffel 1993) with a minimum window setting of 19 amino acids are underlined. The sequence alignment was performed with the PileUp program, Genetics Computer Group Software, GCG, Madison, Wisconsin.

The amino acid exchanges were reversed by site-directed mutagenesis. Single base mutations were introduced one by one into hOAT3 using the QuikChange site-directed mutagenesis kit, as described in Methods. First, the proline 22 was corrected to alanine, and then lysine 271 was corrected to glutaric acid. To verify the corrected clones, both strands of the entire coding region were sequenced by dye terminator cycle sequencing. From the two resulting clones, “partially corrected “(P22A) and “completely corrected” (P22A;K271E), cRNA was synthesized and expressed in oocytes to test the encoded proteins for function. In contrast to original RZPD-hOAT3 clone, both “corrected” hOAT3 clones induced a significant increase in ES and PAH uptake of more then 130-fold and around 4-fold, respectively, compared with water-injected oocytes (Figure 4.3, A and B). All further experiments to functionally characterize hOAT3 were done on the completely corrected hOAT3-RZPD clone.

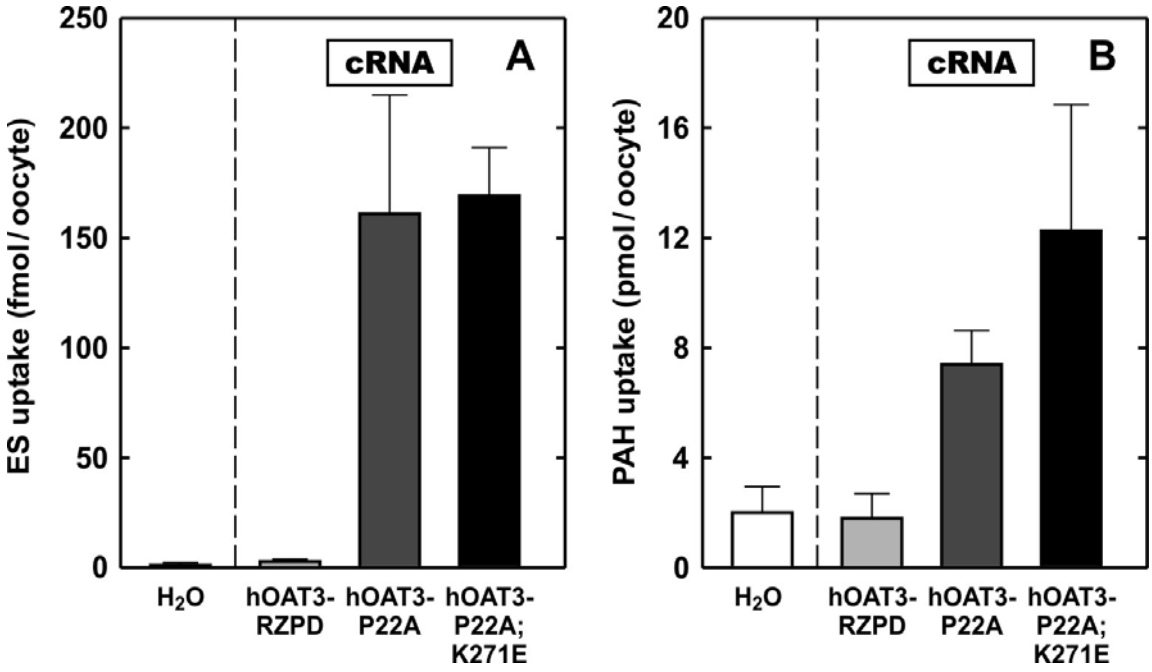

Figure 4.3: Uptakes of ES and PAH by original and corrected hOAT3-RZPD clones. Oocytes were injected with cRNA synthesized from the original RZPD–hOAT3 clone, the “partially corrected” hOAT3 clone P22A, the “completely corrected” clone P22A;K271E-hOAT3 clone, or an equivalent volume of H_2O. After 3 d of incubation, uptake of 10 nM [^{3}H]ES (**A**) or 10µM [^{3}H]PAH (**B**) were assayed for 1 h. Data are expressed in fmol/oocyte (ES) or pmol/oocyte (PAH) as means ± SE of n=4 (ES) or n=3 (PAH) independent experiments, each carried out on 8-11 oocytes per treatment.

4.2 Characterization of hOAT3-mediated transport.

4.2.1 Ion dependence of hOAT3-mediated ES transport

In previous studies on hOAT1, carried out in our laboratory (Wolff *et al* 2003) the hOAT1-mediated PAH uptake was shown to be chloride-dependent: it was decreased by approximately 80% in chloride-free uptake medium. To check whether hOAT3 possesses the same property, ES uptake by hOAT3 was studied in normal ORI medium and in ORI medium in which chloride was replaced with gluconate. As seen in Figure 4.4, hOAT3-mediated ES uptake was decreased by about 60% in chloride-free uptake medium.

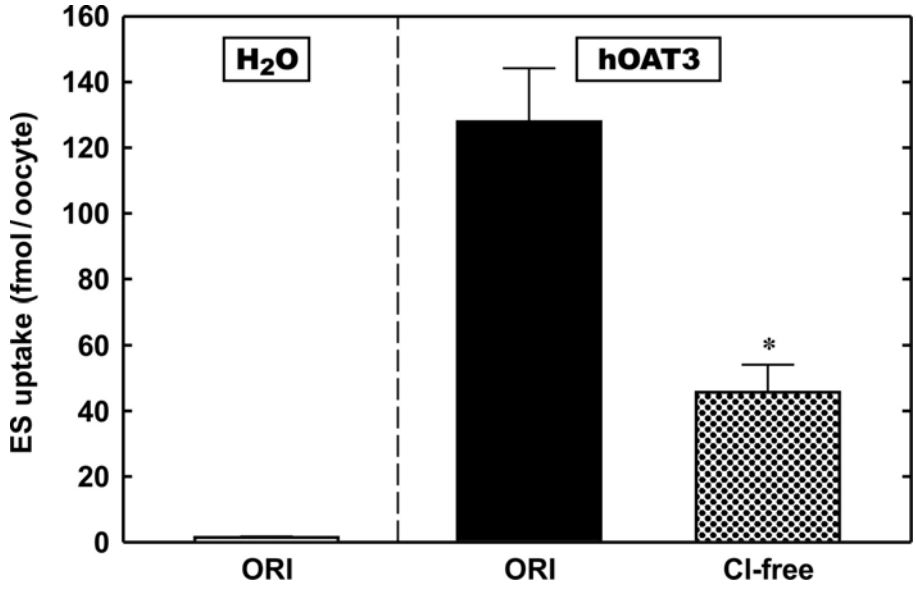

Figure 4.4: The Cl^--dependence of hOAT3-mediated ES uptake. Oocytes were injected with cRNA derived from corrected hOAT3 clone (P22A;K271E) or an equivalent volume of H_2O. After 3 d of incubation, uptake of 10 nM [^{3}H]ES was assayed in the normal transport medium (ORI, control) or in the Cl^--free medium for 1 h. Data are expressed in fmol/oocyte as means ± SE of four independent experiments, each carried out on 8-11 oocytes per treatment. Significance of differences in unpaired Student's t-test of absolute uptake relative to the control is indicated (*: $p < 0.05$)

To study whether hOAT3 can interact with bicarbonate, uptake of ES into hOAT3-expressing oocytes was carried out without or with 25 mM sodium bicarbonate added to the uptake medium (Figure 4.5). Bicarbonate decreased hOAT3-mediated ES uptake by about half of that in normal ORI medium. As a control for potential effects of the increased osmolarity, uptake in one group of oocytes was assayed in the presence of 25 mM sodium methanesulfonate, which did not significantly alter the ES uptake by hOAT3.

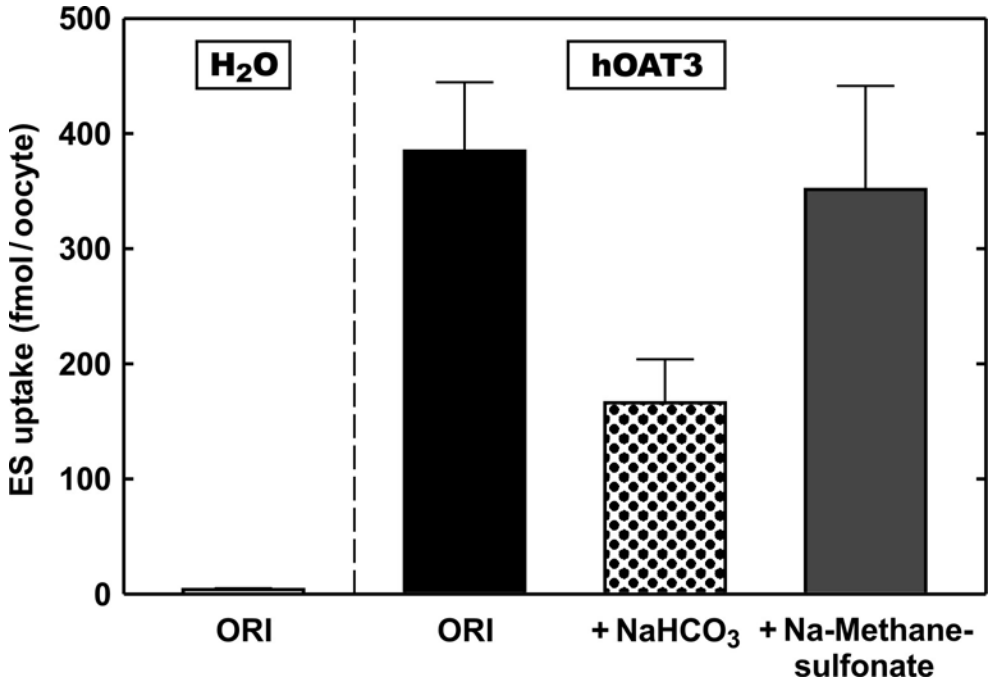

Figure 4.5: Bicarbonate-dependence of hOAT3-mediated ES uptake. Oocytes were injected with cRNA derived from the corrected hOAT3 clone or an equivalent volume of H_2O. After 3 d of incubation, 1 h uptake of 10 nM [^{3}H]ES was assayed in the normal transport medium (ORI), or in the presence of 25 mM $NaHCO_3$ or Na-Methanesulfonate. Data are expressed in fmol/oocyte as means ± SE of two independent experiments, each carried out on 8-11 oocytes per treatment.

4.2.2 Cis-inhibition of hOAT3-mediated ES uptake, and dicarboxylate transport

Several organic anions were tested for their ability to inhibit hOAT3-mediated ES uptake. These include PAH – classical substrate of OAT1; glutarate – a dicarboxylate that was shown to inhibit PAH uptake by hOAT1 by more than 95%; urate - the end product of purine catabolism, and lactate. Therefore, the hOAT3-dependent ES uptake was carried out in the presence of 1 mM of each potential inhibitor. As seen in Figure 4.6, the ES uptake by hOAT3 was greatly reduced by PAH – by about 90%. Glutarate inhibited hOAT3 most potently - by more than 95%. The inhibition by urate was unexpectedly strong – about 85%, whereas in previous studies this anion was inhibiting hOAT1-mediated PAH uptake by less than 50%. Lactate did not significantly alter the hOAT3-mediated ES transport.

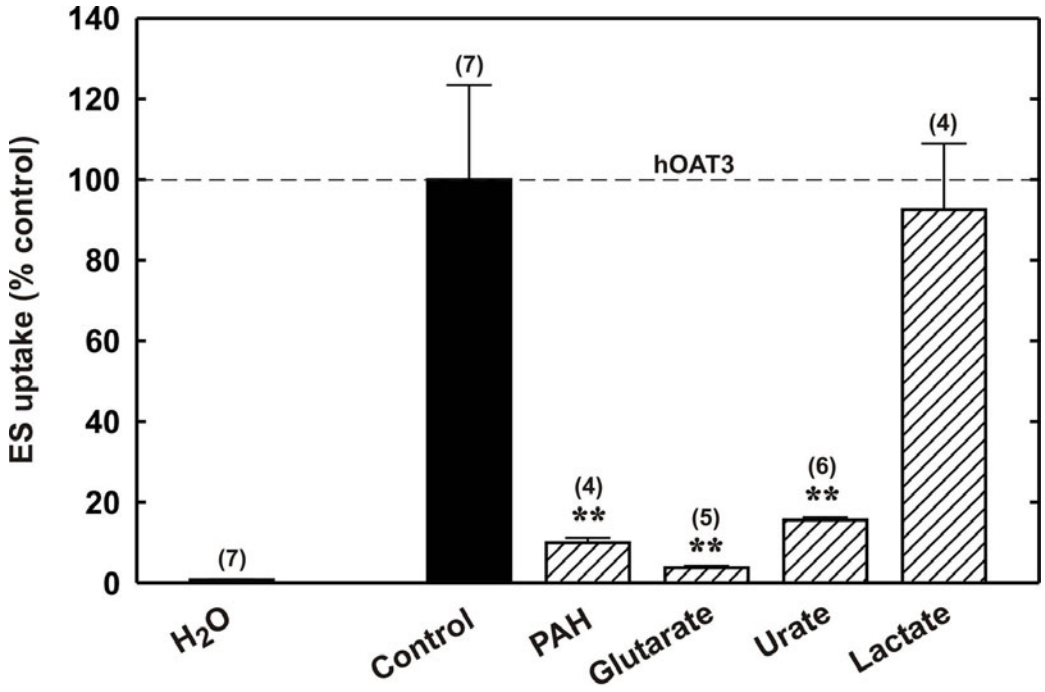

Figure 4.6: Sensitivity of hOAT3-mediated ES uptake to various potential inhibitors. One-hour uptakes of 10 nM [^{3}H]ES into the hOAT3-expressing oocytes were assayed in the absence (control) or presence of 1 mM of organic test ions. Data are expressed in % of the uptake of hOAT3-injected oocytes in the absence of inhibitors as means ± SE of the number of independent experiments given in parentheses, each carried out on 8-11 oocytes per treatment. Significance of differences in unpaired Student's t-test of absolute uptake relative to the control is indicated (*: $p < 0.05$, **: $p < 0.01$).

Since glutarate turned out to be the most potent inhibitor, other dicarboxylates, which could be potential substrates for hOAT3 under physiological conditions were tested for cis-inhibition (Figure 4.7). Of the Krebs-cycle intermediates, α-ketoglutarate (α-KG) reduced ES uptake by hOAT3 most potently – by almost 90%. A similarly strong inhibition by α-KG has previously been observed for hOAT1-mediated PAH uptake (Wolff *et al* 2003). Fumarate and succinate inhibited hOAT3-mediated ES uptake only moderately, yet consistently: fumarate by about 47% and succinate by 30%. Oxaloacetate and the tricarboxylate citrate did not affect ES uptake in hOAT3-expressing oocytes. All the substances tested for inhibition were added at a final concentration of 1 mM to the incubation media. As the ES uptake in oocytes expressing hOAT3 was most greatly inhibited by dicarboxylates with 5 carbons (C-5 dicarboxylates) – glutarate and α-KG – these substances were also tested as substrates for hOAT3. As seen in Figure 4.8, at 100 µM, hOAT3-mediated uptake was indeed observed for both [^{14}C]glutarate - 3.6-fold above H_2O-injected cells, and [^{14}C]α-KG - 3.8-fold above H_2O-injected cells.

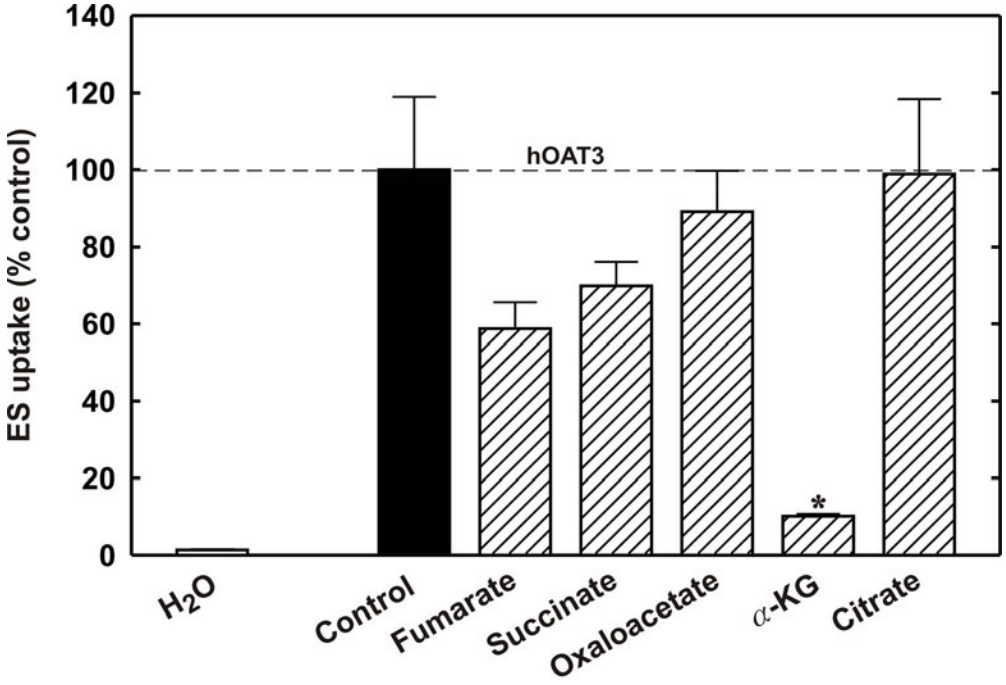

Figure 4.7: Cis-inhibition of hOAT3-mediated ES uptake by Krebs-cycle intermediates. One-hour uptakes of 10 nM [^{3}H]ES into the hOAT3-expressing oocytes were assayed in the absence (control) or presence of 1 mM of organic test ions. Data are expressed in % of the uptake of hOAT3-injected oocytes in the absence of inhibitors as means ± SE of four independent experiments, each carried out on 8-11 oocytes per treatment. Significance of differences in unpaired Student's t-test of absolute uptake relative to the corresponding control is indicated (*: $p < 0.05$)

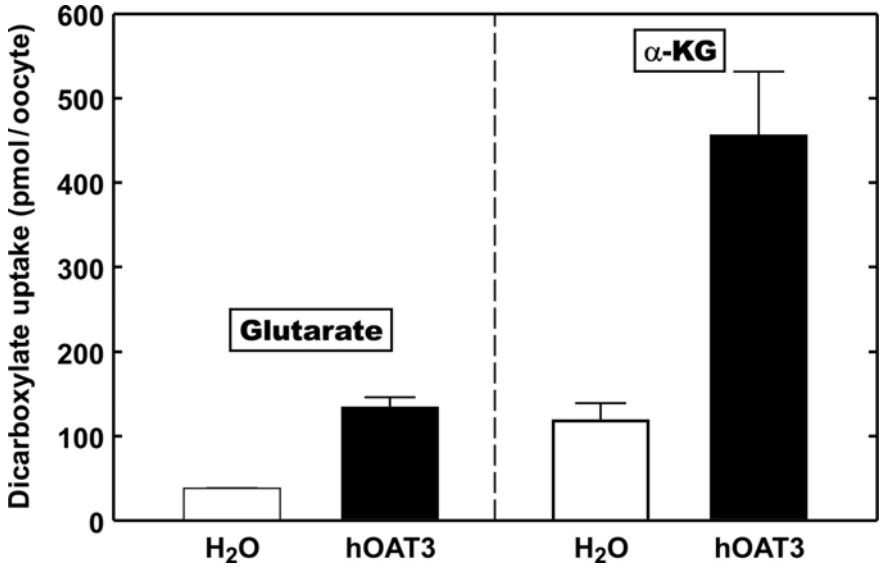

Figure 4.8: Uptake of glutarate and α-KG by hOAT3-expressing oocytes. Oocytes were injected with hOAT3-cRNA or an equivalent volume of H_2O. After 3 d of incubation, uptakes of 100 µM [^{14}C]glutarate or [^{14}C] α-KG were assayed for 1 h. Data are expressed in pmol/oocyte as means ± SE of 9-11 oocytes, one donor.

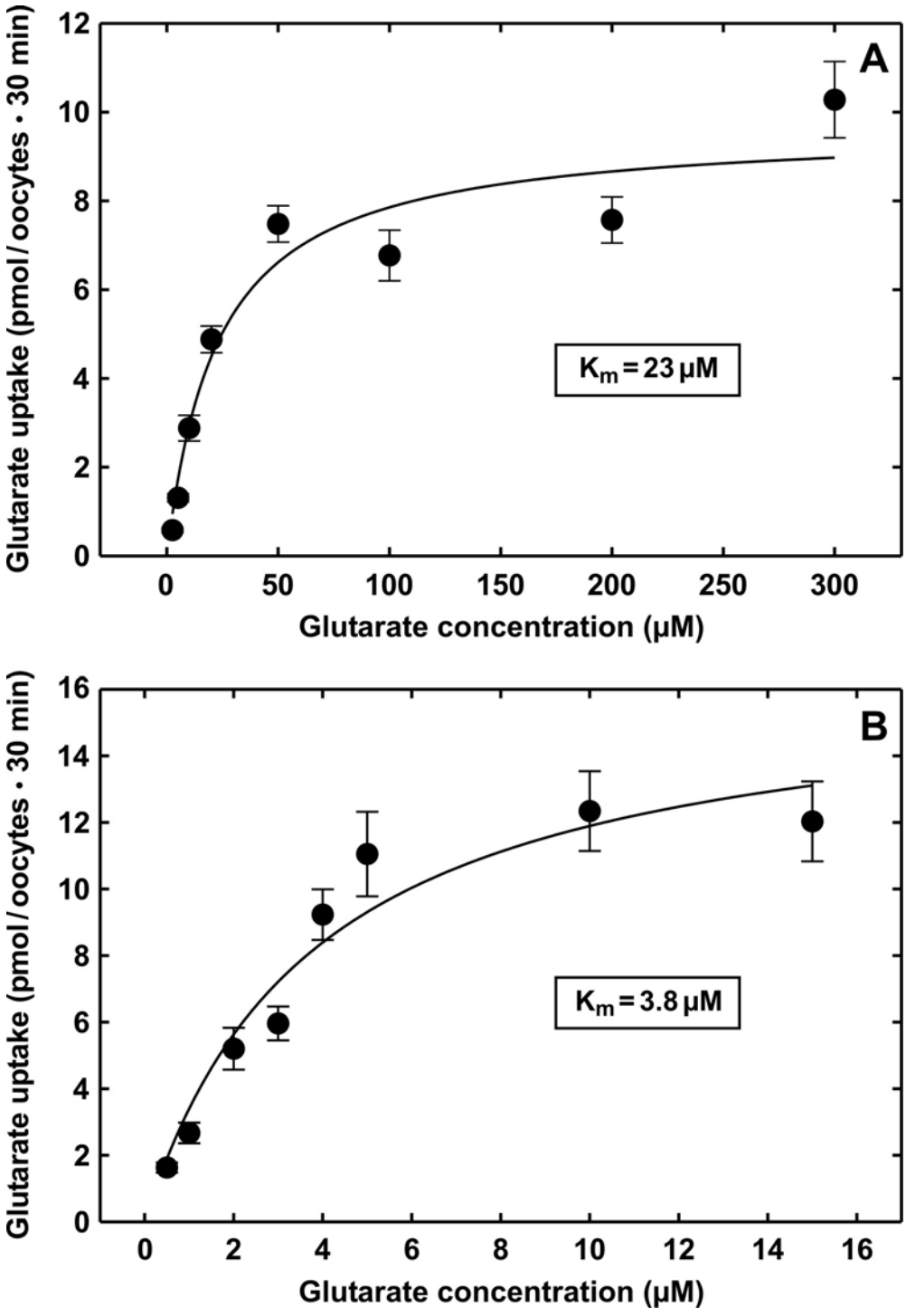

Figure 4.9: Determination of the K_m of hOAT3 (A) and hOAT1 (B) for glutarate. Oocytes were injected with hOAT3 or hOAT1 cRNA or an equivalent volume of H_2O. After 3 d of incubation, 30-min uptakes were determined at 2.5, 5, 10, 20, 50, 100, 200, and 300 µM glutarate (A) of at 0.5, 1, 2, 3, 4, 5, 10 and 15 µM glutarate (B). For each carrier concentration-dependent glutarate uptake is shown as one representative of three independent experiments. Each point represents the mean ± SE of at least eight oocytes.

4.2 3 Determination of K_m of hOAT1 and hOAT3 for glutarate

The uptake of glutarate into hOAT3- and hOAT1- injected oocytes was found to be a linear process from 0-45 minutes at highest glutarate concentration used (400 µM), and should thus represent initial rate uptake (data not shown). Therefore, an uptake period of 30 minutes was chosen when determining the K_m of hOAT3 and hOAT1 for glutarate. To obtain the K_m value of glutarate for both transporters, uptake of glutarate in hOAT3- and hOAT1- injected oocytes was studied in the presence of increasing concentrations of glutarate in the transport media. The K_m was calculated by fitting the data to the following equation: $V=V_{max}[S]/(K_m+[S])$, where V is the rate of glutarate uptake, S is the glutarate concentration in the medium, K_m is the apparent Michaelis Menten constant; and V_{max} is the maximum uptake rate (Neame and Richards 1972). Curve fitting was performed with the SigmaPlot 2000 program (SPSS Science software).

Figure 4.9.A shows a representative out of three independent determinations of the K_m for glutarate of hOAT3-expressing oocytes. The mean K_m value was calculated to be approximately 23.5 µM (n=3 independent experiments, 8-11 oocytes per treatment each). For hOAT1, the K_m-value for glutarate averaged 2 µM (n=3 independent experiments, each carried out on 8-11 oocytes per experimental condition). One representative experiment is shown in Figure 4.9.B.

4.3 Re-evaluation the mode of operation of hOAT3

4.3.1 Trans-stimulation studies

To study if hOAT3 can function as an exchanger, trans-stimulation experiments were performed. This means that the hOAT3-expressing oocytes were injected with the radioactively labeled substrate of hOAT3. Afterwards the influence of various anions present in the extracellular medium – supposed exchange partners - on the efflux of the previously injected substrate from the oocytes was assayed.

As had previously been shown (Cha *et al* 2001), no trans-stimulation of [^{3}H]ES efflux from hOAT3-espressing oocytes was observed when ES, α-KG or PAH were added to the extracellular medium (data not shown). However, ES is a highly lipophilic compound and might thus bind to intracellular components upon injection, in particular to the large number of yolk platelets in the oocyte, thereby lowering the free submembraneous ES concentration available for efflux.

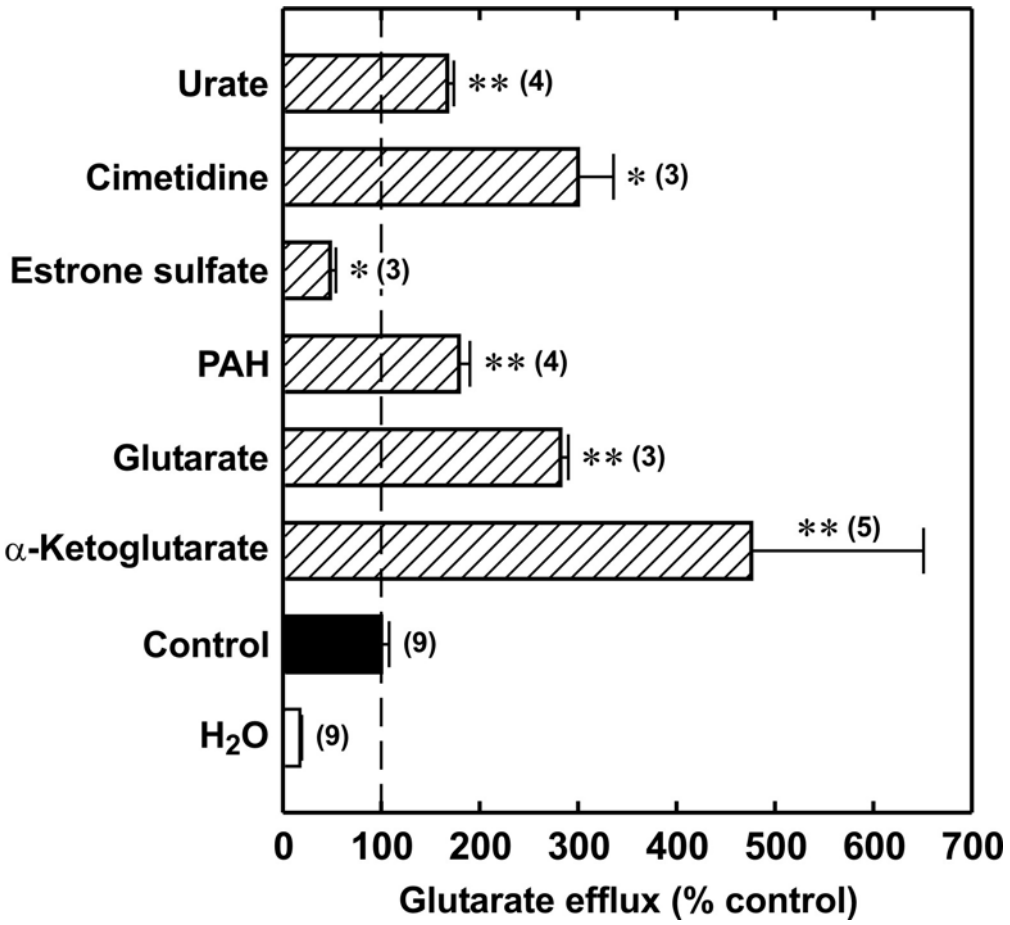

Figure 4.10: Trans-stimulation of GA efflux from oocytes that express hOAT3. Oocytes were injected with hOAT3 cRNA or an equivalent volume of H_2O. After 3 d of incubation, they were injected with 2.6 nCi [^{14}C]GA and placed in efflux medium without (control) or with 2 mM test compound as indicated. After an initial period of 2 min, during which oocytes showed a highly variable leak flux because of the injection, medium was changed and the efflux then assayed over the following 28 min. Data are expressed in % of the efflux from the hOAT3-injected oocytes in the absence of test compound in the efflux medium as means ± SE of the number of independent experiments given in parentheses, each carried out on four to five oocytes per treatment. Significant changes in paired data analysis in absolute efflux after addition of test compound to the 'trans' side are indicated (*: $p < 0.05$, **: $p < 0.01$).

Therefore, next the efflux of the more hydrophilic [^{14}C]glutarate – a non-methabolisable analogue of α-KG – was assayed from hOAT3-expressing oocytes (Figure 4.10). As would be expected for an exchanger, α-KG, glutarate and PAH - at 2 mM concentrations - significantly trans-stimulated glutarate efflux by more than 370%, nearly 200% and 80%, respectively. Of all ions tested, only ES did not stimulate hOAT3-mediated GA efflux, but rather inhibited it by about 50%. Cimetidine - a cationic compound, previously shown to be transported by OAT3 (Cha *et al* 2001,Kusuhara *et al* 1999), increased glutarate efflux by hOAT3 by nearly 200%. Most interestingly, the

physiologically important organic anion urate trans-stimulated GA efflux from hOAT3-oocytes by nearly 70%.

4.3.2 The pH dependence of hOAT3-mediated ES uptake

4.3.2.1 Inhibition of hOAT3-mediated ES uptake by cimetidine

As was reported previously, hOAT3 as well as hOAT1 and fOAT (Burckhardt *et al* 2002) are able to transport cimetidine – a cationic drug compound that is present in solution as positively charged as well as uncharged form at physiological pH. While fOAT has recently been shown to interact preferentially with uncharged cimetidine (Burckhardt *et al* 2002), the charge dependence of hOAT3-mediated cimetidine transport had not yet been elucidated.

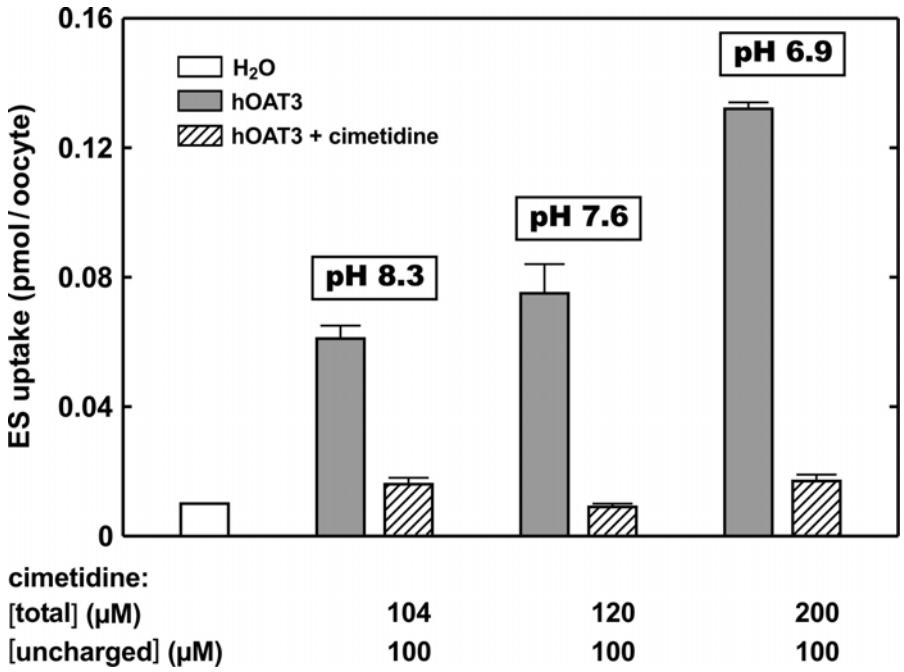

Figure 4.11: Cis-inhibition of hOAT3 mediated ES uptake by cimetidine at different pH values. Oocytes were injected with hOAT3 cRNA or an equivalent volume of H_2O. After 3 d of incubation, 30 min uptake of 50 nM [^{3}H]ES was assayed in the ORI medium at tree different pHs - 6.9, 7.4 and 8.3 in the absence or presence of cimetidine in the uptake medium. Cimetidine concentrations were calculated so that the concentration of uncharged form was constant (100 μM) under all three conditions and total concentration varied. Data are expressed in pmol/oocyte as means ± SE of 9-11 oocytes, and represent one out of 3 independent experiments.

To test whether only the uncharged cimetidine inhibits hOAT3, the ES uptake was studied at different bath pH values of 6.9, 7.6 and 8.3. Given a pKa of 6.9 (Barendt and Wright 2002), the relative abundance of uncharged cimetidine is 50.0, 83.4, and 96.2% at pH 6.9, 7.6, and 8.3, respectively. The concentration of total cimetidine was calculated so that the concentration of uncharged cimetidine was kept constant (100 µM) at all three pH values. If hOAT3 preferred the uncharged cimetidine form, inhibition of hOAT3-mediated ES uptake should be equal at all three pH values, despite the different total cimetidine concentrations. However, as seen in Figure 4.11, the hOAT3-mediated ES uptake itself was found to be pH-dependent - it increased with lowering the extracellular pH. This unexpected finding precluded the interpretation of the cimetidine inhibition data.

4.3.2.2 Elucidation of pH effect on hOAT3-mediated ES uptake

The effect of increasing the hOAT3-mediated ES uptake by lowering the pH could be due to the ability of hOAT3 to exchange for hydroxyl ions for which there exists an outwardly directed gradient at acidic extracellular pH. If this was true and both hydroxyl ions and glutarate anions shared the same binding site, then competitive inhibition of intracellular hydroxyl binding by glutarate should eliminate or at least attenuate the pH effect.

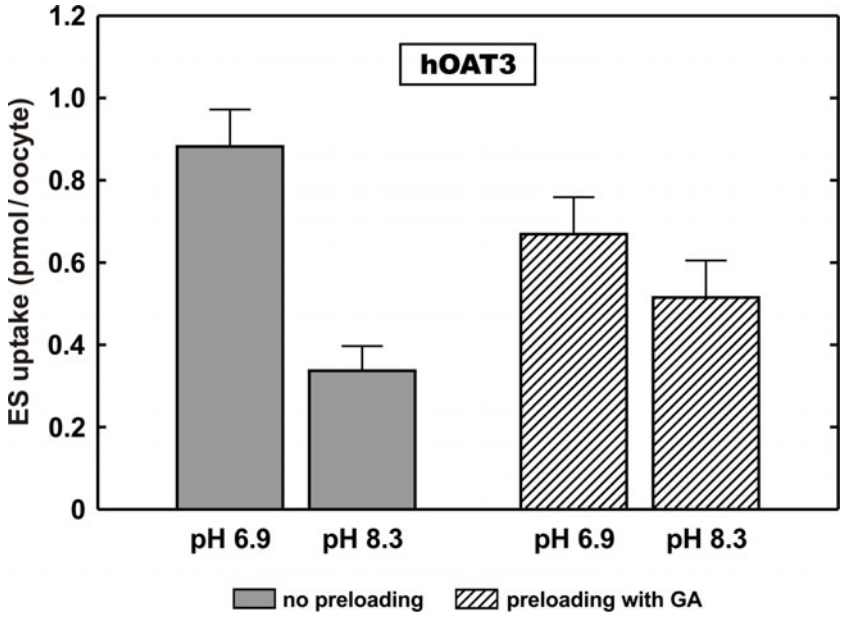

Figure 4.12: hOAT3 mediated ES uptake at different pH values- effect of preloading of the oocytes with glutarate. Oocytes were injected with hOAT3 cRNA or an equivalent volume of H_2O. After 3 d of incubation, uptake of 50 nM [^{3}H]ES was assayed in the ORI medium at two different pHs - 6.9 and 8.3 for 30 min without (no preloading) or with (preloading with GA) prior preloading with 1 mM glutarate for 2 hr. Data are expressed in pmol/oocyte as means ± SE of 9-11 oocytes, and represent one from 3 independent experiments.

Therefore, hOAT3-expressing oocytes were preloaded with 1 mM unlabeled glutarate for 2 hours and then tested for ES uptake at pH 6.9 and 8.3. As controls, uptake in another two groups was carried out at pH 6.9 and 8.3 without preloading. As seen in Figure 4.12, when preloading with glutarate, the pH effect was reduced such that uptakes of ES were nearly equal at both pH values. Moreover, the preloading with glutarate inhibited original ES uptake at the acidic pH. This observation suggests that hOAT3 is able to exchange organic anions for hydroxyl ions.

4.4 Sensitivity of hOAT3 for urate in comparison with hOAT1

4.4.1 Inhibition of hOAT1- and hOAT3-mediated PAH uptake by urate

Because of the strong cis-inhibition by urate of hOAT3-mediated uptake and the trans-stimulation by this anion of glutarate efflux via hOAT3 as observed previously (see Figure 4.6 and Figure 4.10), the further cis-inhibition studies were carried out to test the extent of interaction of hOAT3 with urate.

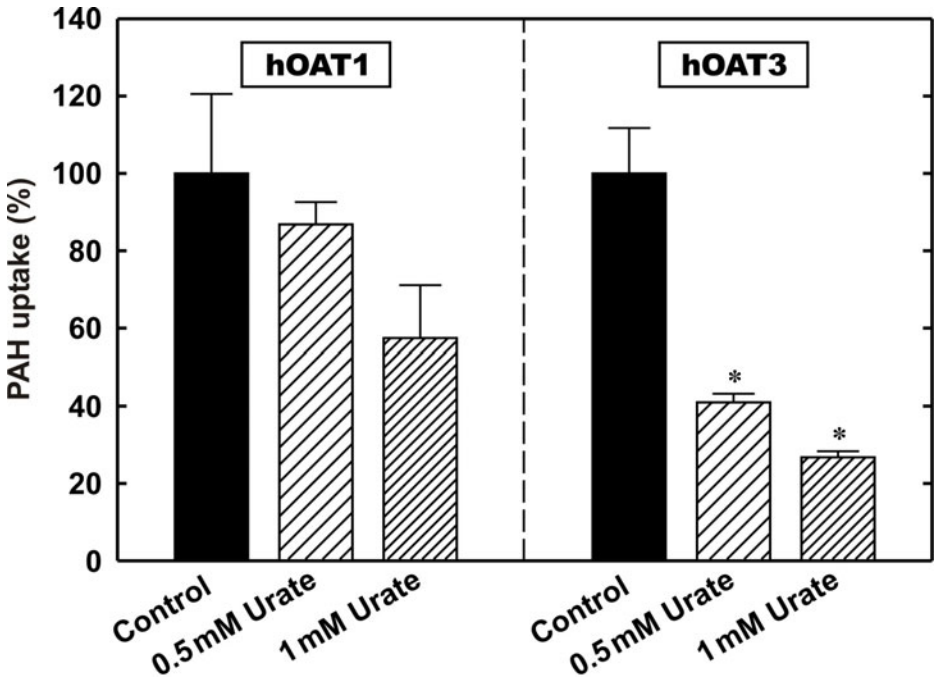

Figure 4.13: Sensitivity of hOAT3-and hOAT1-mediated PAH uptake to urate inhibition. Oocytes were injected with hOAT1-cRNA, hOAT3-cRNA, or an equivalent volume of H_2O. After 3 d of incubation, uptake of 10µM PAH was assayed in the absence (control) or presence of urate (0.5mM or 1mM in the uptake medium). Data are expressed in % of the uptake of hOAT3- and hOAT1-injected oocytes in the absence of urate as means ± SE of three independent experiments, each carried out on 8-11 oocytes per treatment. Significance of differences in unpaired Student's t-test of absolute uptake relative to the corresponding control is indicated (*: $p < 0.05$).

Most recently, hOAT1 has been suggested as the prime candidate driving the energy-dependent step in urate secretion (Ichida *et al* 2003). Therefore, the sensitivity of hOAT1 and hOAT3 to urate was compared by cis-inhibition of uptake of 10 µM PAH as the common substrate for both transporters (Figure 4.13). Under these conditions, hOAT3 appeared to be more sensitive to urate inhibition. Urate at a concentration of 0.5 mM did not significantly alter hOAT1-mediated PAH while it inhibited hOAT3-transport by 60%. At 1 mM concentration, it reduced hOAT1 transport by only 40%, and hOAT3 transport by 75%.

4.4.2 Inhibitory potency of urate on hOAT3-mediated ES uptake.

To obtain the IC_{50} value for urate on ES transport, 30 min ES uptake in hOAT3-oocytes was assayed in the presence of increasing urate concentrations. Uptake was linear at least up to the 30 min time point at the ES concentrations used and should thus represent initial rate uptake (data not shown).

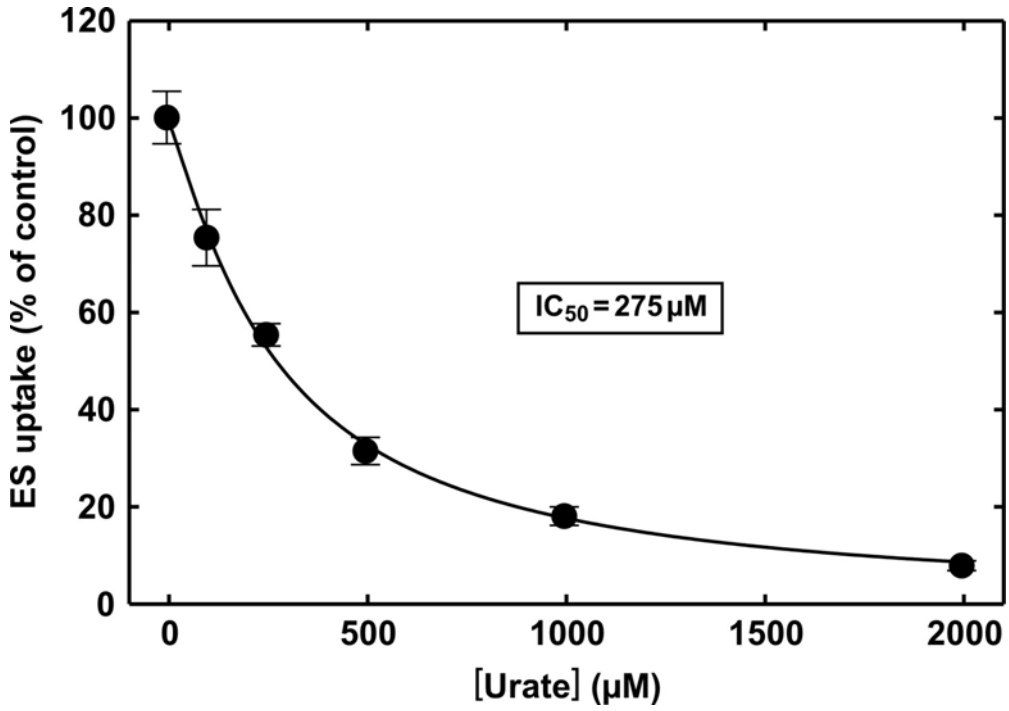

Figure 4.14: Concentration-dependent inhibition of hOAT3-mediated ES uptake by urate. Oocytes were injected with hOAT3 cRNA or an equivalent volume of H_2O. After 3 d of incubation, 30-min uptakes of 50 nM [^{3}H]ES were assayed in the absence or presence of increasing concentrations of urate. Data are expressed in % of the uptake of hOAT3-injected oocytes in the absence of urate (control) and were fitted by non-linear regression as described in the text. Concentration-dependent inhibition of ES uptake is shown in one representative of three independent experiments. Each point represents the mean ± SE of at least eight oocytes.

For determination of the urate concentration that blocked 50% of the ES uptake (IC_{50}), data were fitted to the equation $V=V_0/[1+(I/IC_{50})^h]$, where V is the rate of ES uptake in the presence of urate, V_o is the rate of ES uptake in the absence of urate, I is the urate concentration; and h is the Hill coefficient (Zhang *et al* 1999). The SigmaPlot 2000 program (SPSS Science software) was used to fit the data by non-linear regression. At 50 nM, the IC_{50}-values averaged 290 $\pm$ 16 µM (n=2 independent experiments, each carried out on 8-11 oocytes per experimental condition). One representative inhibition curve is shown in Figure 4.14. When the urate sensitivity of uptake was assayed at 10 nM ES, an average urate IC_{50} value of 255 $\pm$ 34 µM (n=4 independent experiments, 8-11 oocytes per treatment each) was obtained.

4.4.3 Urate studies on HEK293 cells

To further compare the sensitivity of both transporters to urate, additional inhibition experiments were done on T-REx™-HEK-293 cells stably expressing hOAT3 and hOAT1. First, the uptakes of 10 µM PAH as the model substrate for hOAT1 and the 50 nM ES as the substrate of hOAT3 were studied in the two cell lines – hOAT1-T-REx™-HEK-293 and hOAT3-T-REx™-HEK cells, respectively. The uptake of PAH by hOAT1 into the hOAT1-stably expressing cells was found to be a linear process from 0-3 minutes and the uptake of ES by hOAT3 into the hOAT3-stably expressing cells was found to be a linear process from 0-4 minutes (data not shown). Therefore, a period of 2 minutes was chosen for IC_{50} determination of the transporters for urate.

To obtain the IC_{50} value for urate on PAH or ES transport, initial rate uptakes in hOAT1- or hOAT3-HEK cells was assayed in the presence of increasing urate concentrations, and the results were fitted to the equation given above (Chapter 4.4.2). Figure 4.15 shows urate IC_{50} curves for hOAT1 (A) and hOAT3 (B), each curve representing the mean of three independent experiments. From these curves urate IC_{50} values of approximately 380 µM in the case of hOAT1 and 170 µM in the case of hOAT3 were calculated using the SigmaPlot 2000 program (SPSS Science software).

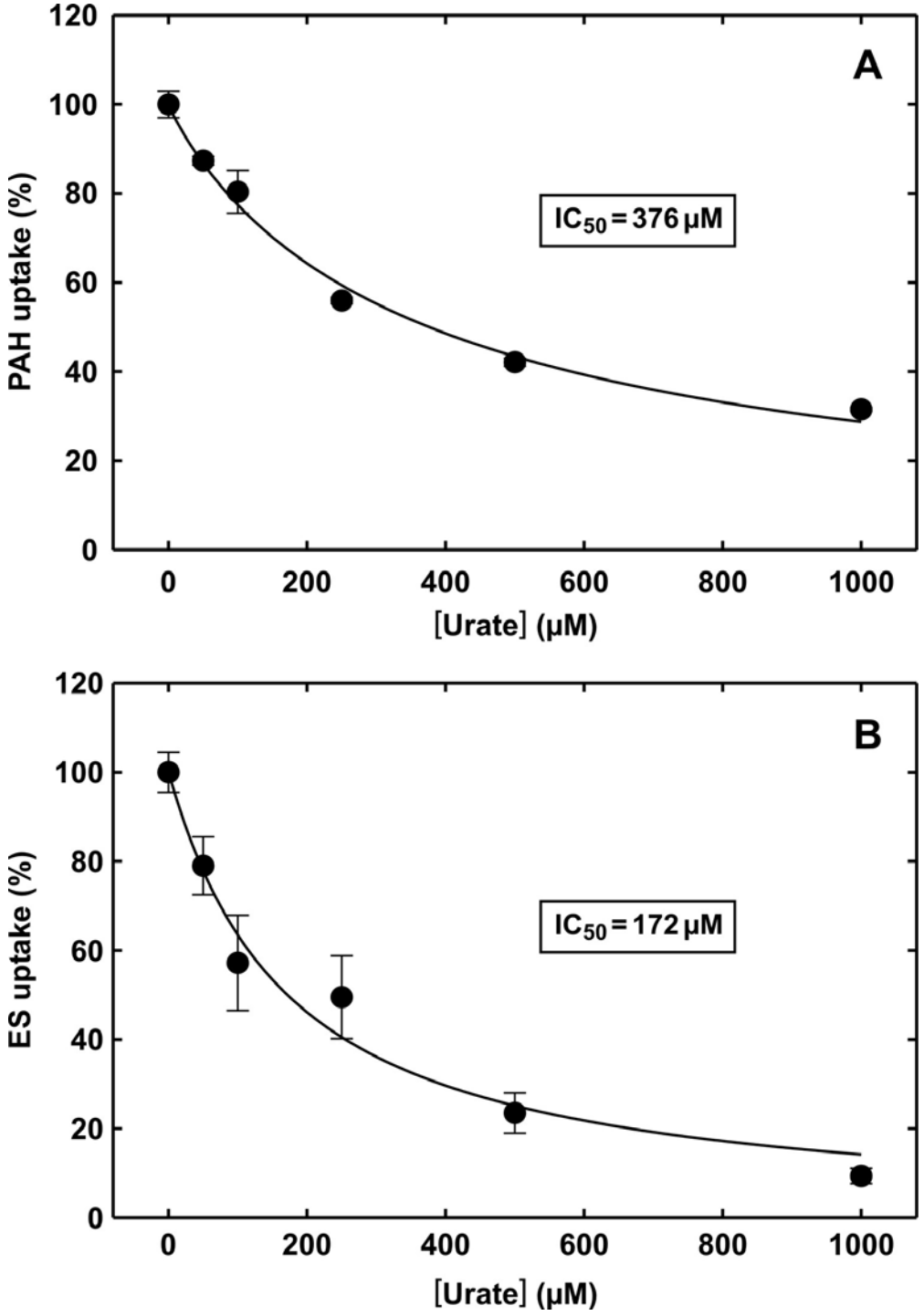

Figure 4.15: Concentration-dependent inhibition of hOAT1-mediated PAH uptake and hOAT3-mediated ES uptake in T-REx™-HEK-293 cells by urate. Uptakes of 10 µM [^{3}H]PAH or (A) 50 nM [^{3}H]ES (B) were assayed by the T-REx™-HEK-293 cells, stably expressing hOAT1 (A) or hOAT3 (B) in the absence or presence of increasing concentrations of urate. The uptake rates are expressed in % of the uptake of hOAT3- or hOAT1-expressing cells minus that of the mock-transfected cells in the absence of urate, and were fitted by non-linear regression as described in the text. Each point represents the mean ± SE of three independent experiments, each carried out in triplicate.

4.5 Interaction of hOAT1 and hOAT3 with diuretics

Although both hOAT1 and hOAT3 have previously been shown to interact with diuretics (Cha *et al* 2001,Race *et al* 1999), neither their ability to actually transport these compounds, nor relative contribution of both transporters in the process of secretion of these drugs were known. Therefore the experiments were performed on the direct comparison of the both transporters with respect to diuretics interaction.

4.5.1 Transport of various organic anions by hOAT1 and hOAT3

For the comparison studies, a substrate that is equally well transported by both transporters was searched for. Therefore, the carriers were compared with respect to PAH, ES and glutarate transport. Figure 4.16 shows the data on uptake rates of these three radioactively labeled organic anions by both transporters in *Xenopus laevis* oocytes.

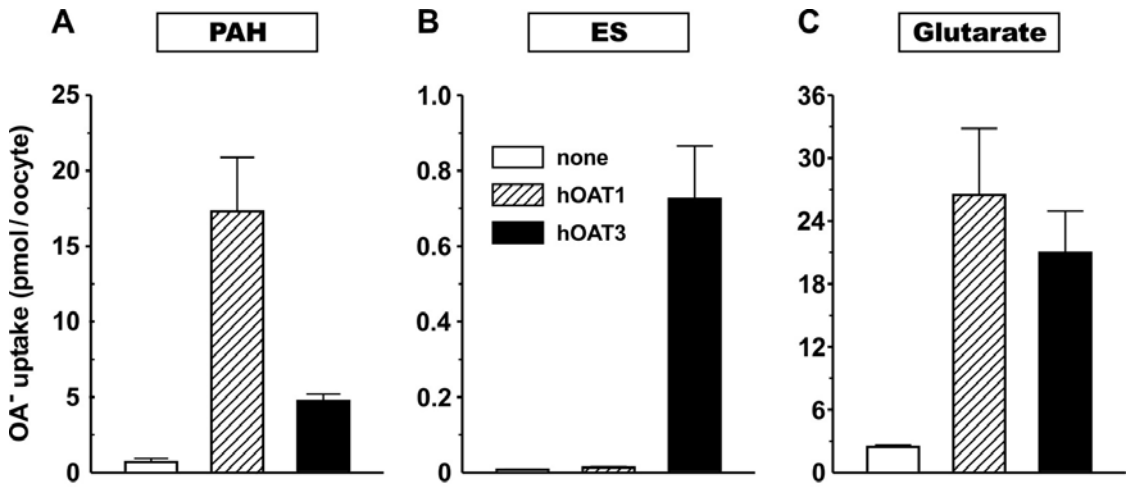

Figure 4.16: Uptake of various organic anions by hOAT1- and hOAT3-expressing oocytes. Oocytes were injected with hOAT1-cRNA, hOAT3-cRNA or an equivalent volume of H_2O. After 3 d of incubation, uptake of 10 µM [^{3}H]PAH (A), 50 nM [^{3}H]ES (B) or 100 µM [^{14}C]glutarate (C) were assayed for 1 hr (PAH) or 30 min (ES and glutarate). Data are expressed in pmol/oocyte as means ± SE of n=4 (PAH), or n=3 (ES and glutarate) independent experiments, each carried out on 8-11 oocytes per treatment.

The uptake of PAH was significantly above that of water-injected oocytes for both transporters (Figure 4.16.A). However, while the oocytes expressing hOAT1 showed an increase of PAH uptake by approximately 25-fold, hOAT3-expressing oocytes increased PAH uptake only to 7.4-fold compared with water-injected oocytes. Thus, PAH uptake by hOAT3 was nearly 3.5 times lower than by hOAT1. Yet, although

hOAT1-mediated PAH transport was inhibited by 250 µM ES to 80.6±5.4% (n=11 oocytes, data not shown), this carrier apparently did not accept ES as a substrate (Fig. 4.16.B). In contrast, a nearly 90-fold uptake over water-injected cells was observed for hOAT3-expressing oocytes. Finally, both hOAT1 and hOAT3 mediated nearly equal uptake rates for glutarate (Fig.4.16.C). hOAT1-expressing oocytes exhibited 11±3 fold, and hOAT3-expressing oocytes 8.5±1 fold, (n=3) uptake of 100 µM glutarate when compared with water-injected cells. Therefore glutarate was the substrate of choice for subsequent experiments on comparison of the sensitivity of hOAT1 and hOAT3 for loop diuretics.

4.5.2 cis-Inhibition of hOAT1 and hOAT3 by loop diuretics

At a glutarate concentration of 100µM the inhibition of hOAT1- and hOAT3-mediated transport by 250 µM of the loop diuretics bumetanide and furosemide was tested.

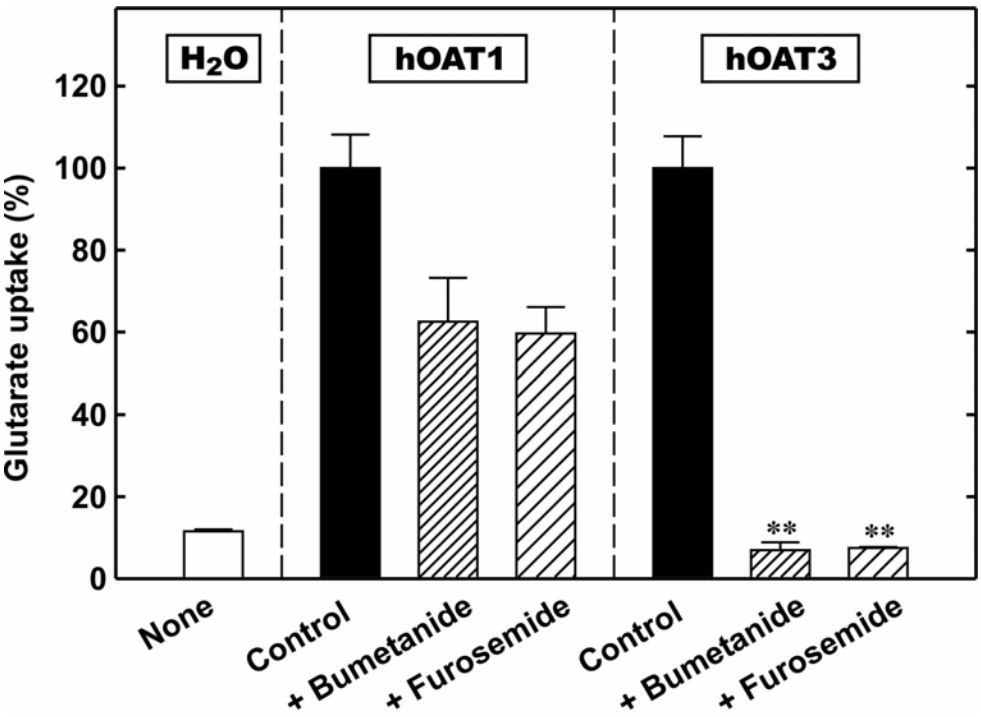

Figure 4.17: Cis-inhibition of hOAT1 and hOAT3 by loop diuretics. Oocytes were injected with hOAT1-cRNA, hOAT3-cRNA or an equivalent volume of H_2O. After 3 d of incubation, inhibition of hOAT1 and hOAT3-mediated glutarate uptake at a concentration of 100µM by 250 µM of the loop diuretics bumetanide and furosemide was assayed. Data are expressed in % of the uptake of hOAT1- and hOAT3-injected oocytes in the absence of inhibitors as means ± SE of two independent experiments, each carried out on 8-11 oocytes per treatment. Significance of differences in unpaired Student's t-test of absolute uptake relative to the corresponding control is indicated (**: $p < 0.01$).

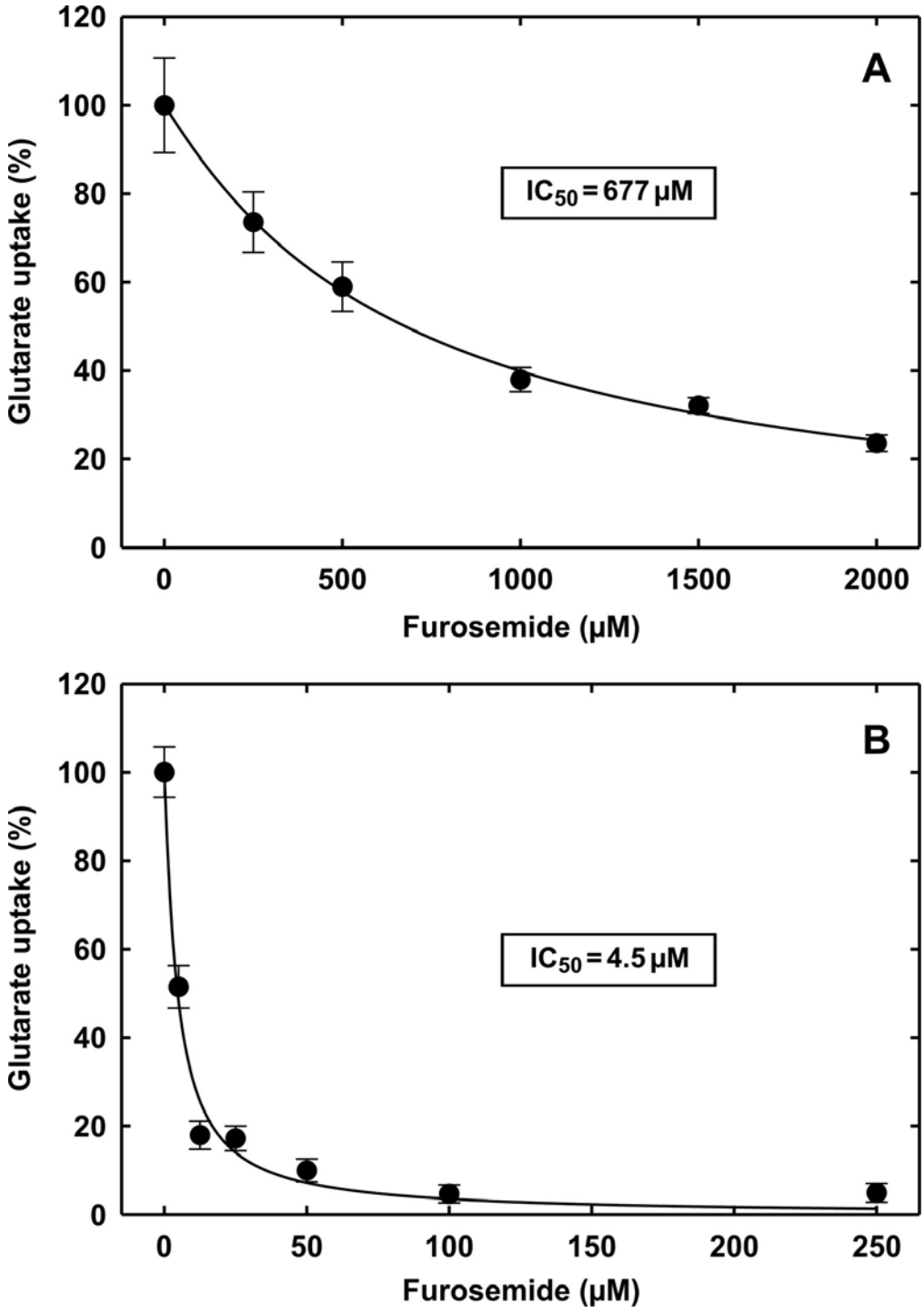

Figure 4.18: Concentration-dependent inhibition of (A) hOAT1- and (B) hOAT3-mediated glutarate uptake by furosemide. Oocytes were injected with hOAT1-cRNA or hOAT3-cRNA, or an equivalent volume of H_2O. After 3 d of incubation, 30-min uptakes of 100 µM [^{14}C]glutarate were assayed in the absence or presence of increasing concentrations of furosemide. The cRNA-dependent uptake rates (uptake of cRNA-injected oocytes minus that of water-injected cells) are expressed in % of the uptake in the absence of furosemide and were fitted by non-linear regression as described in the text. For each carrier, one representative furosemide inhibition curve out of 3 is shown. Each point represents the mean ± SE of at least eight oocytes.

Under these conditions hOAT3 appeared to be more sensitive for loop diuretics. As seen in Figure 4.17, the hOAT1-mediated transport was only inhibited to about 60% by 250 µM furosemide and 250 µM bumetanide. At the same concentration, furosemide and bumetanide reduced hOAT3-mediated transport to approximately 7.5% and 7.0%, respectively, which was equal to the rate of uptake by water-injected cells. To confirm these findings, kinetic studies – a determination of IC_{50} of furosemide for both carriers were performed.

4.5.3 Inhibitory potency of furosemide on hOAT1- and hOAT3-mediated glutarate uptake

To determine the furosemide concentrations inhibiting uptake of glutarate by both carriers by 50%, 30 min glutarate uptakes in hOAT1- and hOAT3-oocytes were assayed in the presence of increasing furosemide concentrations. Uptakes by hOAT1 and hOAT3 were linear at least up to the 30 min time point at 100 µM glutarate concentration used and should thus represent initial rates uptakes (data not shown).

For hOAT1 the IC_{50}-values in averaged 490 µM (n=5 independent experiments, each carried out on 8-11 oocytes per experimental condition). One representative experiment is shown in Figure 4.18(A), in which the IC_{50}-value was calculated as 677 µM. When the furosemide sensitivity of uptake of hOAT3 was assayed, an average furosemide IC_{50} value of 3.2 µM was obtained (n=3 independent experiments, 8-11 oocytes per treatment each). The representative inhibition curve for hOAT3 is shown in Figure 4.18(B). The IC_{50}-value in this experiment was 4.5 µM.

4.5.4 Trans-stimulation of hOAT3-mediated efflux by diuretics

To elucidate whether diuretics are translocated by hOAT1 and hOAT3, trans-stimulation studies were performed. Therefore efflux of [^{14}C]glutarate from hOAT1- and hOAT3-expressing oocytes was assayed in presence of the loop diuretic furosemide and the thiazide diuretic hydrochlorothiazide (HCTZ) in the efflux media.

When used at a concentration of 2 mM, furosemide did not stimulate hOAT3-mediated GA efflux, and bumetanide even inhibited it by about 50% (data not shown). Therefore lower concentrations of diuretics were applied for further trans-stimulation experiments.

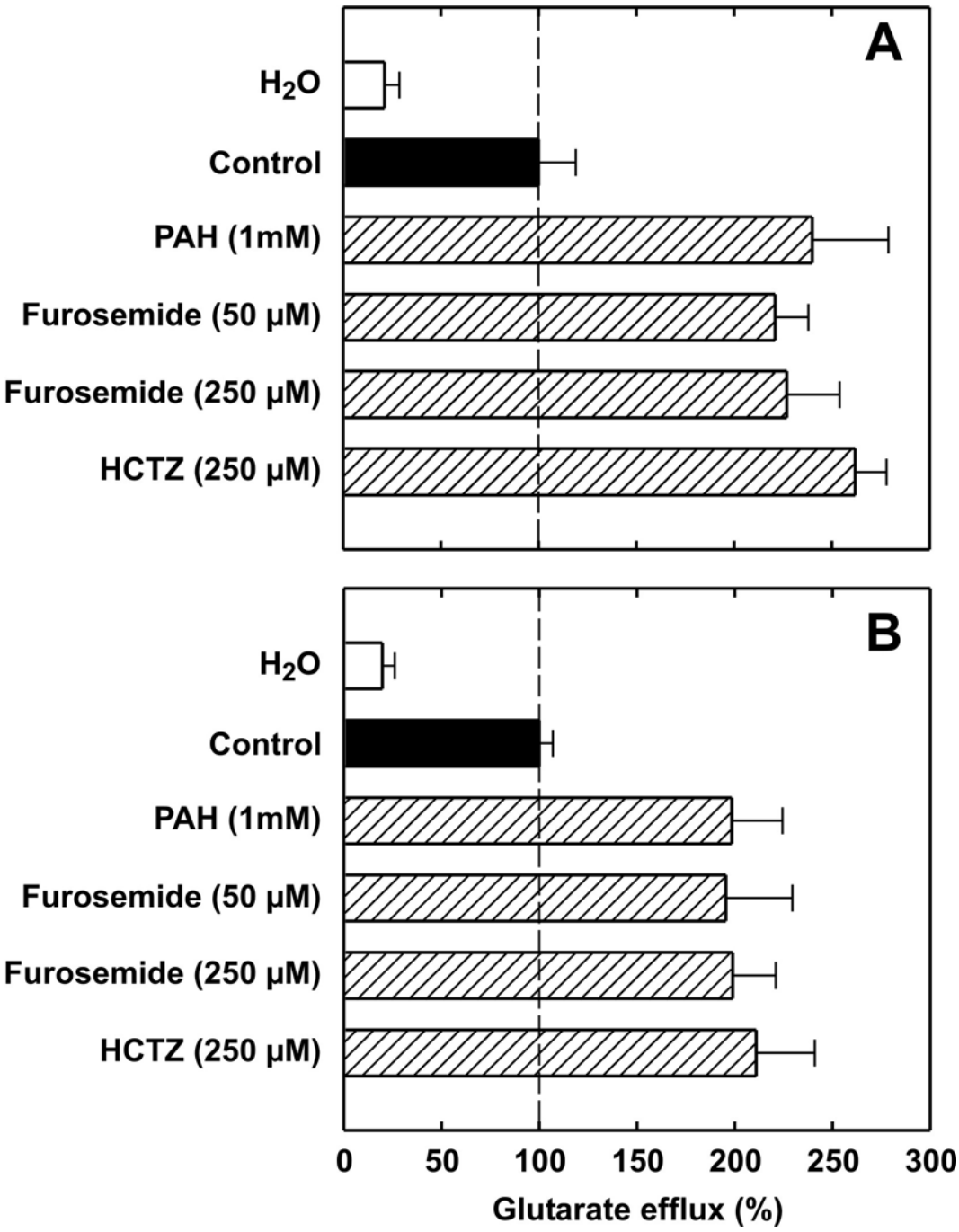

Figure 4.19: Trans-stimulation of glutarate efflux from oocytes that express hOAT1 (A) or hOAT3 (B). Oocytes were injected with hOAT1 or hOAT3 cRNA or an equivalent volume of H_2O. After 3 d of incubation, they were injected with 2.6 nCi [^{14}C]glutarate and placed in efflux medium without or with test compound as indicated. After an initial period of 2 min, medium was changed and the efflux then assayed over the following 28 min. Data are expressed in % of the efflux from the hOAT1- or hOAT3-injected oocytes, respectively, in the absence of test compound in the efflux medium. These are means ± SE of three independent experiments, each carried out on four to five oocytes per treatment. HCTZ stands for hydrochlorothiazide

When applied at concentrations of 50 μM and 250 μM, furosemide trans-stimulated glutarate efflux from hOAT1-expressing oocytes by almost 120% and 130%, respectively. This trans-stimulation was nearly as strong as caused by 1 mM PAH used as a positive control - 140% (Figure 4.19.A). Hydrochlorothiazide at 250 μM trans-stimulated glutarate efflux from hOAT1-oocytes most effectively - by more than 160%. In hOAT3-oocytes (Figure 4.19.B), furosemide trans-stimulated glutarate efflux by 95% and almost 100% in concentrations of 50 and 250 μM respectively. Again, the strongest effect was observed for HCTZ - it trans-stimulated glutarate efflux from hOAT3-oocytes by more that 110% (n=3), which was even higher than the stimulation caused by 1 mM PAH - 98%. These data demonstrate that both transporters can exchange furosemide and hydrochlorothiazide for dicarboxylates.

5 DISCUSSION

5.1 Obtaining the functional hOAT3 clone

The secretion of organic anions including endogenous metabolites, xenobiotics and widely prescribed drugs is an important physiological function of the renal proximal tubules. The molecular mechanisms underling this process has been studied during the last decades and it is now believed to be mediated to a major part by multiple organic anion transporters of the OAT family. The rate-limiting step of this process is the basolateral uptake of organic anions from the blood into the proximal tubules cells. Of the recently cloned organic anion transporters, OAT1 and OAT3 were consistently localized to the basolateral membrane of the proximal tubules and therefore are the main candidate proteins to mediate this translocation event. However, while the transport mode and functional properties of OAT1 have been intensively characterized, similar information was lacking for OAT3. Yet understanding the functional role of hOAT3 and its contribution to overall kidney function (in comparison to hOAT1) is not only of academical interest but has also clinical importance, as these transporters could control the urinary excretion of potentially toxic anionic drugs and, on the other hand, might confer nephrotoxicity of certain pharmaceuticals. The knowledge of substrate specificities of these transporters would also help to avoid undesirable drug-drug interactions.

For the characterization studies it was necessary first to obtain a functional hOAT3 clone. The RT-PCR and 5'- and 3'-RACE yielded products identical in sequence to that published by Cha and colleagues (Cha *et al* 2001). With 5'-RACE, an additional 12 base pairs of the untranslated region were amplified. At this stage of the study, a hOAT3 clone could be obtained from the Resource Center / Primary Database (RZPD) human cDNA library. However, when this original hOAT3-RZPD clone was expressed in *Xenopus laevis* oocytes and the encoded protein tested for its transport ability, it turned out to be not functional. The alignment of the hOAT3-RZPD sequence with the hOAT3 sequence published by Cha and our own RT-PCR data revealed two single nucleotide deviations that resulted in two amino acid exchanges - a proline residue instead of the alanine residue at position 22, and a lysine residue instead of the glutaric acid residue at position 271. As the hOAT3-RZPD clone was derived from a cDNA library, these deviations likely represent single nucleotide polymorphisms (SNPs).

One of the deviating amino-acids in the RZPD-hOAT3 clone – the proline 22 - was found to be situated in the first predicted trans-membrane domain of the hOAT3 protein. After “correction” of this amino acid by site-directed mutagenesis, this deviation in the RZPD clone turned out to be responsible for the total loss of function. This was not unexpected since proline is known as an amino acid that markedly influences protein architecture. Proline tends to disrupt α-helices because of its ring structure, which makes it more conformationally restricted than other amino acids (Berg *et al* 2002). Interestingly, the other nucleotide exchange, which resulted in the glutaric acid to lysine exchange, was also present in the base sequence of the hOAT3 clone isolated by Race and colleagues (Race *et al* 1999), and may thus constitute another SNP. The alignment of hOAT3 with its rat and mouse homologues revealed, however, that this position is not conserved between these species (arginine in mOAT3, lysine in rOAT3) which clearly suggests that it may not be critical for protein function.

As mentioned above, transport ability of hOAT3 was already restored after substitution of proline 22 by alanine, and did not significantly change after the additional replacement of the lysine residue residue by glutaric acid indicating that the A22P mutation, but not the E172K mutation, in the RZPD clone was responsible for the loss function. Oocytes, expressing either “corrected” clone (P22A or P22A;K271E) showed a significant increase of both estrone sulfate (ES) and *p*-aminohippurate (PAH) uptake compared with water-injected oocytes. However, while the uptake of ES was more than 150-fold that of water-injected cells, for PAH this ratio reached maximally 8. This result is consistent with previous observations that ES is a much better substrate for hOAT3 than PAH. While ES was taken up at high rates by hOAT3-expressing oocytes with a K_m of 3.1 µM, for PAH a K_m of 87 µM was determined (Cha *et al* 2001).

5.2 Characterization of hOAT3-mediated organic anion transport

5.2.1 Ion-dependence of hOAT3-mediated ES uptake

The hOAT3-mediated ES uptake was investigated for its sensitivity to the presence of inorganic anions in the uptake media. In order to look for functional characteristics similar to hOAT1, the sensitivity of hOAT3 to the removal of chloride ions was assayed. The chloride dependence has been demonstrated as one of the features of the basolateral organic anion uptake system. In the early experiments with rat renal basolateral membrane vesicles, the carrier-mediated transport of PAH was shown to

be stimulated in the presence of chloride, and the maximal stimulation occurred when chloride was present on the same side as PAH (Inui *et al* 1986, Pritchard 1988). A more detailed study of the modulatory effect of chloride on the PAH transport was done on bovine renal basolateral vesicles (Schmitt and Burckhardt 1993). The authors demonstrated that the anion stimulation was not indirect, but on the PAH transporter itself, and that chloride modulated the carrier at a site distinct from the anion translocation site without being co-transported with PAH. Consequently, when the OAT1 was cloned as a main candidate for the basolateral organic anion/dixarboxylate exchanger, it was tested for chloride dependence. And indeed, as was shown in our department, PAH uptake in hOAT1-injected oocytes was decreased by 80% when chloride was replaced by gluconate in the transport medium (Wolff *et al* 2003). Similar results have been reported for the hOAT1 clones isolated and characterized by other groups (Hosoyamada *et al* 1999,Race *et al* 1999). This hOAT1 characteristic was consistent with the previously determined ion dependence of the organic anion transporting system. Similarly, hOAT3-expressing oocytes also showed significantly reduced substrate (ES) uptake when chloride was replaced with gluconate in the extracellular medium. Taking into consideration the ability of hOAT3 to transport PAH, although at lower rate than hOAT1, and co-localization of both carriers in the basolateral membrane of the proximal tubules, the present data indicate that the chloride-dependent PAH uptake into basolateral membrane vesicles was most likely represented by both hOAT1 and hOAT3.

The proximal tubules reabsorb bicarbonate from the primary filtrate. It enters the cells through the apical membrane as CO_2 and after the intracellular dissociation leaves the cell across the basolateral membrane following its electrochemical potential difference (Murer and Burckhardt 1983). Recently, the organic anion transporter polypeptide family member Oatp1, localized in the apical membrane of the S3 segment of proximal tubule cells, has been shown to mediate taurocholate/HCO_3^- exchange (Hagenbuch and Meier 2003). Therefore, in search for the driving force for hOAT3-mediated organic anion transport, bicarbonate was tested for interaction with hOAT3. Indeed, hOAT3-mediated ES uptake was reduced nearly by half when 25 mM bicarbonate was added to the uptake medium. The observed inhibition of bicarbonate on hOAT3 might suggest that this anion is a substrate of hOAT3 and thus could be a possible counter-ion for the hOAT3-mediated organic anion uptake. Another explanation of the bicarbonate effect could be that it replaces chloride ions on the “modifier side” of the transporter, the presence of which has been shown in the present study to be important for normal

functioning of the hOAT3. In view of the observed pH dependence of the hOAT3-mediated ES uptake, another possible reason of the inhibition might be alkalization of the uptake medium. However, the pH increase, caused by the addition of 25 mM bicarbonate was less than 0.1 pH units, by far not enough to account for the roughly 50% inhibition observation.

5.2.2 Cis-inhibition of hOAT3-mediated ES uptake

Various organic anions were tested for the ability to cis-inhibit ES transport by hOAT3 in order to investigate its substrate selectivity. The inhibition profile of hOAT3 was compatible with that of the classical basolateral PAH uptake system studied earlier by Ullrich and co-workers in the intact rat kidney (Ullrich 1997). Based on multiple inhibition studies of the PAH uptake into microperfused proximal tubule cells, the common structural requirements were determined for interaction with the system, which are based on four factors: hydrophobicity, charge, charge distribution, and charge strength (Ullrich 1997).

In the present study, hOAT3 was inhibited by about 90% by 1 mM PAH. This high inhibitory potency of PAH is in accordance with the previous observation that carrier-mediated anion uptake into mouse proximal tubule cells stably expressing hOAT3 was half-maximally inhibited by 19.6 µM unlabeled PAH (Jung *et al* 2001). As was already mentioned, hOAT3 is also able to transport PAH, although with a lower affinity than hOAT1. While the K_m values of hOAT1 for PAH range between 3.9 and 22 µM depending on expression system used (Burckhardt and Burckhardt 2003), the K_m for PAH determined in hOAT3-expressing oocytes was 87.2 µM (Cha *et al* 2001). The organic anion lactate showed no significant effect on the organic anion transport by hOAT3. As seen from the structural formula of lactate (Figure 5.1), this is a three-carbon monocarboxylate and hence is probably a too hydrophilic and too small compound to fulfill the structural requirements of the basolateral PAH transporter system, which accepts monovalent anions when they have a hydrophobic domain with a minimal length about 4 Å. In contrast urate, which contains an oxypurine ring and is present at physiological pH as a monovalent anion, significantly inhibited anion transport by hOAT3.

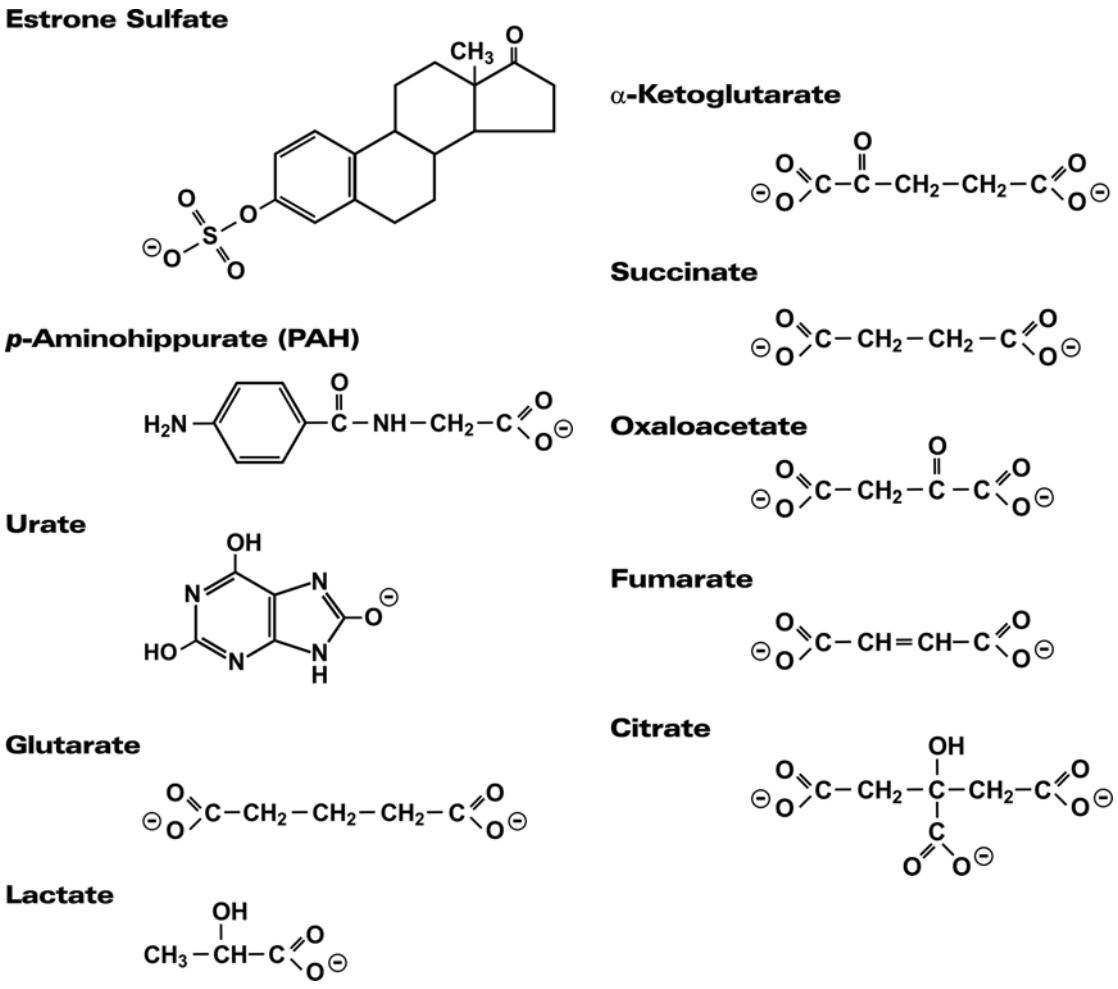

Figure 5.1: Structural formulas of compounds tested in the present study for inhibition of hOAT3-mediated ES uptake.

Among the anions originally tested for cis-inhibition, glutarate inhibited hOAT3-mediated ES uptake most potently - by 95%. Similarly, hOAT3 cloned by Cha and colleagues was strongly inhibited by glutarate (Cha *et al* 2001). Subsequently, the interaction of hOAT3 with other physiological dicarboxylates was investigated. Several TCA cycle intermediates where studied for their cis-inhibitory potency on OAT3-mediated ES uptake. Of this group, hOAT3 was significantly affected only by α-ketoglutarate (α-KG). Although some consistent inhibition was observed by fumarate and succinate, the affinity of hOAT3 for these C-4 dycarboxylates seems to be low. Similarly, the PAH uptake mediated by flounder OAT (fOAT) (Wolff *et al* 1997), rOAT1 (Uwai *et al* 1998) and hOAT1 (Reid, unpublished observation) was only inhibited by unsubstituted dicarboxylates with a carbon backbone of five or more carbons. This pattern of inhibition by dicarboxylates is consistent with the model predicted by Ullrich

and colleagues according to which the basolateral PAH uptake system interacts with divalent anions, with a minimum charge separation (distance) of 6-7 Å (Fritzsch *et al* 1989, Ullrich *et al* 1987).

5.2.3 Dicarboxylate transport by hOAT3

Since hOAT3, similarly to OAT1 (Uwai *et al* 1998) and flounder OAT (Wolff *et al* 1997), which is positioned between the OATs1 and OATs3 in the phylogenetic tree, exhibited a preference for dicarboxylates with at least 5 carbons, and glutarate and α-KG are known to be transported by OAT1s as well as by flounder OAT, these substances were also expected to be substrates for hOAT3. Indeed, in present study hOAT3 was shown to mediate the uptake of radiolabelled glutarate and α-KG. However, the transport rates observed for both dicarboxylates at 100 µM concentration were about 5-fold over control cells, much lower than for ES. The only data on glutarate transport by hOAT3 in the literature are published by Cha and colleagues (Cha *et al* 2001), demonstrating an only 2-fold higher glutarate uptake into hOAT3-expressing oocytes than into controls. Because the concentration used in the latter study was 10 times lower than in the present study, it is not possible to compare these data. Therefore, kinetic studies were performed to evaluate the affinity of hOAT3 for glutarate, and compare it with that of hOAT1. The apparent K_m of hOAT3 for glutarate averaged 23.5 µM, which means a rather high affinity of the carrier for this substrate. This value is only two times higher than the previously reported K_m for glutarate of hOAT1 expressed in CHO cells that averaged 10.7 µM (Cihlar and Ho 2000). However, when determined in oocytes in the present study, the obtained apparent K_m of hOAT1 for glutarate was about 2 µM, which is one order of magnitude lower than that obtained for hOAT3 under the same experimental conditions. The differences in determined affinity of hOAT1 between this and earlier studies might be due to the different expression systems used. This argument holds for the extracellular transport sites of hOAT1 and hOAT3. Whether a similar difference exists also for the intracellular sites of hOAT1 and hOAT3 is unknown at present. Also unknown remain the maximal velocities of both transporters for glutarate. The observation that the maximum achieved glutarate transport into hOAT1- and hOAT3-expressing oocytes was approximately equal does not allow the conclusion that both transporters have the same V_{max}, since there are no data about the amount of transporter molecules expressed in the oocytes' membrane.

5.2.4 Trans-stimulation of hOAT3

Trans-stimulation experiments were used for re-assessment of the transport mode of hOAT3, because they allow to directly demonstrate the ability of carriers to mediate substrate exchange. As was mentioned above, the elucidation of the driving force for OAT3 was important for the understanding of the physiological role of this carrier in renal organic anion handling. When initially characterized, based on the lack of trans-stimulation of efflux of its model substrate, estrone sulfate (ES), from OAT3-expressing oocytes, it was argued that OAT3 is simply a uniporter mediating facilitated diffusion (Cha *et al* 2001,Kusuhara *et al* 1999). Still, OAT3 was regarded as a transporter responsible for the basolateral uptake of its substrates, although it was not explained by the authors, how the uniporter could drive the uptake of negatively charged compounds in the face of opposing electrical and concentrational gradients of the proximal tubule cells. Therefore, in the earlier proposed mode of operation, OAT3 would rather function in the absorptive direction, and as that would compromise secretion of many substrates shared with OAT1, since both transporters co-localize along the basolateral membrane of the proximal tubules (Kojima *et al* 2002, Motohashi *et al* 2002).

Similar to previous observations (Cha *et al* 2001), no trans-stimulation of ES efflux from hOAT3-espressing oocytes was observed in the present study, when ES, α-KG or PAH were added to the extracellular medium (data not shown). However, it was assumed that the absence of trans-stimulation of ES efflux might not be due to the inability of OAT3 to mediate exchange, but rather due to the properties of ES per se. ES is a highly lipophilic compound and the tight binding of ES to a number of proteins was reported (Nicollier *et al* 1992, Rosenthal *et al* 1972, Tan and Pang 2001). As such, ES might bind to intracellular components upon injection, in particular to the large number of yolk platelets in the oocyte, impairing its release and minimizing trans-stimulatory effects of potential exchange partners. As was already discussed, hOAT3 was in the present study shown to transport glutarate with a rather high affinity. Since glutarate is a hydrophilic compound and was used as an exchange partner for the assessment of the transport mode of hOAT1 (Cihlar *et al* 1999,Ho *et al* 2000), as well as rOAT1 (Sekine *et al* 1997, Sweet *et al* 1997), this dicarboxylate was chosen for the subsequent efflux studies. Consistent with the above assumption, when efflux of glutarate was assayed, all organic anions tested with the exception of ES induced a significant trans-stimulation of hOAT3-mediated efflux. It should be noted that the

glutarate efflux in the absence of added organic anion to the extracellular medium was around five times higher from the hOAT3-expressing oocytes that from water-injected control oocytes. This observation could suggest that hOAT3 is able to operate without being completely loaded, or that this carrier can exchange intracellular glutarate for some inorganic anion present in the efflux medium used. The fact that extracellular ES trans-inhibited hOAT3-mediated glutarate efflux might be due to the rapid OAT3-mediated entry of ES into the oocytes, followed by competition of this high affinity substrate (Cha *et al* 2001,Kusuhara *et al* 1999) with glutarate for binding from the intracellular (cis-) side. In contrast, PAH, glutarate, α-KG, urate, and cimetidine significantly stimulated glutarate efflux when applied to the trans-side. This finding indicates that hOAT3 is able to mediate hetero-exchange of its substrates. While this study was in progress (Bakhiya *et al* 2003), similar results have been obtained on rat OAT3 (Sweet *et al* 2003), previously also regarded as a uniporter. Thus, the ability to mediate organic anion / dicarboxylate exchange is not a specific property of the human orthologue, but rather a general characteristic of OAT3.

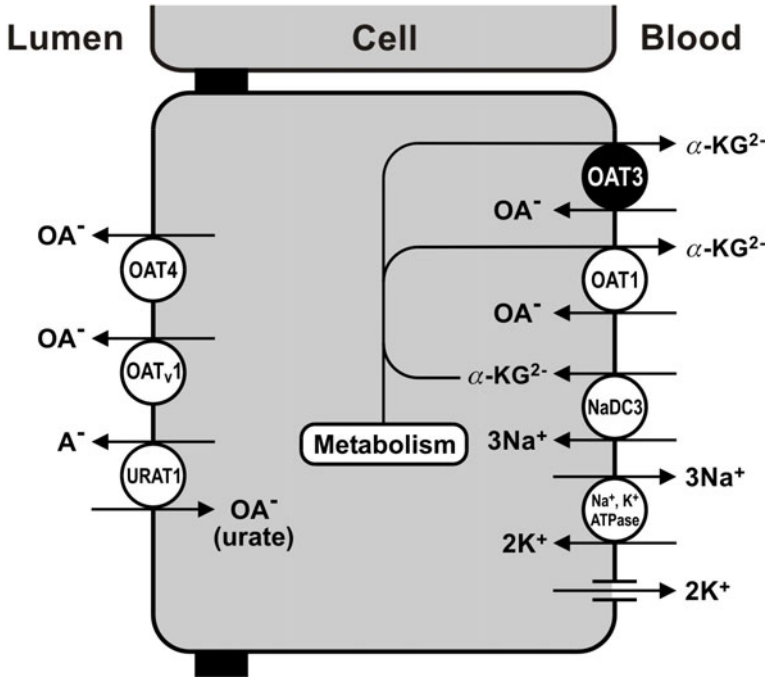

Figure 5.2: Scheme of proximal tubular organic anion secretion, redrawn after elucidation of the mode of operation of hOAT3. A^-, anion; OA^-, organic anion; α-KG^{2-}; α-ketoglutarate; NaDC3; sodium-dicarboxyate cotransporter;

Taken together, the data on trans-stimulation indicate that hOAT3 can indeed operate as an organic anion/dicarboxylate exchanger, and thus its mechanism of organic anion uptake is similar to that of OAT1. This means, that both OAT1 and OAT3 likely share

the same driving force in vivo, i.e. the outwardly directed α-KG gradient and thus function in parallel in the secretory direction (Figure 5.2). Since normal concentrations of α-ketoglutarate within the proximal tubular cell range between 100 and 300 μM (Pritchard 1995), with the determined K_m values for dicarboxylates under 25, μM both hOAT1 and hOAT3 should work in vivo under saturated conditions. This, together with previously reported data on co-localization of both transporters, would suggest that the contribution of each of the two carriers to the overall renal transport function would depend only on the respective affinities and maximal velocities of OAT1 and OAT3 for a certain compound. Since both transporters are likely to play a role in the urinary excretion of potentially toxic drugs and metabolites as well as in the development of nephrotoxicity, the above mentioned identity in the transport energetics and similarity of substrate specificities raised the need of direct comparison of both transporters with respect to their interaction with selected substrates of interest.

5.2.5 pH dependence of hOAT3-mediated ES uptake

The observed dependence of ES uptake by hOAT3 on the extracellular pH raised the question of the existence of other counterions that could drive the organic anion uptake by hOAT3. Since the uptake of ES was found to increase with acidification of the extracellular medium, it may be that hOAT3 is able to exchange organic anions for hydroxyl ions, for which an outwardly directed gradient is established at acidic pH of the medium. Ichida and colleagues (Ichida *et al* 2003) observed an increase of urate transport into mouse proximal tubule cells stably expressing hOAT1, when the uptake solution was acidified from pH 7.4 to pH 6.0. The authors also assumed that one of the explanations of this effect could be the ability of hOAT1 to perform urate/hydroxyl ion exchange. In the present study, the possibility of organic anion/hydroxyl ion exchange by hOAT3 was assessed indirectly. When the carrier's intracellular binding sites were saturated by pre-loading with glutarate, the difference between the rates of organic anion uptake by acidic and alkaline pH should be diminished due to the competition of glutarate with hydroxyl ions. This was indeed the case, suggesting that hOAT3 may exchange organic anion substrates for hydroxyl ions. Whether the hydroxyl ions contribute to the driving forces of hOAT3 in vivo and if so, to what extent, is hard to estimate, because the affinity of the carrier to hydroxyl ions is not known. Nevertheless, since an outwardly directed OH^- gradient exists in the proximal tubular cells due to the functioning of the luminal sodium/proton exchanger that pumps out protons and leaves

hydroxyl ions inside (Burckhardt and Greger 1997), this possibility can not be excluded and requires further testing.

5.3 Assessment of physiological role of hOAT3 in comparison with hOAT1

5.3.1 Sensitivity of hOAT3 for urate

The organic anion urate is the end product of dietary purine degradation in humans, since the uricase gene is not expressed (Roch-Ramel and Guisan 1999). As a result, humans have higher urate plasma levels compared to most other mammals (Johnson *et al* 2003). Urate is freely filtered at the glomerulus. Across the human proximal tubular epithelium it is bidirectionally transported, with reabsorption normally greatly exceeding secretion, resulting in a fractional excretion of only about 10%. The mechanism of urate reabsorption in humans has been intensively studied over the past several years. This process was found to be mediated by a urate/anion exchanger, URAT1 (Enomoto *et al* 2002a). However, the nature of the energy-dependent basolateral uptake step in renal urate secretion in humans was as yet unresolved. The elucidation of the molecular mechanism of this process is of high physiological as well as of clinical importance. Since maintaining constant urate plasma concentration depends on the balance between absorption on the one hand and secretion on the other, alterations of each of these processes leads to changes in urate plasma level. Both the increase (hyperuricemia) as well as decrease (hypouricemia) in urate plasma concentrations is associated with clinical problems. Some types of hypouricemia were shown to result from increased urate secretion and were accompanied by renal calculi formation (urolithiasis) (Hisatome *et al* 1993, Kotake *et al* 1993). Hyperuricemia, which is often due to decreased renal urate clearance, is frequently found in patients with symptoms of gout and arthritis (Roch-Ramel and Diezi 1997). Impairment of the basolateral step in urate secretion might be a cause for some forms of hyperuricemia (Quinones *et al* 1995, Roch-Ramel and Diezi 1997) as has been observed in gouty chicken (Zmuda and Quebbemann 1975).

Recent findings indicated the existence of a basolateral urate / α-KG exchanger both in urate secreting species (Grassl 2002, Werner and Roch-Ramel 1991), as well as in the rat (Rebane *et al* 1998) as a net urate reabsorber, similar to humans. The present observation that hOAT3-mediated ES uptake was strongly inhibited by urate suggested that hOAT3 may be a major basolateral system for renal urate secretion. Moreover, the

present finding that hOAT3-mediated glutarate efflux was significantly trans-stimulated by urate proves the ability of the carrier to mediate urate / dicarboxylate exchange. However, the uptake ratio of hOAT3- over H_2O-injected oocytes observed previously by Cha and colleagues was rather low – only 2.3-fold (Cha *et al* 2001). This could be due to the low substrate concentration of 10 µM used for uptake in these studies, which is well below normal serum urate levels averaging 300 µM (Roch-Ramel and Guisan 1999).

Recently, hOAT1 has also been suggested as the candidate protein driving the energy-dependent step in urate secretion. Conflicting results have however been reported concerning the ability of this transporter to interact with urate. While PAH uptake by the hOAT1 was not inhibited by urate in one study (Race *et al* 1999), an over 90% inhibition by urate was observed in another one (Hosoyamada *et al* 1999). As the concentrations of urate applied differed between these studies, i.e. 100 µM in the former and 2 mM in the latter, the observed discrepancy could be explained by a rather low affinity of hOAT1 for urate. This is supported by the study of Ichida and colleagues who showed that hOAT1 is be able to transport urate when expressed in the mouse S2 cell line (Ichida *et al* 2003), yet with a K_m value as high as about 940 µM, far higher than the normal urate serum concentration. Some observations are also not compatible with hOAT1 as the only urate secretory mechanism. Urate fractional excretion in humans has been found not to be significantly changed by PAH infusion (Boner and Steele 1973). While urate reabsorption would not be expected to be affected by PAH, because the urate / anion exchange pathways present in human brush-border membranes have little or no affinity for PAH (Roch-Ramel *et al* 1994, Roch-Ramel *et al* 1997), urate secretion - if mediated predominantly by hOAT1 - should be strongly inhibited by PAH, as this carrier has a very high PAH affinity (Burckhardt and Burckhardt 2003). Thus, whether OAT1 contributes significantly in the urate transport under physiological conditions has become questionable.

Based on the results obtained in the present study, hOAT3 is proposed to be the major pathway for renal urate secretion. When the sensitivity of hOAT3 for urate was assayed in parallel with that of hOAT1 by cis-inhibition of uptake of PAH as the common substrate for both transporters, hOAT3 appeared to be much more sensitive for urate. Kinetic studies were performed to evaluate the inhibitory potency of urate on hOAT3-mediated transport more accurately. Urate inhibited hOAT3-mediated uptake of 10 nM ES with an average IC_{50} of 255 µM. As the ES concentration (10 nM) is more than 100

times lower than the reported K_m value of hOAT3 for ES of 3.1 µM (Cha *et al* 2001), the obtained IC_{50} value should approximate the K_i (Neame and Richards 1972). This is further supported by the observation that increasing the ES concentration by a factor of 5 yielded an only insignificantly higher urate IC_{50} value of 290 µM. Thus, a mean IC_{50} of below 300 µM was determined, which is in the range of physiological serum urate levels. In contrast, the K_m of hOAT1 for urate is 3-fold higher, as mentioned above. Additionally, the affinities of both transporters for urate were compared using HEK-293 cells stably transfected with hOAT1 and hOAT3 as an alternative expression system. Notably, that the affinity for urate of hOAT1 expressed in HEK293 cells was higher than shown previously in mouse S2 cells (Ichida *et al* 2003). Nevertheless, the difference between hOAT1 and hOAT3 in urate sensitivity remained. The urate concentration that half-maximally inhibited hOAT1-mediated PAH uptake into HEK293 cells was around 380 µM, nearly two times higher than that for hOAT3-mediated ES uptake (~170 µM).
Taken together, these data suggest that hOAT3 has a higher affinity for urate than hOAT1, and may therefore play the predominant role in urate secretion under normal physiological conditions.

5.3.2 Involvement of hOAT3 and hOAT1 in the secretion of diuretics

Diuretics are drugs widely used for the clinical management of hypertension and edema. Loop diuretics and thiazides both act at the luminal side of the tubule: loop diuretics by inhibiting the Na^+-K^+-$2Cl^-$ cotransporter (NKCC) in the thick ascending limb of Henle's loop, and thiazides by inhibiting the Na^+-Cl^- cotransporter (NCC) of the distal convoluted tubule (Okusa and Ellison 2000). Diuretics are poorly filtered in the glomerulus because of binding to plasma proteins. Therefore, to reach their luminal sites of action these compounds have to be secreted. Loop diuretics and thiazides belong to the class of sulfonamide diuretics as they carry a sulfamoyl group (Figure 5.3), and at physiological pH are present predominantly as organic anions. Thus, by their chemical structure loop diuretics and thiazides fulfill the specificity requirements of the basolateral organic anion transport system - hydrophobic molecules carrying one or two negative charges as established earlier by Ullrich and co-workers (Ullrich 1997). Moreover, sulfamoyl diuretics have been shown to inhibit the contraluminal PAH transport in the intact rat kidney (Ullrich *et al* 1989) and in the isolated S_2 segment of rabbit kidney proximal tubules (Bartel *et al* 1993). Likewise, the transport of labeled furosemide into rabbit kidney basolateral membrane vesicles was inhibited by

probenecid – the classical inhibitor of the organic anion transport system (Gloff *et al* 1988).

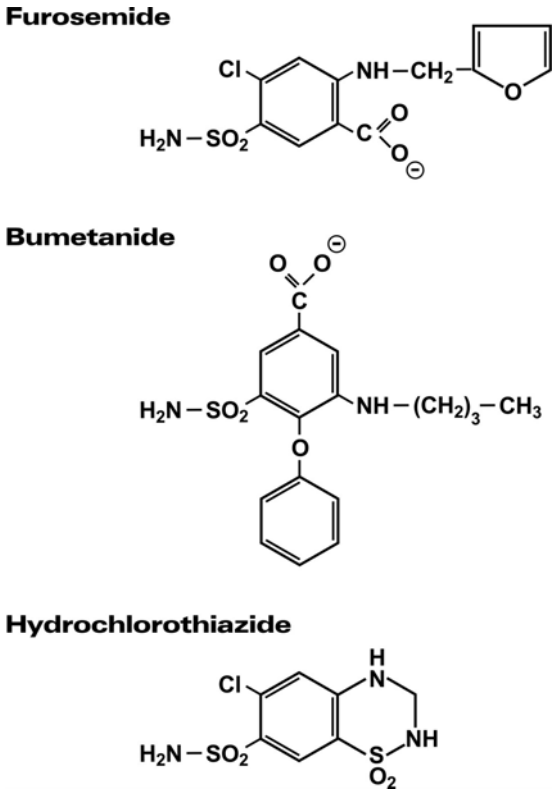

Figure 5.3. Structural formulas of diuretic drugs tested for interaction with hOAT1 and hOAT3 in the present study.

Due to their localization and functional properties, hOAT1 and hOAT3 are the main candidates for mediating secretion of these diuretics. Despite the high clinical importance, few data existed concerning the involvement of hOAT1 and hOAT3 in this process. While the uptake of substrates by hOAT1 and hOAT3 was inhibited by the loop diuretics furosemide and bumetanide (Cha *et al* 2001, Race *et al* 1999), nothing was known about the affinities of these interactions. While rOAT1 had been shown to mediate uptake of furosemide when expressed in oocytes (Uwai *et al* 2000), and the flounder OAT was shown by electrophysiologic techniques to translocate bumetanide (Burckhardt *et al* 2000), the ability of hOAT1 and hOAT3 to translocate diuretics had not been demonstrated.

In the present study, in order to assess the contribution of hOAT1 and hOAT3 to diuretic secretion, both transporters were directly compared with respect to interaction with these drugs under identical conditions in the same expression system. Glutarate

was chosen as the common substrate of hOAT1 and hOAT3, since at a saturating concentration of 100 µM the uptake rates were similar for both transporters. Although a relatively low concentration of loop diuretics was used (250 µM), the hOAT3-mediated transport was already suppressed to the level of water-injected control oocytes. This was consistent with the previously observed strong inhibition of hOAT3-mediated ES uptake by bumetanide and furosemide at 5 µM (Cha *et al* 2001). Under the same conditions, hOAT1-mediated glutarate uptake was inhibited less than 50%, suggesting a lower affinity of this transporter for loop diuretics. Similarly, a low inhibitory potency of bumetanide and furosemide on hOAT1-mediated PAH uptake has been reported by Race and colleagues (Race *et al* 1999). Thus, already preliminary inhibition studies indicated a much higher sensitivity of hOAT3 than of hOAT1 for the loop diuretics furosemide and bumetanide. These data were further supported by kinetic studies of the inhibitory potency of furosemide on hOAT1- and hOAT3-mediated glutarate transport. The furosemide IC_{50}-value for hOAT1-mediated glutarate uptake averaged 490 µM, while for hOAT3 this value was around 3 µM. Thus, the sensitivity of hOAT3 appeared to be more than two orders of magnitude (~150 times) higher than that of hOAT1. It might be argued that the observed difference in IC_{50}-values could be the consequence of the different affinities of the two transporters for glutarate. However, it can account for the difference in IC_{50} only partially, as detailed below. Assuming competitive inhibition between glutarate and furosemide, as both substances are substrates for hOAT1 and hOAT3, and nothing is known about a second high-affinity binding site of both transporters, an estimate for K_i can be obtained from the IC_{50} value. From the competitive inhibition kinetics we know that $IC_{50} = K_i(1+\frac{S}{K_m})$, where K_i is the real constant of inhibition, S the concentration of substrate used, K_m the apparent Michaelis-Menten constant (Neame and Richards 1972). This can be rearranged as $K_i = \frac{IC_{50}}{1+\frac{S}{K_m}}$. Thus, by substitution of the values obtained for hOAT1 of 490 µM as IC_{50} value for furosemide and 2.4 µM as K_m for glutarate, as well as 100 µM for the concentration of glutarate used as substrate, one can calculate a K_i value of hOAT1 for furosemide of 11.5 µM. Making the same calculation for hOAT3, with the furosemide IC_{50} value of 3.2 µM, and a glutarate K_m of 23.5 µM, the real K_i value of hOAT3 for furosemide would approach 0.6 µM, which is 19 times smaller than that of hOAT1. The therapeutically relevant concentrations of unbound furosemide are considered to be around 0.4 µM (Hasannejad *et al* 2004). Taken together with its furosemide affinity

established in the current study, hOAT3 might be assumed to be the major pathway for furosemide secretion in human proximal tubules in vivo. Moreover, the previous in vivo studies on rabbit kidneys revealed that furosemide secretion was depressed by probenecid by 95% while PAH exerted only 44 to 66% inhibition (Bidiville and Roch-Ramel 1986). Likewise, in studies on basolateral membrane vesicles of rabbit proximal tubules, the furosemide transport was inhibited by probenecid, but the inhibition by PAH was not significant (Gloff *et al* 1988). Since hOAT3 has a lower affinity for PAH than hOAT1, these data are in line with the present finding that hOAT3 may be the main transporter mediating furosemide excretion. In a most recent paper, which appeared after finishing the experiments of the current study, Hasannejad with coworkers reported on the interactions of hOATs with diuretics (Hasannejad *et al* 2004). The authors used cells of the second segment of the proximal tubule (S2) stably expressing hOAT1, hOAT2, hOAT3, or hOAT4. The furosemide concentration half-maximally inhibiting the hOAT3-mediated ES uptake was around 7 µM, and IC_{50} value of furosemide for hOAT1 (measured on PAH uptake) was 18 µM. Thus, consistent with the present study, hOAT3 was shown to have a higher affinity for furosemide than hOAT1. However the difference between hOAT1 and hOAT3 IC_{50} values in the above-mentioned study was much lower (2.5 times). The reason for this discrepancy is not clear. One of the factors influencing the kinetic constants may be the different expression systems used.

In order to prove the ability of hOAT1 and hOAT3 to translocate loop diuretics (furosemide) and thiazide diuretics (hydrochlorothiazide), trans-stimulation experiments were performed. When taken at low concentrations (50 µM and 250 µM), furosemide trans-stimulated efflux of glutarate from hOAT1- and hOAT3-expressing oocytes with the same potency as did PAH as a positive control. Interestingly, the rate of trans-stimulation caused by furosemide was also similar for both transporters. Possible reasons of the discrepancy between this finding and the affinity studies could be potential opposing effects under efflux conditions. At lower concentrations of trans-anion, trans-stimulation should predominate, whereas at higher concentrations - especially of high-affinity substrates applied from the extracellular side - the trans-stimulation effect may be superimposed by cis-inhibition of test compound having already entered the cell via the carrier, resulting in a biphasic curve. Thus, since hOAT3 has the high affinity for furosemide, part of the trans-stimulation effect could be masked by cis-inhibition by furosemide from the intracellular side. Notably, hydrochlorothiazide stimulated the glutarate efflux most potently by both transporters,

in both cases even more strongly than PAH. Taken together, the trans-stimulation data indicate that both hOAT1 and hOAT3 are not only inhibited by diuretics, but actually able to translocate furosemide and hydrochlorothiazide in exchange for dicarboxylates and thus participate in the secretion of these drugs in vivo.

5.4 Conclusions and outlook

In the present study the mechanism of hOAT3-mediated organic anion transport was re-investigated. The data presented here demonstrated that OAT3 does not represent a uniporter, as was assumed before, but can operate as an organic anion / dicarboxylate exchanger, similar to hOAT1. Thus, hOAT3 together with hOAT1 mediate the secretory flux of their substrates and both carriers can share the same driving force in vivo - the outwardly directed α-KG gradient. This finding has some important implications. First, the mode of operation of other OAT family members, such as OAT2 and OAT4, should be more carefully studied. Second, it is necessary to re-evaluate the relative roles of hOAT1 and hOAT3 in the transport of shared substrates by their comparison with respect to selectivity and specificity under identical conditions. Such comparisons have been carried out in the present study, namely for the naturally occurring substrate urate and for selected diuretics. The ability of hOAT3 to translocate urate, and the sensitivity of the transporter to this metabolite was estimated and compared to that of hOAT1. From the obtained data the conclusion was drawn that hOAT3 is probably the main basolateral carrier involved in renal urate secretion under physiological conditions. With respect to the interaction with diuretics, both hOAT3 and hOAT1 have been shown to translocate the loop diuretic furosemide as well as hydrochlorothiazide. Thus, both carriers can participate in diuretic secretion, although because of its higher affinity at least for furosemide, hOAT3 might predominate over hOAT1 in this process. However, accurate assessment of the contribution of both carriers to the secretion of these compounds in vivo requires knowledge about hOAT1 and hOAT3 transport capacities in the kidney. Therefore, studies on intact human proximal tubules are required under conditions, at which one of these carriers is selectively inhibited, to evaluate their contribution to overall kidney function. Further compounds which are known as hOAT1 and/or hOAT3 substrates await comparison studies, which are particularly important in view of potential drug-drug interactions that could occur at the sites of these carriers.

REFERENCES

Alebouyeh M, Takeda M, Onozato ML, Tojo A, Noshiro R, Hasannejad H, Inatomi J, Narikawa S, Huang XL, Khamdang S, Anzai N, Endou H (2003), Expression of human organic anion transporters in the choroid plexus and their interactions with neurotransmitter metabolites, *J.Pharmacol.Sci.* 93: 430-436

Apiwattanakul N, Sekine T, Chairoungdua A, Kanai Y, Nakajima N, Sophasan S, Endou H (1999), Transport properties of nonsteroidal anti-inflammatory drugs by organic anion transporter 1 expressed in Xenopus laevis oocytes, *Molecular Pharmacology* 55: 847-854

Babu E, Takeda M, Narikawa S, Kobayashi Y, Enomoto A, Tojo A, Cha SH, Sekine T, Sakthisekaran D, Endou H (2002), Role of human organic anion transporter 4 in the transport of ochratoxin A, *Biochimica et Biophysica Acta* 1590: 64-75

Bakhiya N, Bahn A, Burckhardt G, Wolff NA. Human organic anion transporter 3 (hOAT3) can operate as an exchanger. The Faseb Journal 17, A477. 2003.

Barendt WM, Wright SH (2002), The human organic cation transporter (hOCT2) recognizes the degree of substrate ionization, *The Journal of Biological Chemistry* 277: 22491-22496

Bartel C, Wirtz C, Brandle E, Greven J (1993), Interaction of thiazide and loop diuretics with the basolateral para-aminohippurate transport system in isolated S2 segments of rabbit kidney proximal tubules, *Journal of Pharmacology and Experimental Therapeutics* 266: 972-977

Berg JM, Tymoczko JL, Stryer L. (2002), *Biochemistry* 5th.edition. Published by W. H. Freeman and Company, New York, USA

Bidiville J, Roch-Ramel F (1986), Competition of organic anions for furosemide and p-aminohippurate secretion in the rabbit, *Journal of Pharmacology and Experimental Therapeutics* 237: 636-643

Boner G, Steele TH (1973), Relationship of urate and p-aminohippurate secretion in man, *Am.J.Physiol* 225: 100-104

Buist SC, Cherrington NJ, Choudhuri S, Hartley DP, Klaassen CD (2002), Gender-specific and developmental influences on the expression of rat organic anion transporters, *Journal of Pharmacology and Experimental Therapeutics* 301: 145-151

Burckhardt BC, Brai S, Wallis S, Krick W, Wolff NA, Burckhardt G (2002), Transport of cimetidine by flounder and human renal organic anion transporter 1, *Am.J.Physiol Renal Physiol* 284: 503-509

Burckhardt BC, Burckhardt G (2003), Transport of organic anions across the basolateral membrane of proximal tubule cells, *Rev.Physiol Biochem.Pharmacol.* 146: 95-158

Burckhardt BC, Wolff NA, Burckhardt G (2000), Electrophysiologic characterization of an organic anion transporter cloned from winter flounder kidney (fROAT), *Journal of the American Society of Nephrology* 11: 9-17

Burckhardt G, Greger R (1997), Principles of electrolyte transport across plasma membranes of renal tubular cells, in *Handbook of Physiology - Renal Physiology*, p 639-657

Burckhardt G, Pritchard JB (2000), Organic anion and cation antiporters, in *The kidney: Physiology and pathophysiology*, ed. Seldin DW and Giebisch G, Lippincott Williams and Wilkins, Philadelphia p 193-222

Burckhardt G, Wolff NA (2000), Structure of renal organic anion and cation transporters, *Am.J.Physiol Renal Physiol* 278: F853-F866

Cha SH, Sekine T, Fukushima JI, Kanai Y, Kobayashi Y, Goya T, Endou H (2001), Identification and characterization of human organic anion transporter 3 expressing predominantly in the kidney, *Molecular Pharmacology* 59: 1277-1286

Cha SH, Sekine T, Kusuhara H, Yu E, Kim JY, Kim DK, Sugiyama Y, Kanai Y, Endou H (2000), Molecular cloning and characterization of multispecific organic anion transporter 4 expressed in the placenta, *The Journal of Biological Chemistry* 275: 4507-4512

Cihlar T, Ho ES (2000), Fluorescence-based assay for the interaction of small molecules with the human renal organic anion transporter 1, *Anal.Biochem.* 283: 49-55

Cihlar T, Lin DC, Pritchard JB, Fuller MD, Mendel DB, Sweet DH (1999), The antiviral nucleotide analogs cidofovir and adefovir are novel substrates for human and rat renal organic anion transporter 1, *Molecular Pharmacology* 56: 570-580

Enomoto A, Kimura H, Chairoungdua A, Shigeta Y, Jutabha P, Cha SH, Hosoyamada M, Takeda M, Sekine T, Igarashi T, Matsuo H, Kikuchi Y, Oda T, Ichida K, Hosoya T, Shimokata K, Niwa T, Kanai Y, Endou H (2002a), Molecular identification of a renal urate-anion exchanger that regulates blood urate levels, *Nature* 417: 447-452

Enomoto A, Takeda M, Shimoda M, Narikawa S, Kobayashi Y, Kobayashi Y, Yamamoto T, Sekine T, Cha SH, Niwa T, Endou H (2002b), Interaction of Human Organic Anion Transporters 2 and 4 with Organic Anion Transport Inhibitors, *Journal of Pharmacology and Experimental Therapeutics* 301: 797-802

Enomoto A, Takeda M, Taki K, Takayama F, Noshiro R, Niwa T, Endou H (2003), Interactions of human organic anion as well as cation transporters with indoxyl sulfate, *European Journal of Pharmacology* 466: 13-20

Eraly SA, Hamilton BA, Nigam SK (2003), Organic anion and cation transporters occur in pairs of similar and similarly expressed genes, *Biochemical and Biophysical Research Communications* 300: 333-342

Fritzsch G, Rumrich G, Ullrich KJ (1989), Anion transport through the contraluminal cell membrane of renal proximal tubule. The influence of hydrophobicity and molecular charge distribution on the inhibitory activity of organic anions, *Biochimica et Biophysica Acta* 978: 249-256

Gloff CA, Mamelok RD, Benet LZ (1988), Organic anion transport by basal-lateral membranes: effect of PAH and furosemide on each other's transport, *Pharmacology* 37: 268-276

Grassl SM (2002), Urate/a-ketoglutarate exchange in avian basolateral membrane vesicles, *Am.J.Physiol Cell Physiol* 283: C1144-C1154

Hagenbuch B, Meier PJ (2003), The superfamily of organic anion transporting polypeptides, *Biochimica et Biophysica Acta* 1609: 1-18

Hasannejad H, Takeda M, Taki K, Shin HJ, Babu E, Jutabha P, Khamdang S, Aleboyeh M, Onozato ML, Tojo A, Enomoto A, Anzai N, Narikawa S, Huang XL, Niwa T, Endou H (2004), Interactions of human organic anion transporters with diuretics, *Journal of Pharmacology and Experimental Therapeutics* 308: 1021-1029

Hisatome I, Tanaka Y, Kotake H, Kosaka H, Hirata N, Fujimoto Y, Yoshida A, Shigemasa C, Mashiba H, Sato R, . (1993), Renal hypouricemia due to enhanced tubular secretion of urate associated with urolithiasis: successful treatment of urolithiasis by alkalization of urine K+, Na(+)-citrate, *Nephron* 65: 578-582

Ho ES, Lin DC, Mendel DB, Cihlar T (2000), Cytotoxicity of antiviral nucleotides adefovir and cidofovir is induced by the expression of human renal organic anion transporter 1, *Journal of the American Society of Nephrology* 11: 383-393

Hofmann K and Stoffel W (1993), TMbase - a database of membrane spanning proteins segments, *Biol. Chem. Hoppe-Seyler* 374, 166

Horowitz SB, Miller DS (1984), Solvent properties of ground substance studied by cryomicrodissection and intracellular reference-phase techniques, *J.Cell Biol.* 99: 172s-179s

Hosoyamada M, Sekine T, Kanai Y, Endou H (1999), Molecular cloning and functional expression of a multispecific organic anion transporter from human kidney, *American Journal of Physiology* 276: F122-F128

Ichida K, Hosoyamada M, Kimura H, Takeda M, Utsunomiya Y, Hosoya T, Endou H (2003), Urate transport via human PAH transporter hOAT1 and its gene structure, *Kidney International* 63: 143-155

Inui K, Takano M, Okano T, Hori R (1986), Role of chloride on carrier-mediated transport of *p*-aminohippurate in rat renal basolateral membrane vesicles, *Biochimica et Biophysica Acta* 855: 425-428

Islinger F, Gekle M, Wright SH (2001), Interaction of 2,3-dimercapto-1-propane sulfonate with the human organic anion transporter hOAT1, *Journal of Pharmacology and Experimental Therapeutics* 299: 741-747

Jariyawat S, Sekine T, Takeda M, Apiwattanakul N, Kanai Y, Sophasan S, Endou H (1999), The interaction and transport of beta-lactam antibiotics with the cloned rat renal organic anion transporter 1, *Journal of Pharmacology and Experimental Therapeutics* 290: 672-677

Johnson RJ, Kang DH, Feig D, Kivlighn S, Kanellis J, Watanabe S, Tuttle KR, Rodriguez-Iturbe B, Herrera-Acosta J, Mazzali M (2003), Is there a pathogenetic role for uric acid in hypertension and cardiovascular and renal disease?, *Hypertension* 41: 1183-1190

Jung KY, Takeda M, Kim DK, Tojo A, Narikawa S, Yoo BS, Hosoyamada M, Cha SH, Sekine T, Endou H (2001), Characterization of ochratoxin A transport by human organic anion transporters, *Life Sci.* 69: 2123-2135

Jutabha P, Kanai Y, Hosoyamada M, Chairoungdua A, Kim dK, Iribe Y, Babu E, Kim JY, Anzai N, Chatsudthipong V, Endou H (2003), Identification of a novel voltage-driven organic anion transporter present at apical membrane of renal proximal tubule, *The Journal of Biological Chemistry* 278: 27930-27938

Khamdang S, Takeda M, Noshiro R, Narikawa S, Enomoto A, Anzai N, Piyachaturawat P, Endou H (2002), Interactions of human organic anion transporters and human organic cation transporters with nonsteroidal anti-inflammatory drugs, *Journal of Pharmacology and Experimental Therapeutics* 303: 534-539

Kimura H, Takeda M, Narikawa S, Enomoto A, Ichida K, Endou H (2002), Human organic anion transporters and human organic cation transporters mediate renal transport of prostaglandins, *Journal of Pharmacology and Experimental Therapeutics* 301: 293-298

Kobayashi Y, Ohshiro N, Shibusawa A, Sasaki T, Tokuyama S, Sekine T, Endou H, Yamamoto T (2002), Isolation, characterization and differential gene expression of multispecific organic anion transporter 2 in mice, *Molecular Pharmacology* 62: 7-14

Kojima R, Sekine T, Kawachi M, Cha SH, Suzuki Y, Endou H (2002), Immunolocalization of multispecific organic anion transporters, OAT1, OAT2, and OAT3, in rat kidney, *Journal of the American Society of Nephrology* 13: 848-857

Kok LD, Siu SS, Fung KP, Tsui SK, Lee CY, Waye MM (2000), Assignment of liver-specific organic anion transporter (SLC22A7) to human chromosome 6 bands p21.2-->p21.1 using radiation hybrids, *Cytogenet.Cell Genet.* 88: 76-77

Kotake T, Miura N, Ito H (1993), Renal tubular hypouricemia and calcium urolithiasis, *Scanning Microsc.* 7: 417-421

Kudo N, Katakura M, Sato Y, Kawashima Y (2002), Sex hormone-regulated renal transport of perfluorooctanoic acid, *Chem.Biol.Interact.* 139: 301-316

Kusuhara H, Sekine T, Utsunomiya-Tate N, Tsuda M, Kojima R, Cha SH, Sugiyama Y, Kanai Y, Endou H (1999), Molecular cloning and characterization of a new multispecific organic anion transporter from rat brain, *The Journal of Biological Chemistry* 274: 13675-13680

Kuze K, Graves P, Leahy A, Wilson P, Stuhlmann H, You G (1999), Heterologous expression and functional characterization of a mouse renal organic anion transporter in mammalian cells, *The Journal of Biological Chemistry* 274: 1519-1524

Lopez-Nieto CE, You G, Bush KT, Barros EJ, Beier DR, Nigam SK (1997), Molecular cloning and characterization of NKT, a gene product related to the organic cation transporter family that is almost exclusively expressed in the kidney, *The Journal of Biological Chemistry* 272: 6471-6478

Lu R, Chan BS, Schuster VL (1999), Cloning of the human kidney PAH transporter: narrow substrate specificity and regulation by protein kinase C, *American Journal of Physiology* 276: F295-F303

Miller DS, Stewart DE, Pritchard JB (1993), Intracellular compartmentation of organic anions within renal cells, *Am.J.Physiol.Regul.Integr.Comp.Physiol.* 264: R882-R890

Motohashi H, Sakurai Y, Saito H, Masuda S, Urakami Y, Goto M, Fukatsu A, Ogawa O, Inui KI (2002), Gene expression levels and immunolocalization of organic ion transporters in the human kidney, *Journal of the American Society of Nephrology* 13: 866-874

Motojima M, Hosokawa A, Yamato H, Muraki T, Yoshioka T (2002), Uraemic toxins induce proximal tubular injury via organic anion transporter 1-mediated uptake, *Br.J.Pharmacol.* 135: 555-563

Mulato AS, Ho ES, Cihlar T (2000), Nonsteroidal anti-inflammatory drugs efficiently reduce the transport and cytotoxicity of adefovir mediated by the human renal organic anion transporter 1, *Journal of Pharmacology and Experimental Therapeutics* 295: 10-15

Murer H, Burckhardt G (1983), Membrane transport of anions across epithelia of mammalian small intestine and kidney proximal tubule, *Rev.Physiol Biochem.Pharmacol.* 96: 1-51

Nagata Y, Kusuhara H, Endou H, Sugiyama Y (2002), Expression and functional characterization of rat organic anion transporter 3 (rOat3) in the choroid plexus, *Molecular Pharmacology* 61: 982-988

Neame KD, Richards TG (1972), *Elementary kinetics of membrane carrier transport*, Blackwell Scientific Publications, Oxford, London, Edinburgh, Melbourne

Nicollier M, Roblin S, Cypriani B, Remy-Martin JP, Adessi GL (1992), Purification and characterization of a binding protein related to the Z class of cytosolic proteins in guinea-pig liver cytosol (guinea-pig Z protein), *European Journal of Biochemistry* 205: 1137-1144

Okusa MD, Ellison DH (2000), Physiology and pathophysiology of diuretic action, in *The kidney. Physiology and pathophysiology*, ed. Seldin DW and Giebisch G, Lippincott Williams & Wilkins, Philadelphia p 2877-2922

Pritchard JB (1988), Coupled transport of p-aminohippurate by rat kidney basolateral membrane vesicles, *Am.J.Physiol* 255: F597-F604

Pritchard JB (1995), Intracellular alpha-ketoglutarate controls the efficacy of renal organic anion transport, *Journal of Pharmacology and Experimental Therapeutics* 274: 1278-1284

Pritchard JB, Miller DS (1991), Comparative insights into the mechanisms of renal organic anion and cation secretion, *Am.J.Physiol* 261: R1329-R1340

Pritchard JB, Miller DS (1993), Mechanisms mediating renal secretion of organic anions and cations, *Physiol Rev.* 73: 765-796

Quinones GA, Natali A, Baldi S, Frascerra S, Sanna G, Ciociaro D, Ferrannini E (1995), Effect of insulin on uric acid excretion in humans, *Am.J.Physiol* 268: E1-E5

Race JE, Grassl SM, Williams WJ, Holtzman EJ (1999), Molecular cloning and characterization of two novel human renal organic anion transporters (hOAT1 and hOAT3), *Biochemical and Biophysical Research Communications* 255: 508-514

Rebane EN, Orlov Y, Kazbekov EN, Lyubimov Y, Bulat MN (1998), The mechanism of coupling of the organic anion exchange to Na(+)-dicarboxylate symport in basolateral membrane vesicles, *Membr.Cell Biol.* 12: 51-56

Reid G, Wolff NA, Dautzenberg FM, Burckhardt G (1998), Cloning of a human renal p-aminohippurate transporter, hROAT1, *Kidney Blood Press Res.* 21: 233-237

Roch-Ramel F (1998), Renal transport of organic anions
1, *Curr.Opin.Nephrol.Hypertens.* 7: 517-524

Roch-Ramel F, Diezi J (1997), Renal transport of organic ions and uric acid, in *Diseases of the kidney*, ed. Schrier RW and Gottschalk CW, Little,Brown and Company, Boston,New York,Toronto,London p 231-249

Roch-Ramel F, Guisan B (1999), Renal Transport of Urate in Humans, *News Physiol Sci.* 14: 80-84

Roch-Ramel F, Guisan B, Diezi J (1997), Effects of uricosuric and antiuricosuric agents on urate transport in human brush-border membrane vesicles, *Journal of Pharmacology and Experimental Therapeutics* 280: 839-845

Roch-Ramel F, Werner D, Guisan B (1994), Urate transport in brush-border membrane of human kidney, *American Journal of Physiology* 266: F797-F805

Rosenthal HE, Pietrzak E, Slaunwhite WR, Jr., Sandberg AA (1972), Binding of estrone sulfate in human plasma, *J.Clin.Endocrinol.Metab* 34: 805-813

Schmitt C, Burckhardt G (1993), Modulation by anions of p-aminohippurate transport in bovine renal basolateral membrane vesicles, *Pflugers Arch.* 425: 241-247

Sekine T, Cha SH, Endou H (2000), The multispecific organic anion transporter (OAT) family, *Pflugers Arch.* 440: 337-350

Sekine T, Watanabe N, Hosoyamada M, Kanai Y, Endou H (1997), Expression cloning and characterization of a novel multispecific organic anion transporter, *The Journal of Biological Chemistry* 272: 18526-18529

Shimada H, Moewes B, Burckhardt G (1987), Indirect coupling to Na^+ of *p*-aminohippuric acid uptake into rat renal basolateral membrane vesicles, *American Journal of Physiology* 253: F795-F801

Shuprisha A, Lynch RM, Wright SH, Dantzler WH (1999), Real-time assessment of alpha-ketoglutarate effect on organic anion secretion in perfused rabbit proximal tubules, *Am.J.Physiol* 277: F513-F523

Simonson GD, Vincent AC, Roberg KJ, Huang Y, Iwanij V (1994), Molecular cloning and characterization of a novel liver-specific transport protein, *Journal of Cell Science* 107 (Pt 4): 1065-1072

Sun W, Wu RR, van Poelje PD, Erion MD (2001), Isolation of a family of organic anion transporters from human liver and kidney, *Biochemical and Biophysical Research Communications* 283: 417-422

Sweet DH, Bush KT, Nigam SK (2001), The organic anion transporter family: from physiology to ontogeny and the clinic, *Am.J.Physiol Renal Physiol* 281: F197-F205

Sweet DH, Chan LMS, Walden R, Yang X-P, Miller DS, Pritchard JB (2003), Organic anion transporter 3 (*Slc22a8*) is a dicarboxylate exchanger indirectly coupled to the Na^+ gradient. *Am.J.Physiol Renal Physiol* 284: 763-769

Sweet DH, Miller DS, Pritchard JB, Fujiwara Y, Beier DR, Nigam SK (2002), Impaired organic anion transport in kidney and choroid plexus of organic anion transporter 3 (Oat3 [Slc22a8]) knockout mice, *The Journal of Biological Chemistry* 277: 26934-26943

Sweet DH, Wolff NA, Pritchard JB (1997), Expression cloning and characterization of ROAT1. The basolateral organic anion transporter in rat kidney, *The Journal of Biological Chemistry* 272: 30088-30095

Takeda M, Babu E, Narikawa S, Endou H (2002a), Interaction of human organic anion transporters with various cephalosporin antibiotics, *European Journal of Pharmacology* 438: 137-142

Takeda M, Hosoyamada M, Cha SH, Sekine T, Endou H (2000a), Hydrogen peroxide downregulates human organic anion transporters in the basolateral membrane of the proximal tubule, *Life Sci.* 68: 679-687

Takeda M, Khamdang S, Narikawa S, Kimura H, Hosoyamada M, Cha SH, Sekine T, Endou H (2002b), Characterization of methotrexate transport and its drug interactions with human organic anion transporters, *Journal of Pharmacology and Experimental Therapeutics* 302: 666-671

Takeda M, Khamdang S, Narikawa S, Kimura H, Kobayashi Y, Yamamoto T, Cha SH, Sekine T, Endou H (2002c), Human organic anion transporters and human organic cation transporters mediate renal antiviral transport, *Journal of Pharmacology and Experimental Therapeutics* 300: 918-924

Takeda M, Narikawa S, Hosoyamada M, Cha SH, Sekine T, Endou H (2001), Characterization of organic anion transport inhibitors using cells stably expressing human organic anion transporters, *European Journal of Pharmacology* 419: 113-120

Takeda M, Noshiro R, Onozato ML, Tojo A, Hasannejad H, Huang XL, Narikawa S, Endou H (2004), Evidence for a role of human organic anion transporters in the muscular side effects of HMG-CoA reductase inhibitors, *European Journal of Pharmacology* 483: 133-138

Takeda M, Sekine T, Endou H (2000b), Regulation by protein kinase C of organic anion transport driven by rat organic anion transporter 3 (rOAT3), *Life Sci.* 67: 1087-1093

Tan E, Pang KS (2001), Sulfation is rate limiting in the futile cycling between estrone and estrone sulfate in enriched periportal and perivenous rat hepatocytes, *Drug Metab Dispos.* 29: 335-346

Tojo A, Sekine T, Nakajima N, Hosoyamada M, Kanai Y, Kimura K, Endou H (1999), Immunohistochemical localization of multispecific renal organic anion transporter 1 in rat kidney, *Journal of the American Society of Nephrology* 10: 464-471

Ullrich KJ (1997), Renal transporters for organic anions and organic cations. Structural requirements for substrates, *J.Membr.Biol.* 158: 95-107

Ullrich KJ, Rumrich G, Fritzsch G, Kloss S (1987), Contraluminal para-aminohippurate (PAH) transport in the proximal tubule of the rat kidney. II. Specificity: aliphatic dicarboxylic acids, *Pflugers Arch.* 408: 38-45

Ullrich KJ, Rumrich G, Kloss S (1989), Contraluminal organic anion and cation transport in the proximal renal tubule: V. Interaction with sulfamoyl- and phenoxy diuretics, and with beta-lactam antibiotics, *Kidney International* 36: 78-88

Uwai Y, Okuda M, Takami K, Hashimoto Y, Inui K (1998), Functional characterization of the rat multispecific organic anion transporter OAT1 mediating basolateral uptake of anionic drugs in the kidney, *FEBS Letters* 438: 321-324

Uwai Y, Saito H, Hashimoto Y, Inui KI (2000), Interaction and transport of thiazide diuretics, loop diuretics, and acetazolamide via rat renal organic anion transporter rOAT1, *Journal of Pharmacology and Experimental Therapeutics* 295: 261-265

Werner D, Roch-Ramel F (1991), Indirect Na+ dependency of urate and p-aminohippurate transport in pig basolateral membrane vesicles, *Am.J.Physiol* 261: F265-F272

Wolff NA, Thies K, Kuhnke N, Reid G, Friedrich B, Lang F, Burckhardt G (2003), Protein Kinase C Activation Downregulates Human Organic Anion Transporter 1-Mediated Transport through Carrier Internalization, *Journal of the American Society of Nephrology* 14: 1959-1968

Wolff NA, Werner A, Burkhardt S, Burckhardt G (1997), Expression cloning and characterization of a renal organic anion transporter from winter flounder, *FEBS Letters* 417: 287-291

Zhang L, Gorset W, Dresser MJ, Giacomini KM (1999), The interaction of n-tetraalkylammonium compounds with a human organic cation transporter, hOCT1, *Journal of Pharmacology and Experimental Therapeutics* 288: 1192-1198

Zmuda MJ, Quebbemann AJ (1975), Localization of renal tubular uric acid transport defect in gouty chickens, *Am.J.Physiol* 229: 820-825

ACKNOWLEDGEMENTS

This work was supported by the Deutsche Forschungsgemeinschaft, GRK 335.

I would like to express my gratitude to following people

Professor Burckhardt, head of the department, speaker of the Graduiertenkolleg, and my Ph.D. adviser, for support and direction

My supervisor Dr. Natascha Wolff for her professional and personal help and care

Professor Dr R Hardeland and Prof Dr K. von Figura for acting as Referent and Korreferent, respectively

All my colleagues in the Abteilung Vegetative Physiologie und Pathophysiologie for their assistance and nice attitude, specially to Gesche Dallmeyer and Simone Schindelmann who have been always helpful and kind to me

Elke Thelen for helping with the illustration design

And I am always grateful to my parents for their love and support

LEBENSLAUF

Angaben zur Person:	
Name:	Bakhiya
Vorname:	Nadiya
Geburtsdatum:	30.08.1976
Geburtsort:	Sochi, Krasnodarsky Kray, Russland
Staatsangehörigkeit:	Ukrainisch
Schulbildung:	
1983 -1993	Kiew Schule №116
Studium:	
10/1993	Immatrikulation an der Taras-Shevchenko-Universität in Kiew im Studiengang Biologie
6/1997	Bakkalaureusdiplom im Fach Biologie, Anfertigung der Diplomarbeit mit dem Titel ”The modulating effect of autoantibodies on aminoacylation activity of tyrosyl-tRNA synthetase“
6/1998	Magisterdiplom im Fach Biochemie, Anfertigung der Diplomarbeit mit dem Titel: ”Development of new methods for purification of the high-molecular-weight complex of aminoacyl-tRNA synthetases from bovine liver”
6/1998 – 5/2001	Wissenschaftliche Mitarbeiterin, Institut für Molekulare Biologie und Genetik, Kiev
6/2001 – 3/2004	Doktorarbeit in der Abteilung Vegetative Physiologie, Zentrum Physiologie und Pathophysiologie, Georg-August-Universität Göttingen
6/2001 – 11/2003	Mitgleid des Graduiertenkolleg 335 (”Clinical, cellular and molecular biology of internal organs“)
seit 11/2003	Wissenschaftliche Angestellte, Zentrum Physiologie und Pathophysiologie, Georg-August-Universität Göttingen
3/2004	Abgabe der vorliegenden Dissertation

Göttingen, 16.03.2004

Bakhiya, Nadiya